

A dream comes true: Room-temperature superconductivity

Prof. Gianni Profeta

Dipartimento di Scienze Fisiche e Chimiche & CNR-SPIN

Universita' degli Studi dell'Aquila



Vostok base in Antarctica

In 1983 a temperature of $-89.2\text{ }^{\circ}\text{C}$ was registered

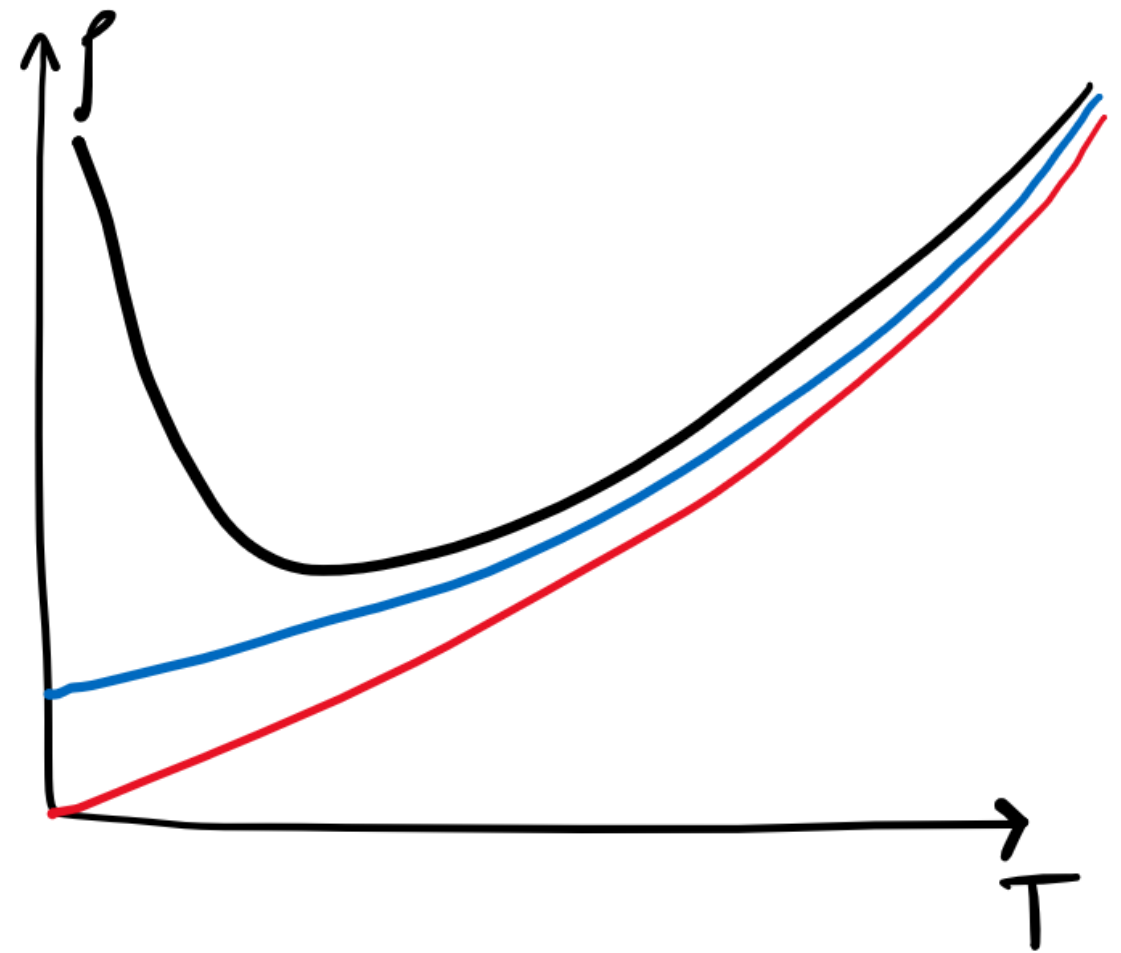


Fontana Luminosa, L'Aquila

In January 2017 a temperature of $-12.0\text{ }^{\circ}\text{C}$ was registered

What happens to the electrical resistivity when we lower the temperature?

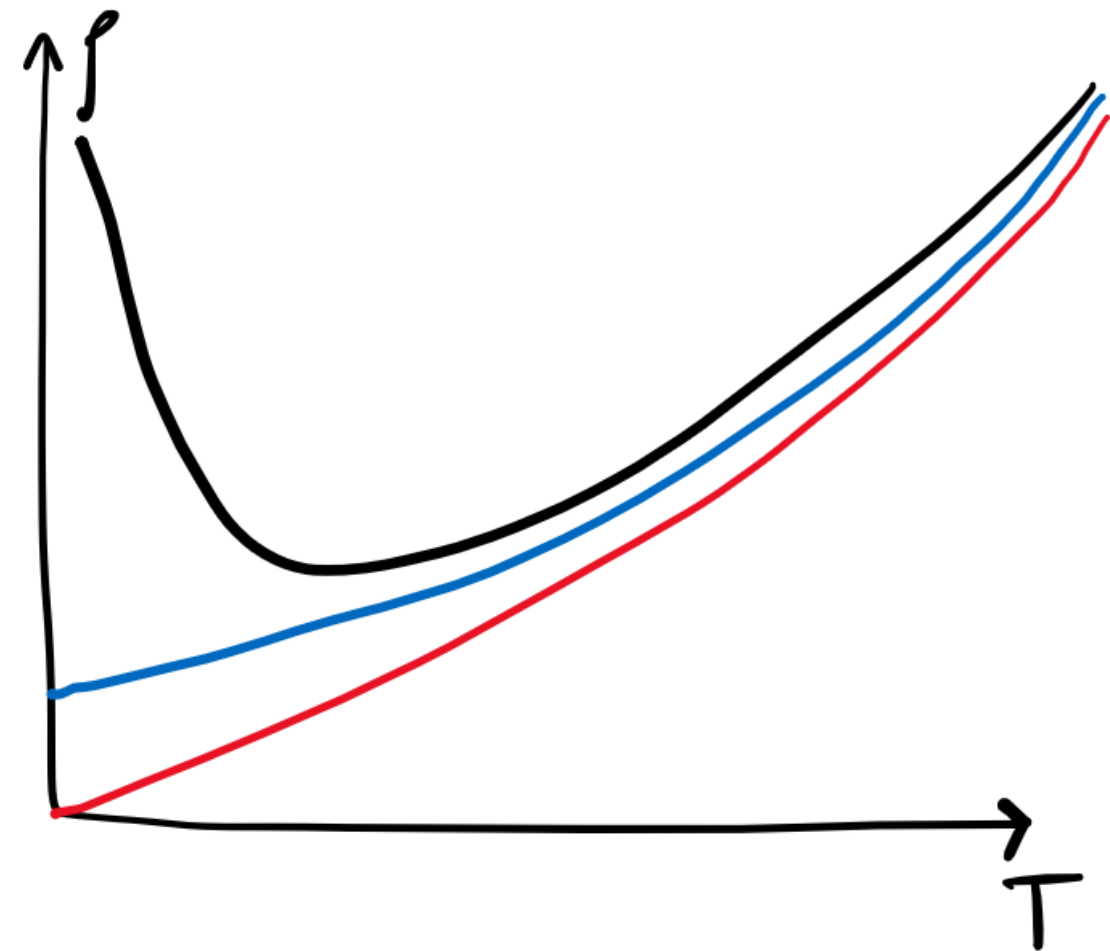
What happens to the electrical resistivity when we lower the temperature?



What happens to the electrical resistivity when we lower the temperature?



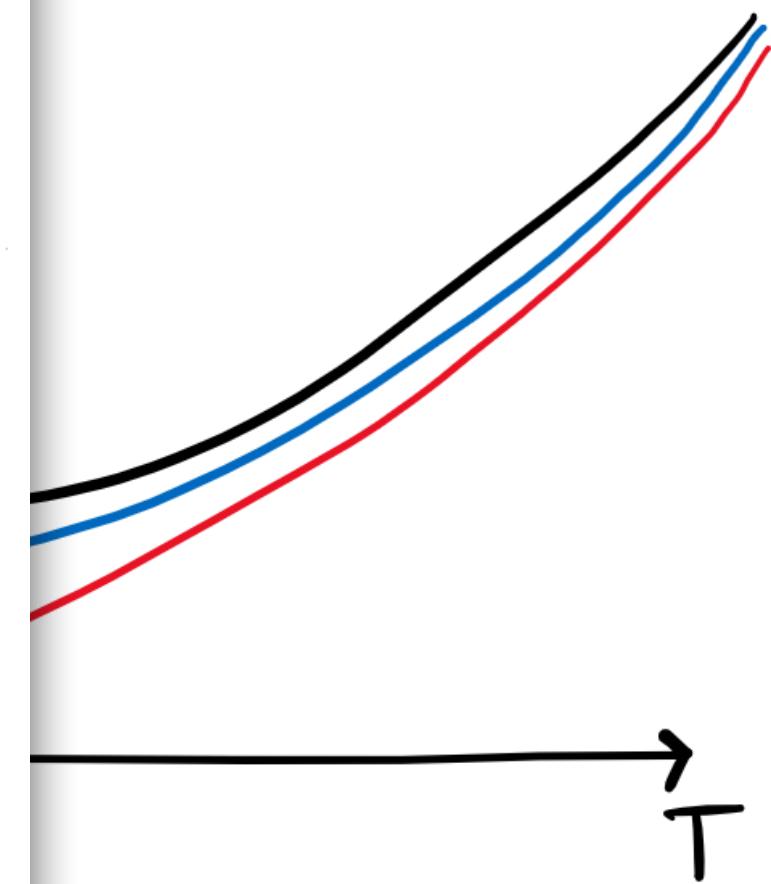
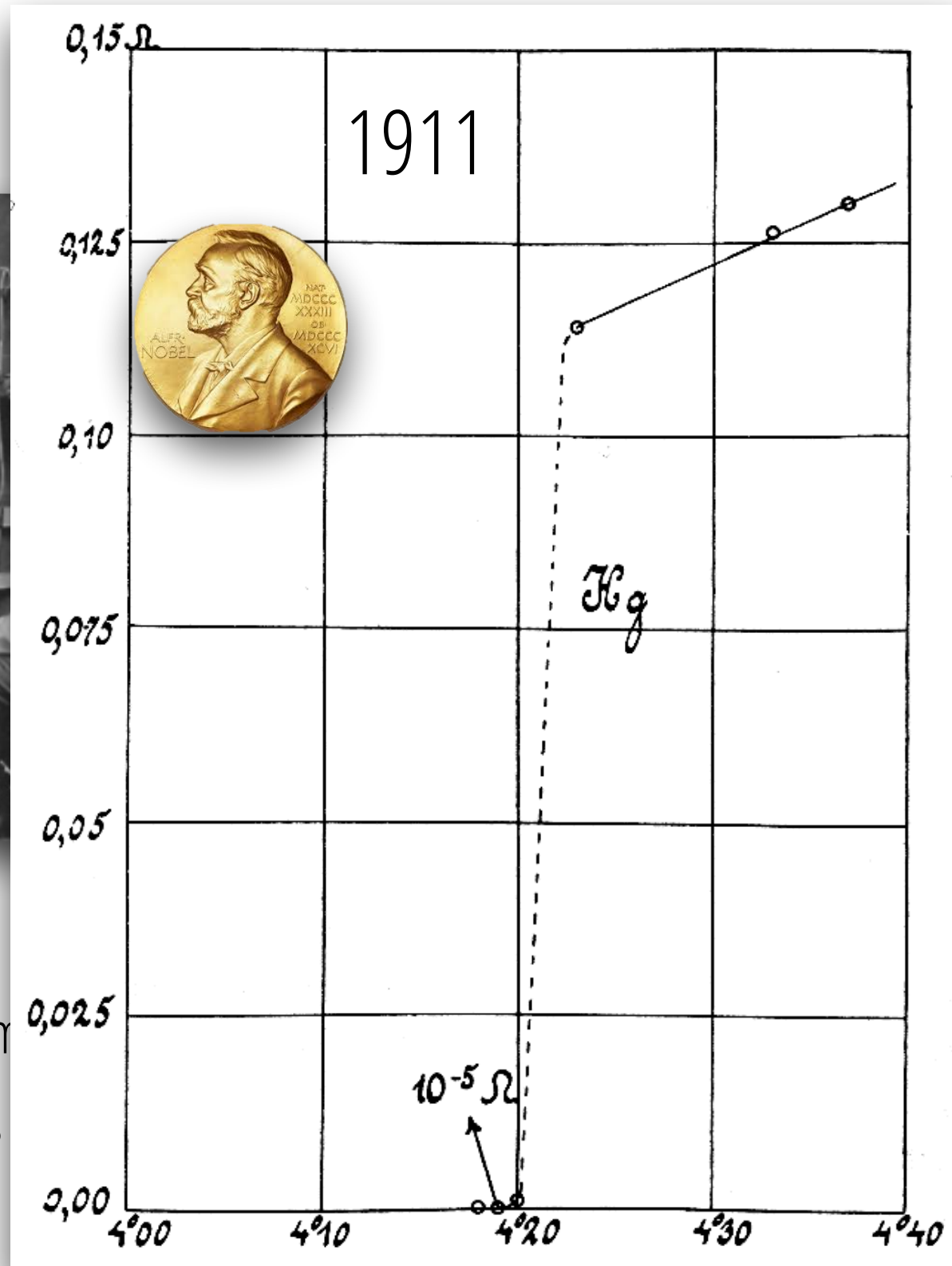
In 1908 liquid helium was realised by Kamerling Onnes



What happens to the electrical resistivity when we lower the temperature?



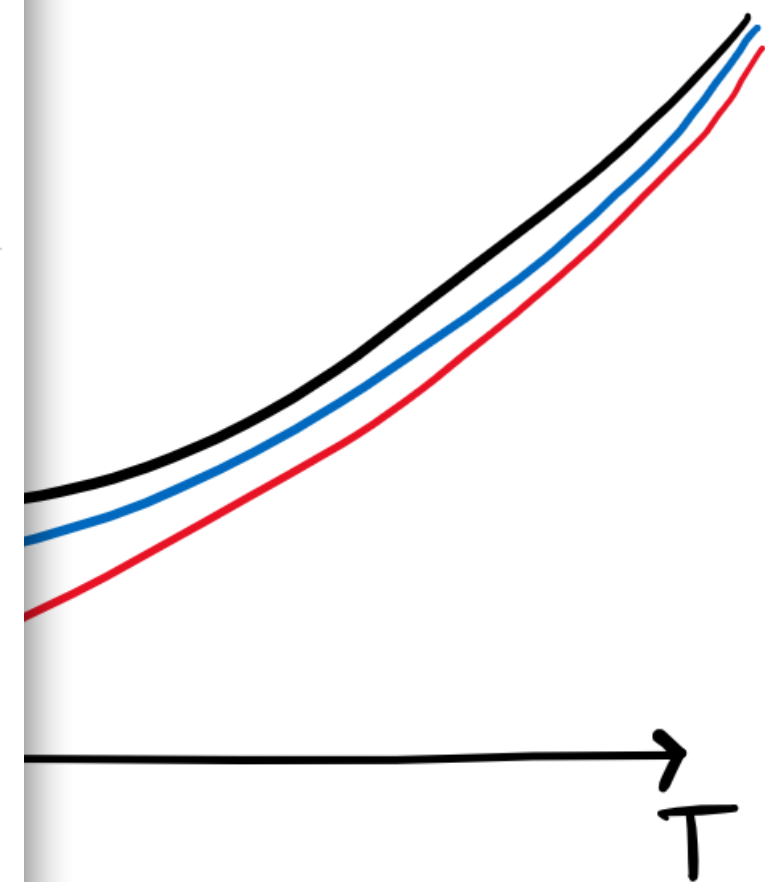
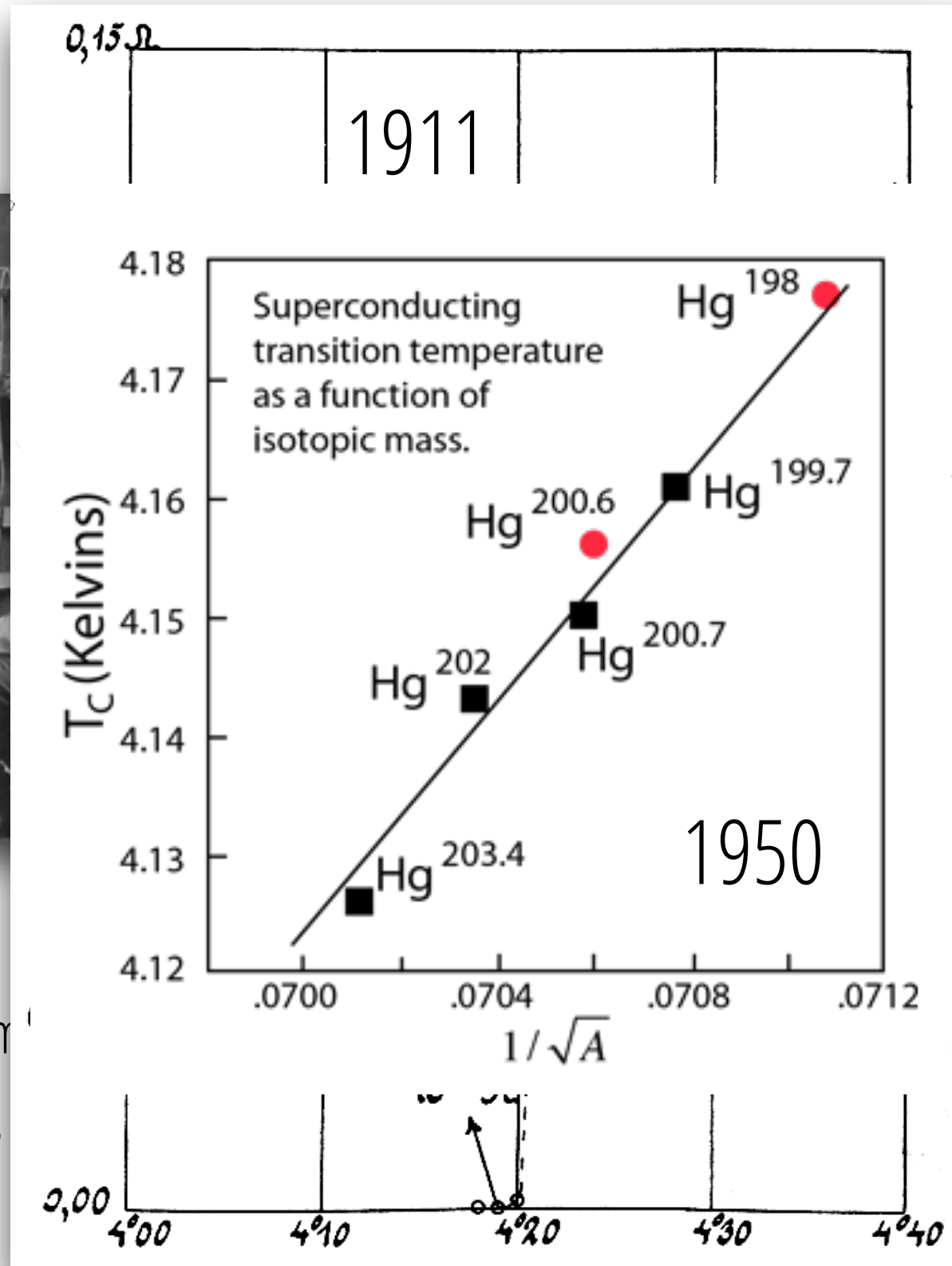
In 1908 liquid helium
Kamerling



What happens to the electrical resistivity when we lower the temperature?



In 1908 liquid helium
Kamerling



Superconductors

It is a common phenomenon

Persistent current: no Joule effect

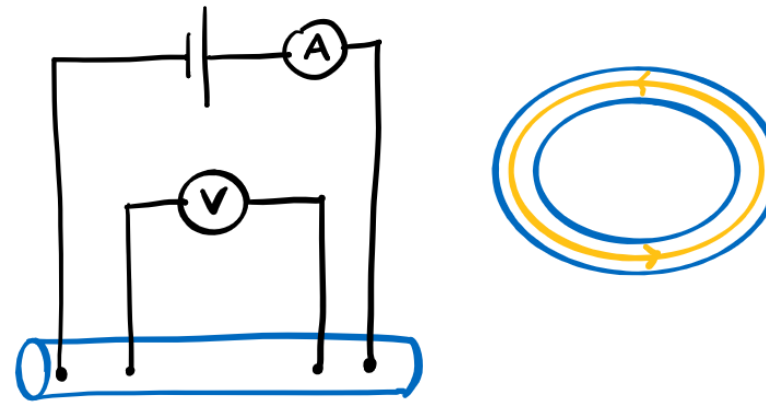
KNOWN SUPERCONDUCTIVE ELEMENTS

■ BLUE = AT AMBIENT PRESSURE
■ GREEN = ONLY UNDER HIGH PRESSURE

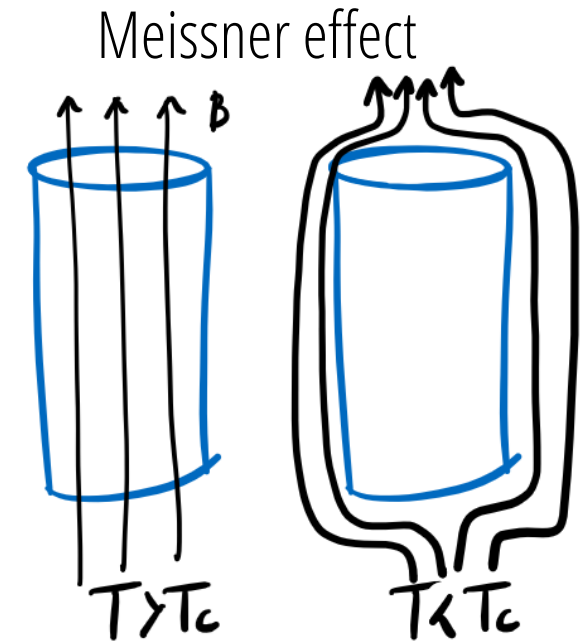
1	2																	10
3	4																	10
11	12																	18
19	20	21	22	23	24	25	26	27	28	29	30	31	32	33	34	35	36	
37	38	39	40	41	42	43	44	45	46	47	48	49	50	51	52	53	54	
55	56	57	58	59	60	61	62	63	64	65	66	67	68	69	70	71		
87	88	89	90	91	92	93	94	95	96	97	98	99	100	101	102	103		

* Lanthanide Series: Ce, Pr, Nd, Pm, Sm, Eu, Gd, Tb, Dy, Ho, Er, Tm, Yb, Lu
+ Actinide Series: Th, Pa, U, Np, Pu, Am, Cm, Bk, Cf, Es, Fm, Md, No, Lr

SUPERCONDUCTORS.ORG



$J_c = 50 \text{ kA}$



$H_c = 13-18 \text{ Tesla}$

Superconductors

It is a common phenomenon

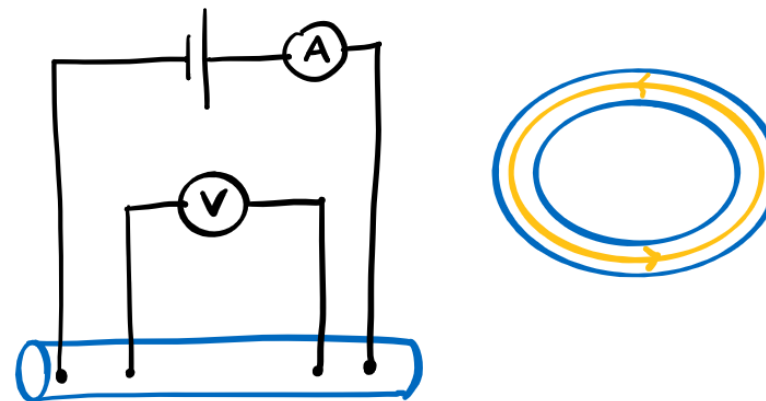
Persistent current: no Joule effect

KNOWN SUPERCONDUCTIVE ELEMENTS

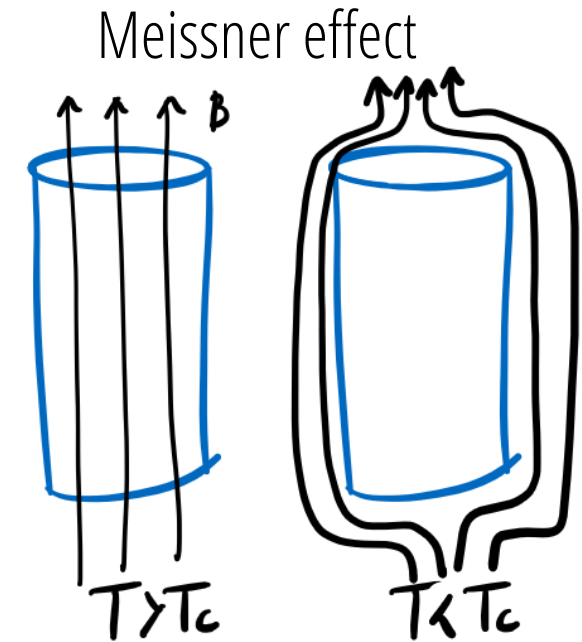
■ BLUE = AT AMBIENT PRESSURE
■ GREEN = ONLY UNDER HIGH PRESSURE

1	H																	2	He
2	Li	Be											B	C	N	O	F	Ne	
3	Na	Mg					Al	Si	P	S	Cl	Ar							
4	K	Ca	Sc	Ti	V	Cr	Mn	Fe	Co	Ni	Cu	Zn	Ga	Ge	As	Se	Br	Kr	
5	Rb	Sr	Y	Zr	Nb	Mo	Tc	Ru	Rh	Pd	Ag	Cd	In	Sn	Sb	Te	I	Xe	
6	Cs	Ba	*La	Hf	Ta	W	Re	Os	Ir	Pt	Au	Hg	Tl	Pb	Bi	Po	At	Rn	
7	Fr	Ra	+Ac	Rf	Ha	106	107	108	109	110	111	112							
		* Lanthanide Series		59	60	61	62	63	64	65	66	67	68	69	70	71			
		+ Actinide Series		90	91	92	93	94	95	96	97	98	99	100	101	102	103		
				Th	Pa	U	Np	Pu	Am	Cm	Bk	Cf	Es	Fm	Md	No	Lr		

SUPERCONDUCTORS.ORG



$J_c = 50 \text{ kA}$



$H_c = 13-18 \text{ Tesla}$

ITER

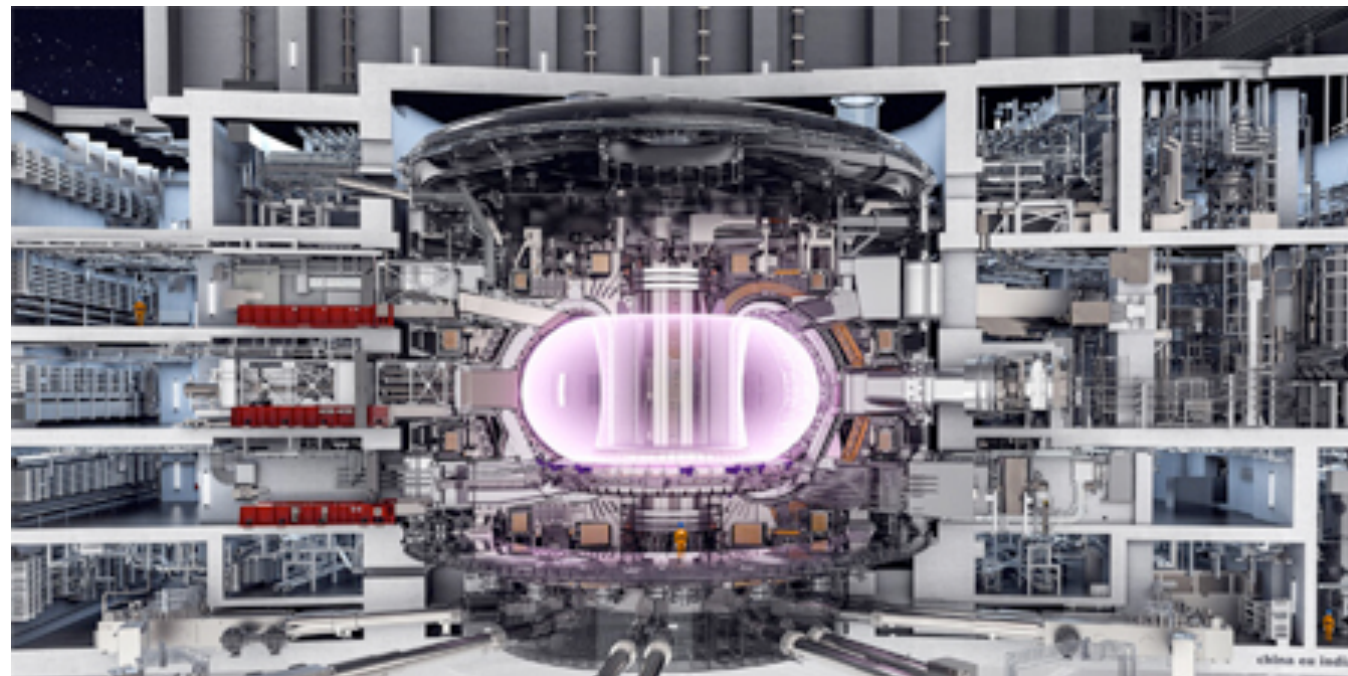
Nb₃Sn@ 4K (ASG)

100.000 Km of cables

41 GJ energy

13.5 Tesla

80 kA



Input power: 620 MW

Output power: 500-700 MW

Large fraction for refrigeration

Theory of Superconductivity*

J. BARDEEN, L. N. COOPER,[†] AND J. R. SCHRIEFFER[‡]
Department of Physics, University of Illinois, Urbana, Illinois

(Received July 8, 1957)

A theory of superconductivity is presented, based on the fact that the interaction between electrons resulting from virtual exchange of phonons is attractive when the energy difference between the electrons states involved is less than the phonon energy, $\hbar\omega$. It is favorable to form a superconducting phase when this attractive interaction dominates the repulsive screened Coulomb interaction. The normal phase is described by the Bloch individual-particle model. The ground state of a superconductor, formed from a linear combination of normal state configurations in which electrons are virtually excited in pairs of opposite spin and momentum, is lower in energy than the normal state by amount proportional to an average $(\hbar\omega)^2$, consistent with the isotope effect. A mutually orthogonal set of excited states in

one-to-one correspondence with those of the normal phase is obtained by specifying occupation of certain Bloch states and by using the rest to form a linear combination of virtual pair configurations. The theory yields a second-order phase transition and a Meissner effect in the form suggested by Pippard. Calculated values of specific heats and penetration depths and their temperature variation are in good agreement with experiment. There is an energy gap for individual-particle excitations which decreases from about $3.5kT_c$ at $T=0^\circ\text{K}$ to zero at T_c . Tables of matrix elements of single-particle operators between the excited-state superconducting wave functions, useful for perturbation expansions and calculations of transition probabilities, are given.

Theory of Superconductivity*

J. BARDEEN, L. N. COOPER,[†] AND J. R. SCHRIEFFER[‡]
Department of Physics, University of Illinois, Urbana, Illinois

(Received July 8, 1957)

A theory of superconductivity is presented, based on the fact that the interaction between electrons resulting from virtual exchange of phonons is attractive when the energy difference between the electrons states involved is less than the phonon energy, $\hbar\omega$. It is favorable to form a superconducting phase when this attractive interaction dominates the repulsive screened Coulomb interaction. The normal phase is described by the Bloch individual-particle model. The ground state of a superconductor, formed from a linear combination of normal state configurations in which electrons are virtually excited in pairs of opposite spin and momentum, is lower in energy than the normal state by amount proportional to an average $(\hbar\omega)^2$, consistent with the isotope effect. A mutually orthogonal set of excited states in

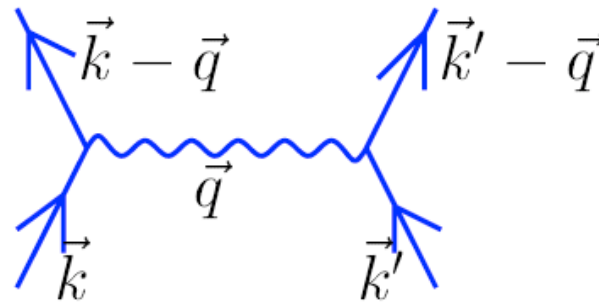
one-to-one correspondence with those of the normal phase is obtained by specifying occupation of certain Bloch states and by using the rest to form a linear combination of virtual pair configurations. The theory yields a second-order phase transition and a Meissner effect in the form suggested by Pippard. Calculated values of specific heats and penetration depths and their temperature variation are in good agreement with experiment. There is an energy gap for individual-particle excitations which decreases from about $3.5kT_c$ at $T=0^\circ\text{K}$ to zero at T_c . Tables of matrix elements of single-particle operators between the excited-state superconducting wave functions, useful for perturbation expansions and calculations of transition probabilities, are given.

Cooper instability

$$\tilde{H}_F = \sum_{k\sigma} \epsilon_k c_{k\sigma}^\dagger c_{k\sigma} + \frac{1}{2} \sum_{\substack{kk'qG \\ \sigma\sigma'}} V_{ph} c_{k+q+G\sigma}^\dagger c_{k'-q-G\sigma'}^\dagger c_{k'\sigma'} c_{k\sigma}$$

$$V_{ph} = \sum_{\lambda} \frac{\hbar\omega_{q\lambda} |g(q+G; \lambda)|^2}{[\epsilon_k - \epsilon_{k+q+G}]^2 - [\hbar\omega_{q\lambda}]^2}$$

if < 0 attraction !!



Theory of Superconductivity*

J. BARDEEN, L. N. COOPER,† AND J. R. SCHRIEFFER‡
Department of Physics, University of Illinois, Urbana, Illinois

(Received July 8, 1957)

A theory of superconductivity is presented, based on the fact that the interaction between electrons resulting from virtual exchange of phonons is attractive when the energy difference between the electrons states involved is less than the phonon energy, $\hbar\omega$. It is favorable to form a superconducting phase when this attractive interaction dominates the repulsive screened Coulomb interaction. The normal phase is described by the Bloch individual-particle model. The ground state of a superconductor, formed from a linear combination of normal state configurations in which electrons are virtually excited in pairs of opposite spin and momentum, is lower in energy than the normal state by amount proportional to an average $(\hbar\omega)^2$, consistent with the isotope effect. A mutually orthogonal set of excited states in

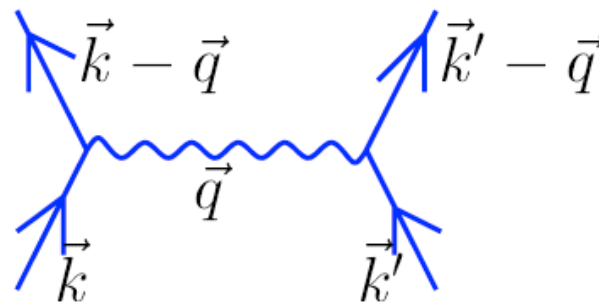
one-to-one correspondence with those of the normal phase is obtained by specifying occupation of certain Bloch states and by using the rest to form a linear combination of virtual pair configurations. The theory yields a second-order phase transition and a Meissner effect in the form suggested by Pippard. Calculated values of specific heats and penetration depths and their temperature variation are in good agreement with experiment. There is an energy gap for individual-particle excitations which decreases from about $3.5kT_c$ at $T=0^\circ\text{K}$ to zero at T_c . Tables of matrix elements of single-particle operators between the excited-state superconducting wave functions, useful for perturbation expansions and calculations of transition probabilities, are given.

Cooper instability

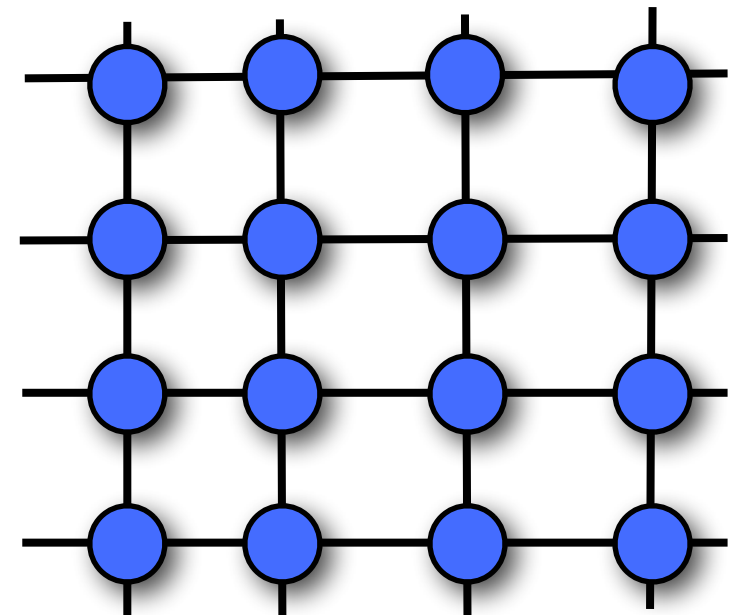
$$\tilde{H}_F = \sum_{k\sigma} \epsilon_k c_{k\sigma}^\dagger c_{k\sigma} + \frac{1}{2} \sum_{\substack{kk'qG \\ \sigma\sigma'}} V_{ph} c_{k+q+G\sigma}^\dagger c_{k'-q-G\sigma'}^\dagger c_{k'\sigma'} c_{k\sigma}$$

$$V_{ph} = \sum_{\lambda} \frac{\hbar\omega_{q\lambda} |g(q+G; \lambda)|^2}{[\epsilon_k - \epsilon_{k+q+G}]^2 - [\hbar\omega_{q\lambda}]^2}$$

if < 0 attraction !!



BCS ansatz



Theory of Superconductivity*

J. BARDEEN, L. N. COOPER,† AND J. R. SCHRIEFFER‡
 Department of Physics, University of Illinois, Urbana, Illinois

(Received July 8, 1957)

A theory of superconductivity is presented, based on the fact that the interaction between electrons resulting from virtual exchange of phonons is attractive when the energy difference between the electrons states involved is less than the phonon energy, $\hbar\omega$. It is favorable to form a superconducting phase when this attractive interaction dominates the repulsive screened Coulomb interaction. The normal phase is described by the Bloch individual-particle model. The ground state of a superconductor, formed from a linear combination of normal state configurations in which electrons are virtually excited in pairs of opposite spin and momentum, is lower in energy than the normal state by amount proportional to an average $(\hbar\omega)^2$, consistent with the isotope effect. A mutually orthogonal set of excited states in

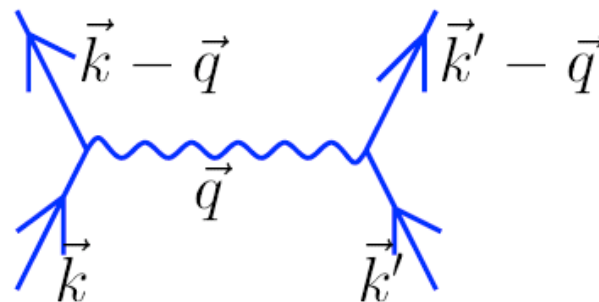
one-to-one correspondence with those of the normal phase is obtained by specifying occupation of certain Bloch states and by using the rest to form a linear combination of virtual pair configurations. The theory yields a second-order phase transition and a Meissner effect in the form suggested by Pippard. Calculated values of specific heats and penetration depths and their temperature variation are in good agreement with experiment. There is an energy gap for individual-particle excitations which decreases from about $3.5kT_c$ at $T=0^\circ\text{K}$ to zero at T_c . Tables of matrix elements of single-particle operators between the excited-state superconducting wave functions, useful for perturbation expansions and calculations of transition probabilities, are given.

Cooper instability

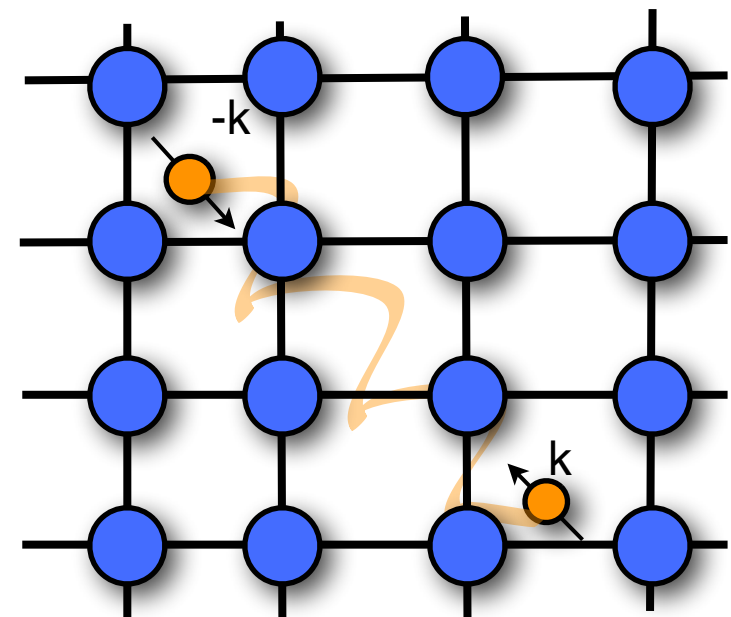
$$\tilde{H}_F = \sum_{k\sigma} \epsilon_k c_{k\sigma}^\dagger c_{k\sigma} + \frac{1}{2} \sum_{\substack{kk'qG \\ \sigma\sigma'}} V_{ph} c_{k+q+G\sigma}^\dagger c_{k'-q-G\sigma'}^\dagger c_{k'\sigma'} c_{k\sigma}$$

$$V_{ph} = \sum_{\lambda} \frac{\hbar\omega_{q\lambda} |g(q+G; \lambda)|^2}{[\epsilon_k - \epsilon_{k+q+G}]^2 - [\hbar\omega_{q\lambda}]^2}$$

if < 0 attraction !!



BCS ansatz



Theory of Superconductivity*

J. BARDEEN, L. N. COOPER,† AND J. R. SCHRIEFFER‡
Department of Physics, University of Illinois, Urbana, Illinois

(Received July 8, 1957)

A theory of superconductivity is presented, based on the fact that the interaction between electrons resulting from virtual exchange of phonons is attractive when the energy difference between the electrons states involved is less than the phonon energy, $\hbar\omega$. It is favorable to form a superconducting phase when this attractive interaction dominates the repulsive screened Coulomb interaction. The normal phase is described by the Bloch individual-particle model. The ground state of a superconductor, formed from a linear combination of normal state configurations in which electrons are virtually excited in pairs of opposite spin and momentum, is lower in energy than the normal state by amount proportional to an average $(\hbar\omega)^2$, consistent with the isotope effect. A mutually orthogonal set of excited states in

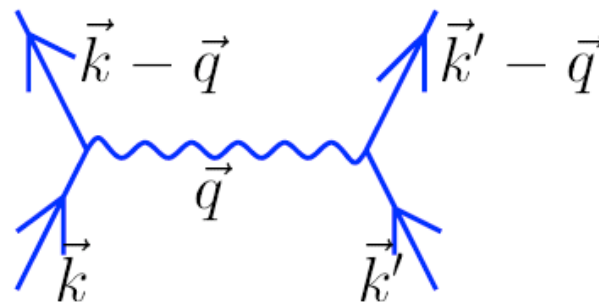
one-to-one correspondence with those of the normal phase is obtained by specifying occupation of certain Bloch states and by using the rest to form a linear combination of virtual pair configurations. The theory yields a second-order phase transition and a Meissner effect in the form suggested by Pippard. Calculated values of specific heats and penetration depths and their temperature variation are in good agreement with experiment. There is an energy gap for individual-particle excitations which decreases from about $3.5kT_c$ at $T=0^\circ\text{K}$ to zero at T_c . Tables of matrix elements of single-particle operators between the excited-state superconducting wave functions, useful for perturbation expansions and calculations of transition probabilities, are given.

Cooper instability

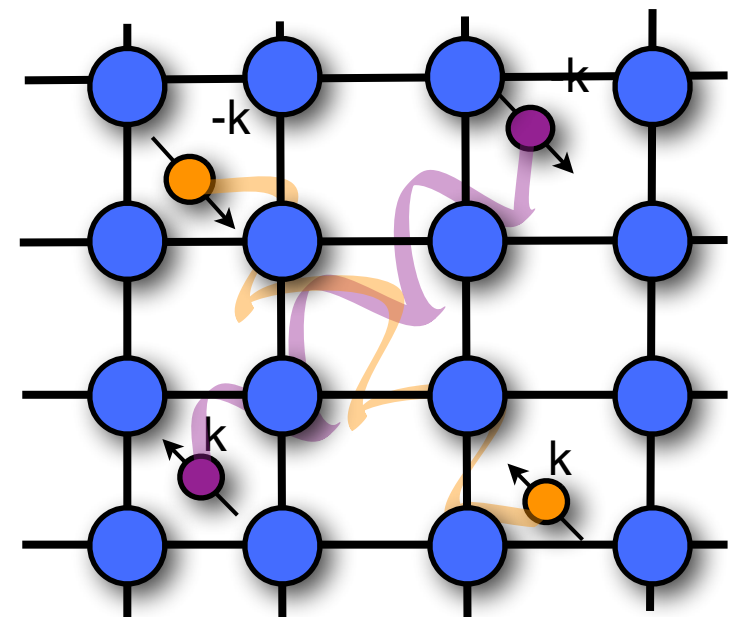
$$\tilde{H}_F = \sum_{k\sigma} \epsilon_k c_{k\sigma}^\dagger c_{k\sigma} + \frac{1}{2} \sum_{\substack{kk'qG \\ \sigma\sigma'}} V_{ph} c_{k+q+G\sigma}^\dagger c_{k'-q-G\sigma'}^\dagger c_{k'\sigma'} c_{k\sigma}$$

$$V_{ph} = \sum_{\lambda} \frac{\hbar\omega_{q\lambda} |g(q+G; \lambda)|^2}{[\epsilon_k - \epsilon_{k+q+G}]^2 - [\hbar\omega_{q\lambda}]^2}$$

if < 0 attraction !!



BCS ansatz



Theory of Superconductivity*

J. BARDEEN, L. N. COOPER,† AND J. R. SCHRIEFFER‡
 Department of Physics, University of Illinois, Urbana, Illinois

(Received July 8, 1957)

A theory of superconductivity is presented, based on the fact that the interaction between electrons resulting from virtual exchange of phonons is attractive when the energy difference between the electrons states involved is less than the phonon energy, $\hbar\omega$. It is favorable to form a superconducting phase when this attractive interaction dominates the repulsive screened Coulomb interaction. The normal phase is described by the Bloch individual-particle model. The ground state of a superconductor, formed from a linear combination of normal state configurations in which electrons are virtually excited in pairs of opposite spin and momentum, is lower in energy than the normal state by amount proportional to an average $(\hbar\omega)^2$, consistent with the isotope effect. A mutually orthogonal set of excited states in

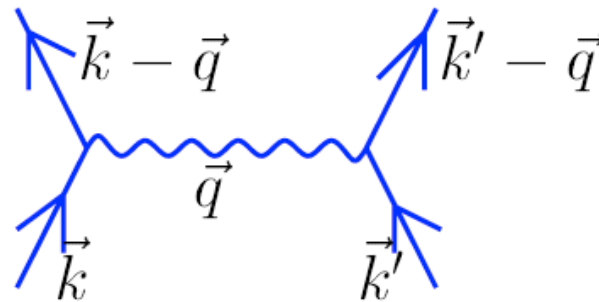
one-to-one correspondence with those of the normal phase is obtained by specifying occupation of certain Bloch states and by using the rest to form a linear combination of virtual pair configurations. The theory yields a second-order phase transition and a Meissner effect in the form suggested by Pippard. Calculated values of specific heats and penetration depths and their temperature variation are in good agreement with experiment. There is an energy gap for individual-particle excitations which decreases from about $3.5kT_c$ at $T=0^\circ\text{K}$ to zero at T_c . Tables of matrix elements of single-particle operators between the excited-state superconducting wave functions, useful for perturbation expansions and calculations of transition probabilities, are given.

Cooper instability

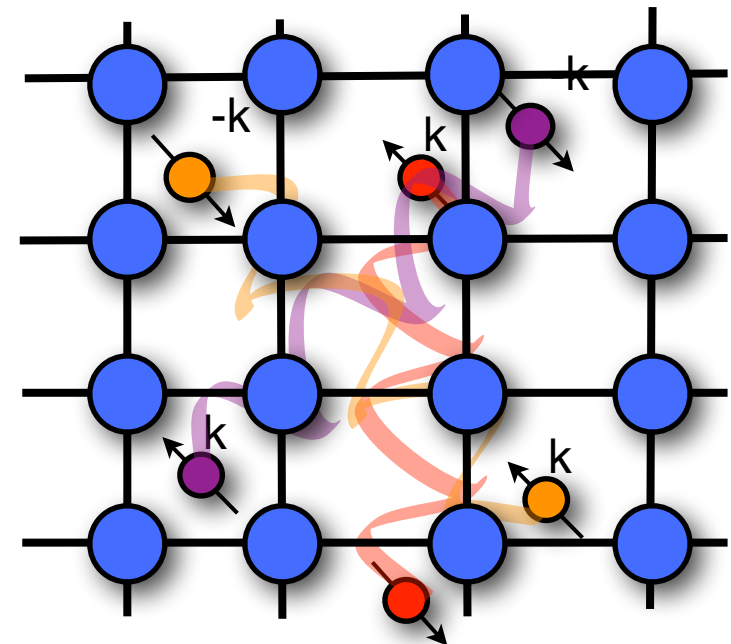
$$\tilde{H}_F = \sum_{k\sigma} \epsilon_k c_{k\sigma}^\dagger c_{k\sigma} + \frac{1}{2} \sum_{\substack{kk'qG \\ \sigma\sigma'}} V_{ph} c_{k+q+G\sigma}^\dagger c_{k'-q-G\sigma'}^\dagger c_{k'\sigma'} c_{k\sigma}$$

$$V_{ph} = \sum_{\lambda} \frac{\hbar\omega_{q\lambda} |g(q+G; \lambda)|^2}{[\epsilon_k - \epsilon_{k+q+G}]^2 - [\hbar\omega_{q\lambda}]^2}$$

if < 0 attraction !!



BCS ansatz



Theory of Superconductivity*

J. BARDEEN, L. N. COOPER,† AND J. R. SCHRIEFFER‡
Department of Physics, University of Illinois, Urbana, Illinois

(Received July 8, 1957)

A theory of superconductivity is presented, based on the fact that the interaction between electrons resulting from virtual exchange of phonons is attractive when the energy difference between the electrons states involved is less than the phonon energy, $\hbar\omega$. It is favorable to form a superconducting phase when this attractive interaction dominates the repulsive screened Coulomb interaction. The normal phase is described by the Bloch individual-particle model. The ground state of a superconductor, formed from a linear combination of normal state configurations in which electrons are virtually excited in pairs of opposite spin and momentum, is lower in energy than the normal state by amount proportional to an average $(\hbar\omega)^2$, consistent with the isotope effect. A mutually orthogonal set of excited states in

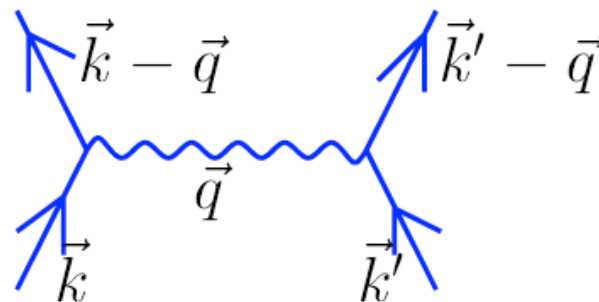
one-to-one correspondence with those of the normal phase is obtained by specifying occupation of certain Bloch states and by using the rest to form a linear combination of virtual pair configurations. The theory yields a second-order phase transition and a Meissner effect in the form suggested by Pippard. Calculated values of specific heats and penetration depths and their temperature variation are in good agreement with experiment. There is an energy gap for individual-particle excitations which decreases from about $3.5kT_c$ at $T=0^\circ\text{K}$ to zero at T_c . Tables of matrix elements of single-particle operators between the excited-state superconducting wave functions, useful for perturbation expansions and calculations of transition probabilities, are given.

Cooper instability

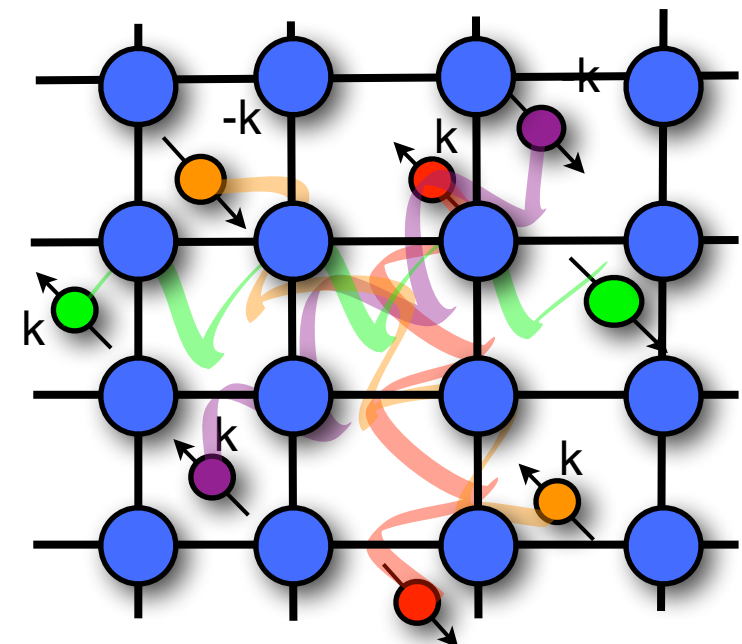
$$\tilde{H}_F = \sum_{k\sigma} \epsilon_k c_{k\sigma}^\dagger c_{k\sigma} + \frac{1}{2} \sum_{\substack{kk'qG \\ \sigma\sigma'}} V_{ph} c_{k+q+G\sigma}^\dagger c_{k'-q-G\sigma'}^\dagger c_{k'\sigma'} c_{k\sigma}$$

$$V_{ph} = \sum_{\lambda} \frac{\hbar\omega_{q\lambda} |g(q+G; \lambda)|^2}{[\epsilon_k - \epsilon_{k+q+G}]^2 - [\hbar\omega_{q\lambda}]^2}$$

if < 0 attraction !!



BCS ansatz

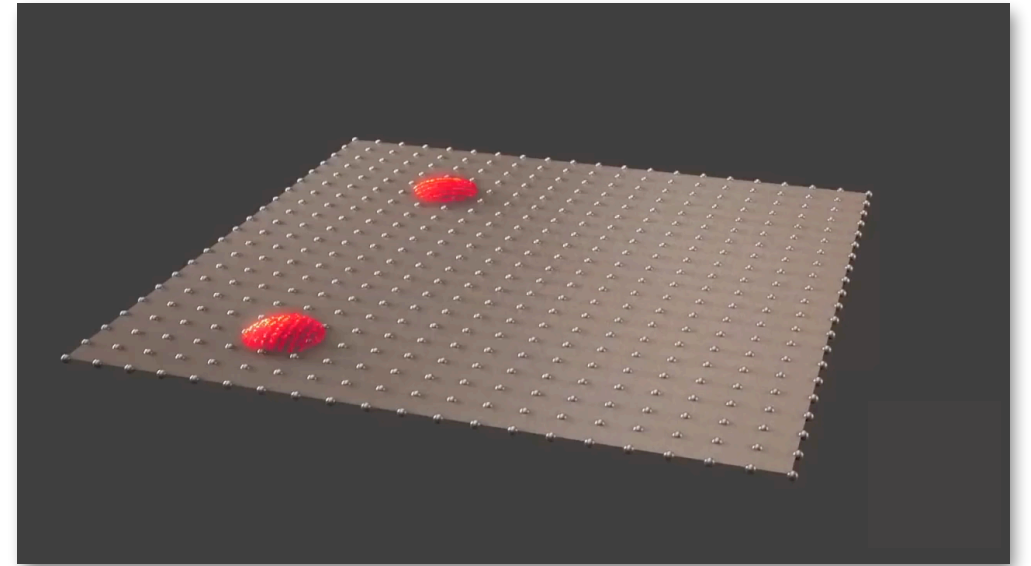


Coherent (macroscopic) state

$$\Psi_N(\mathbf{r}_1, \mathbf{r}_2, \dots, \mathbf{r}_N) = \mathcal{A} \psi(\mathbf{r}_1, \mathbf{r}_2) \psi(\mathbf{r}_3, \mathbf{r}_4) \cdots \psi(\mathbf{r}_{N-1}, \mathbf{r}_N) (1 \uparrow)(2 \downarrow)(3 \uparrow)(4 \downarrow) \cdots (N-1 \uparrow)(N \downarrow).$$

$$|\Psi_{BCS}\rangle = \text{const.} \prod_{\mathbf{k}} \exp(\alpha_{\mathbf{k}} \hat{P}_{\mathbf{k}}^+) |0\rangle$$

$$\Psi = \prod_{\mathbf{k}=\mathbf{k}_1, \dots, \mathbf{k}_{N/2}} \left(u_{\mathbf{k}} + v_{\mathbf{k}} a_{\mathbf{k}\uparrow}^\dagger a_{-\mathbf{k}\downarrow}^\dagger \right) |0\rangle$$

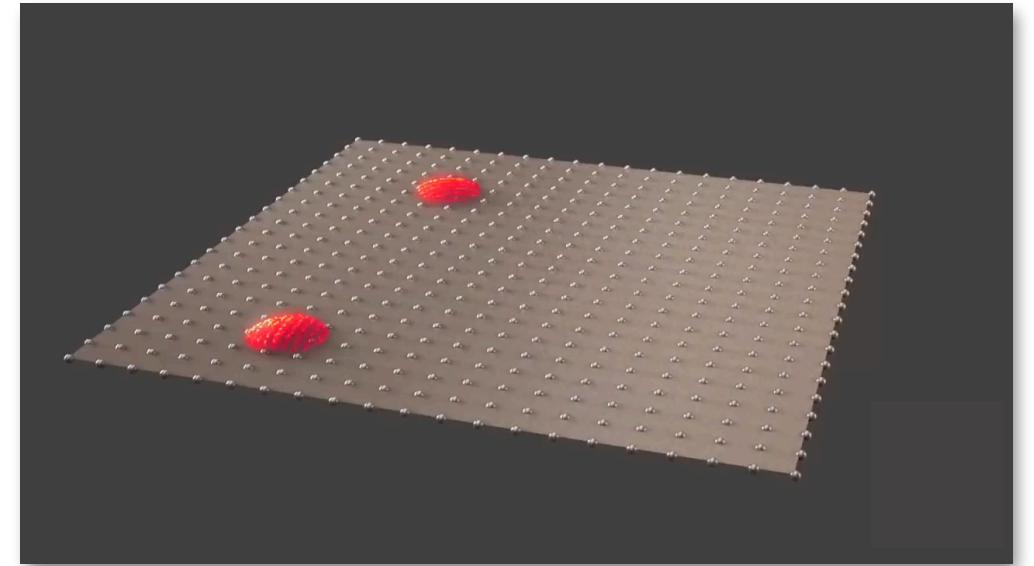


Coherent (macroscopic) state

$$\Psi_N(\mathbf{r}_1, \mathbf{r}_2, \dots, \mathbf{r}_N) = \mathcal{A} \psi(\mathbf{r}_1, \mathbf{r}_2) \psi(\mathbf{r}_3, \mathbf{r}_4) \cdots \psi(\mathbf{r}_{N-1}, \mathbf{r}_N) (1 \uparrow)(2 \downarrow)(3 \uparrow)(4 \downarrow) \cdots (N-1 \uparrow)(N \downarrow).$$

$$|\Psi_{BCS}\rangle = \text{const.} \prod_{\mathbf{k}} \exp(\alpha_{\mathbf{k}} \hat{P}_{\mathbf{k}}^+) |0\rangle$$

$$\Psi = \prod_{\mathbf{k}=\mathbf{k}_1, \dots, \mathbf{k}_{N/2}} \left(u_{\mathbf{k}} + v_{\mathbf{k}} a_{\mathbf{k}\uparrow}^\dagger a_{-\mathbf{k}\downarrow}^\dagger \right) |0\rangle$$



BCS predictions

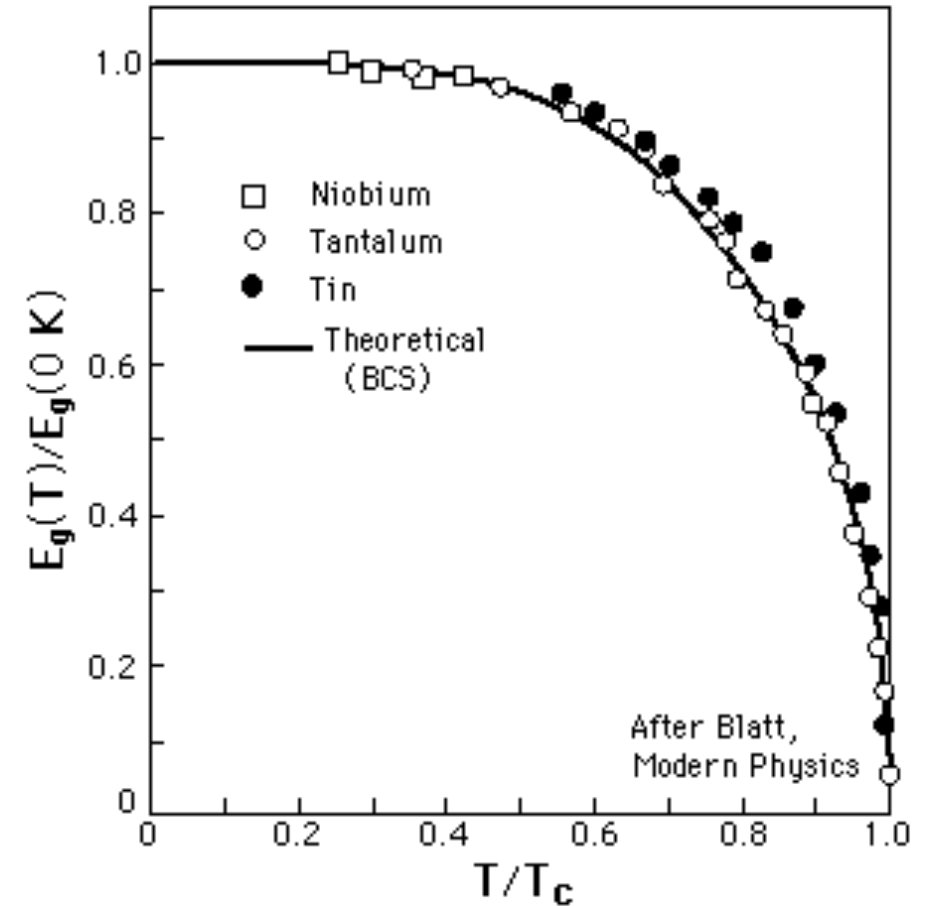
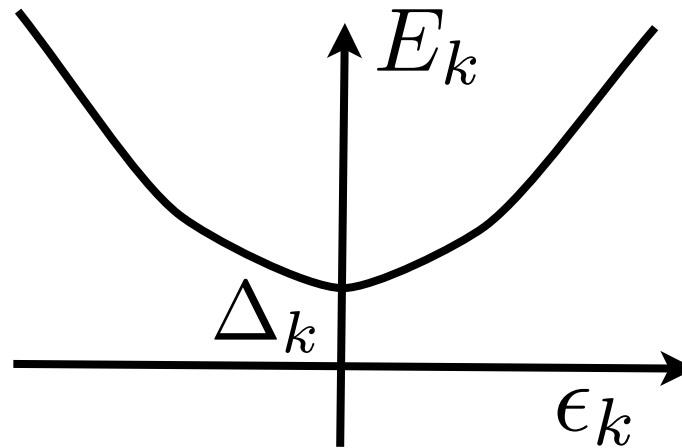
The BCS ground state has a lower energy Δ wrt the free-electron state, which depends on the temperature

$$E_k = \sqrt{\epsilon_k^2 + |\Delta_k|^2}$$

$$\frac{\Delta(T)}{\Delta(0)} = 1.74 \left(1 - \frac{T}{T_c}\right)^{\frac{1}{2}}$$

$$T_c^{BCS} = \omega_D e^{-\frac{1}{\lambda}}$$

$$\lambda = N(0) V_{ph}$$



BCS predictions

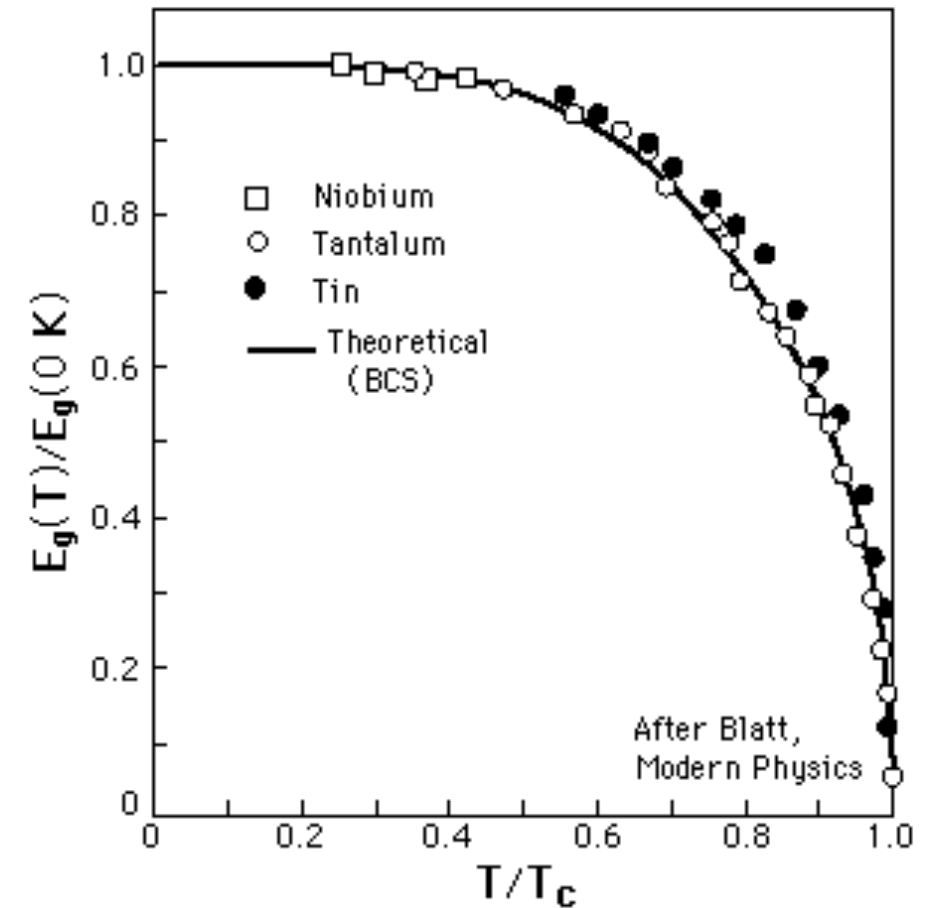
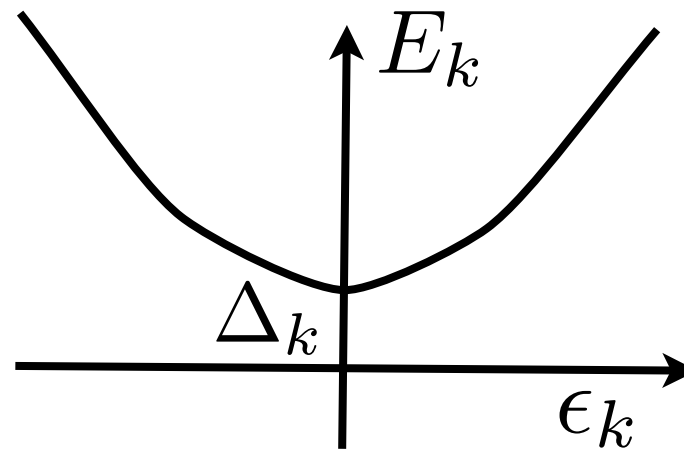
The BCS ground state has a lower energy Δ wrt the free-electron state, which depends on the temperature

$$E_k = \sqrt{\epsilon_k^2 + |\Delta_k|^2}$$

$$\frac{\Delta(T)}{\Delta(0)} = 1.74 \left(1 - \frac{T}{T_c}\right)^{\frac{1}{2}}$$

$$T_c^{BCS} = \omega_D e^{-\frac{1}{\lambda}}$$

$$\lambda = N(0) V_{ph}$$



Pros

The first microscopic theory of SC

Explains many experimental evidences

The T_c formula is simple

Cons

The T_c formula is wrong

No Coulomb interaction

No retardation effects

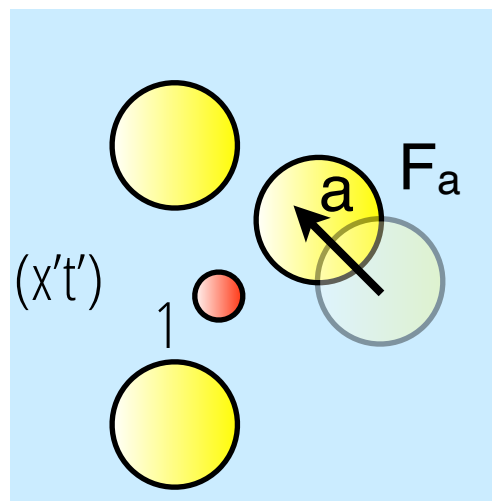
The Migdal - Eliashberg theory ('58-'60)

The electron-electron interaction mediated by phonons is time-dependent



The Migdal - Eliashberg theory ('58-'60)

The electron-electron interaction mediated by phonons is time-dependent

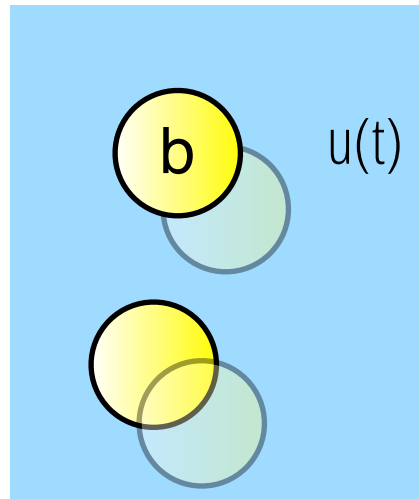
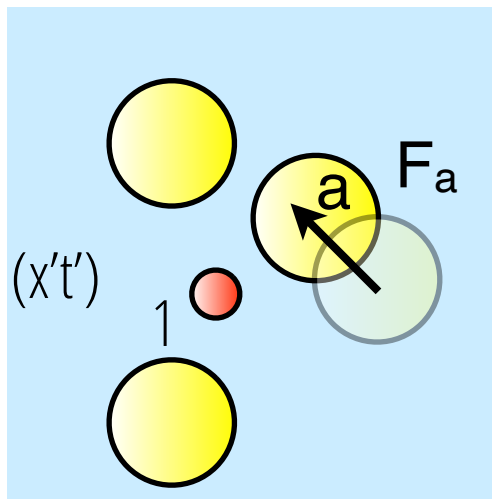


The electron 1 at $(x't')$
causes an impulsive
force F on a ion a
 $F_a = -\nabla V(x_1 - X_a)$

space-time

The Migdal - Eliashberg theory ('58-'60)

The electron-electron interaction mediated by phonons is time-dependent



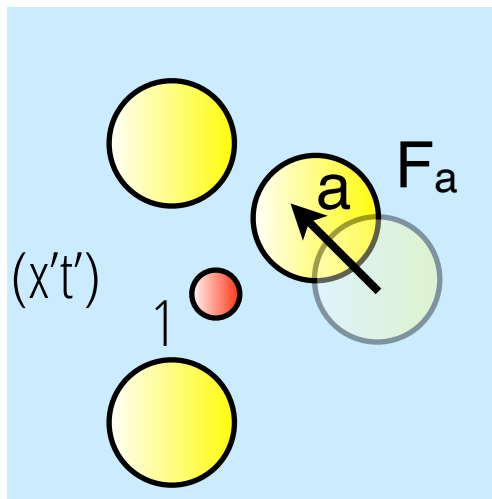
The electron 1 at (x', t')
causes an impulsive
force F on a ion a
 $F_a = - \nabla V(x_1 - X_a)$

The displacement
propagates in time (t) and
space (on ion b)
 $u_b(t) = D(a, b; t - t') F_a(t)$

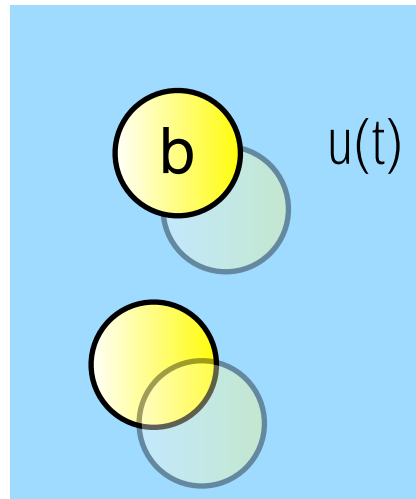
space-time

The Migdal - Eliashberg theory ('58-'60)

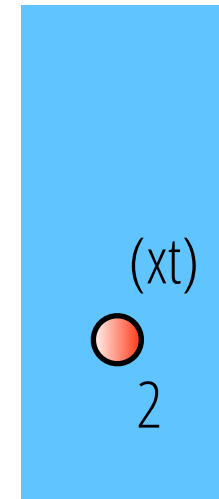
The electron-electron interaction mediated by phonons is time-dependent



The electron 1 at $(x't')$
causes an impulsive
force F on a ion a
 $F_a = - \nabla V(x_1 - X_a)$



The displacement
propagates in time (t) and
space (on ion b)
 $u_b(t) = D(a, b; t-t') F_a(t)$

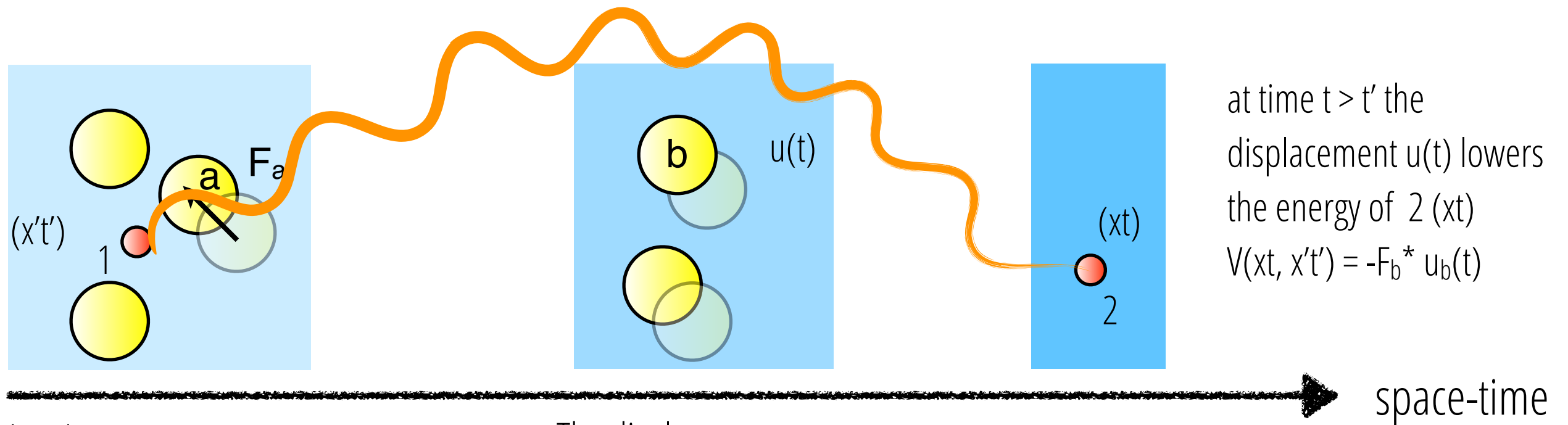


at time $t > t'$ the
displacement $u(t)$ lowers
the energy of 2 (x, t)
 $V(x, t, x't') = -F_b^* u_b(t)$

space-time

The Migdal - Eliashberg theory ('58-'60)

The electron-electron interaction mediated by phonons is time-dependent



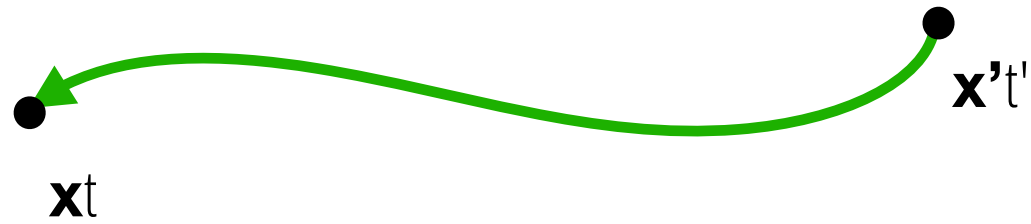
The electron 1 at (x', t') causes an impulsive force F on a ion a
 $F_a = -\nabla V(x_1 - X_a)$

The displacement propagates in time (t) and space (on ion b)
 $u_b(t) = D(a, b; t - t') F_a(t)$

....with Green-functions

$$G(\mathbf{x}t, \mathbf{x}'t') = -\frac{i}{\hbar} \langle N | \hat{T} \hat{\psi}(\mathbf{x}t) \hat{\psi}^\dagger(\mathbf{x}'t') | N \rangle \quad \text{Electrons}$$

$$\mathbf{D}_{\kappa\kappa'}(tt') = -\frac{i}{\hbar} \langle \hat{T} \Delta \hat{\tau}_\kappa(t) \Delta \hat{\tau}_{\kappa'}^T(t') \rangle \quad \text{Phonons}$$



....with Green-functions

$$G(\mathbf{x}t, \mathbf{x}'t') = -\frac{i}{\hbar} \langle N | \hat{T} \hat{\psi}(\mathbf{x}t) \hat{\psi}^\dagger(\mathbf{x}'t') | N \rangle$$

Electrons

$$\mathbf{D}_{\kappa\kappa'}(tt') = -\frac{i}{\hbar} \langle \hat{T} \Delta \hat{\tau}_\kappa(t) \Delta \hat{\tau}_{\kappa'}^T(t') \rangle$$

Phonons

Dyson equation

$$G^{-1}(\omega, k) = G_0^{-1}(\omega, k) - \Sigma(\omega, k)$$

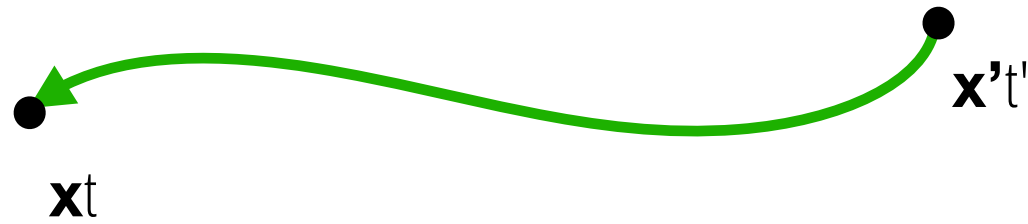
$$D^{-1}(\omega, Q) = D_0^{-1}(\omega, Q) - \Pi(\omega, Q)$$



....with Green-functions

$$G(\mathbf{x}t, \mathbf{x}'t') = -\frac{i}{\hbar} \langle N | \hat{T} \hat{\psi}(\mathbf{x}t) \hat{\psi}^\dagger(\mathbf{x}'t') | N \rangle$$

$$\mathbf{D}_{\kappa\kappa'}(tt') = -\frac{i}{\hbar} \langle \hat{T} \Delta \hat{\tau}_\kappa(t) \Delta \hat{\tau}_{\kappa'}^T(t') \rangle$$



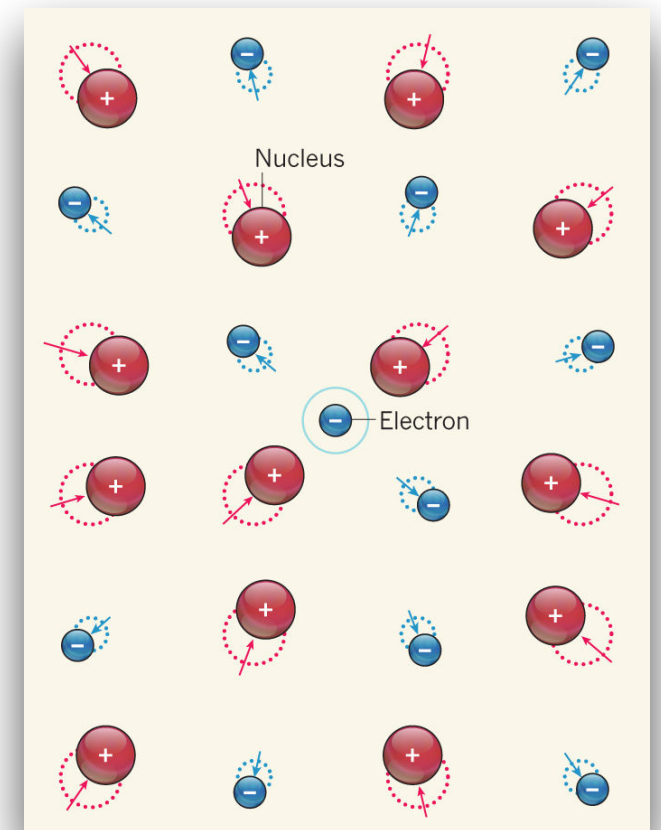
Electrons

$$G^{-1}(\omega, k) = G_0^{-1}(\omega, k) - \Sigma(\omega, k)$$

Phonons

$$D^{-1}(\omega, Q) = D_0^{-1}(\omega, Q) - \Pi(\omega, Q)$$

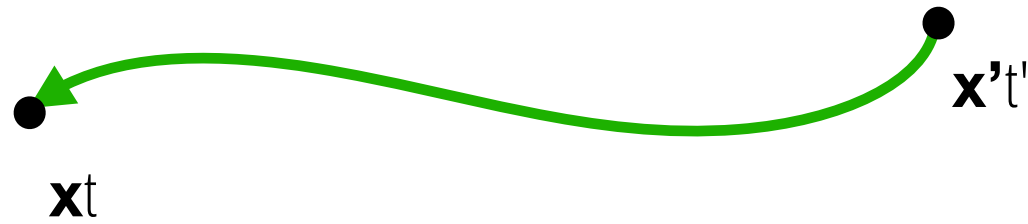
Dyson equation



....with Green-functions

$$G(\mathbf{x}t, \mathbf{x}'t') = -\frac{i}{\hbar} \langle N | \hat{T} \hat{\psi}(\mathbf{x}t) \hat{\psi}^\dagger(\mathbf{x}'t') | N \rangle$$

$$\mathbf{D}_{\kappa\kappa'}(tt') = -\frac{i}{\hbar} \langle \hat{T} \Delta \hat{\tau}_\kappa(t) \Delta \hat{\tau}_{\kappa'}^T(t') \rangle$$



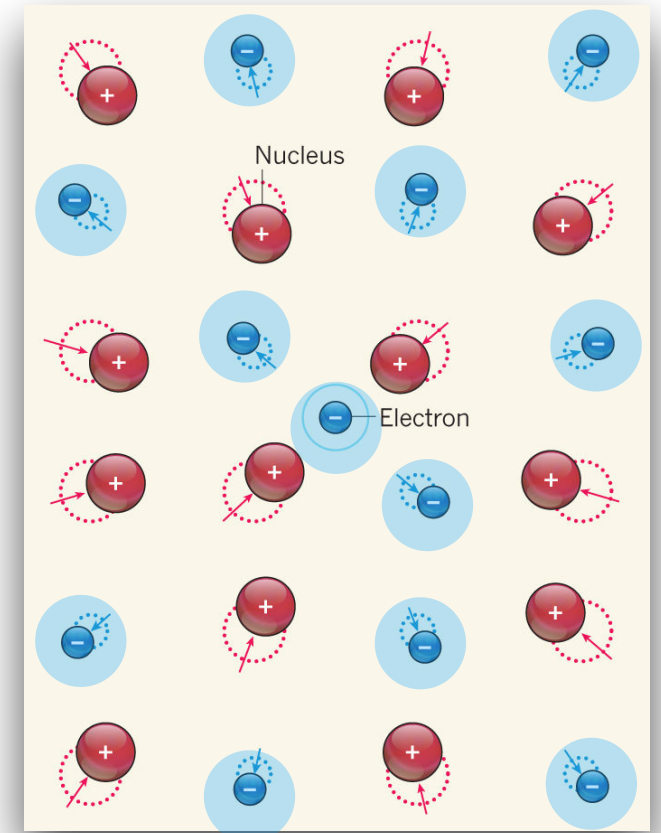
Electrons

$$G^{-1}(\omega, k) = G_0^{-1}(\omega, k) - \Sigma(\omega, k)$$

Phonons

$$D^{-1}(\omega, Q) = D_0^{-1}(\omega, Q) - \Pi(\omega, Q)$$

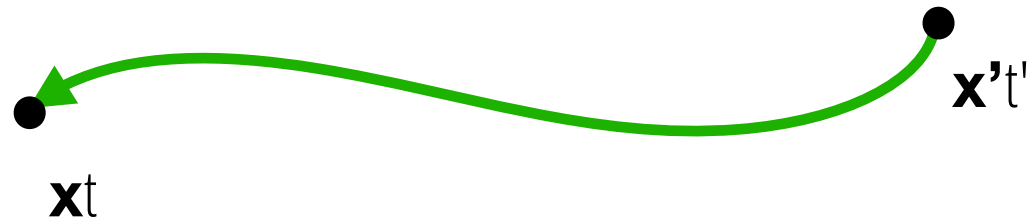
Dyson equation



....with Green-functions

$$G(\mathbf{x}t, \mathbf{x}'t') = -\frac{i}{\hbar} \langle N | \hat{T} \hat{\psi}(\mathbf{x}t) \hat{\psi}^\dagger(\mathbf{x}'t') | N \rangle$$

$$\mathbf{D}_{\kappa\kappa'}(tt') = -\frac{i}{\hbar} \langle \hat{T} \Delta \hat{\tau}_\kappa(t) \Delta \hat{\tau}_{\kappa'}^T(t') \rangle$$



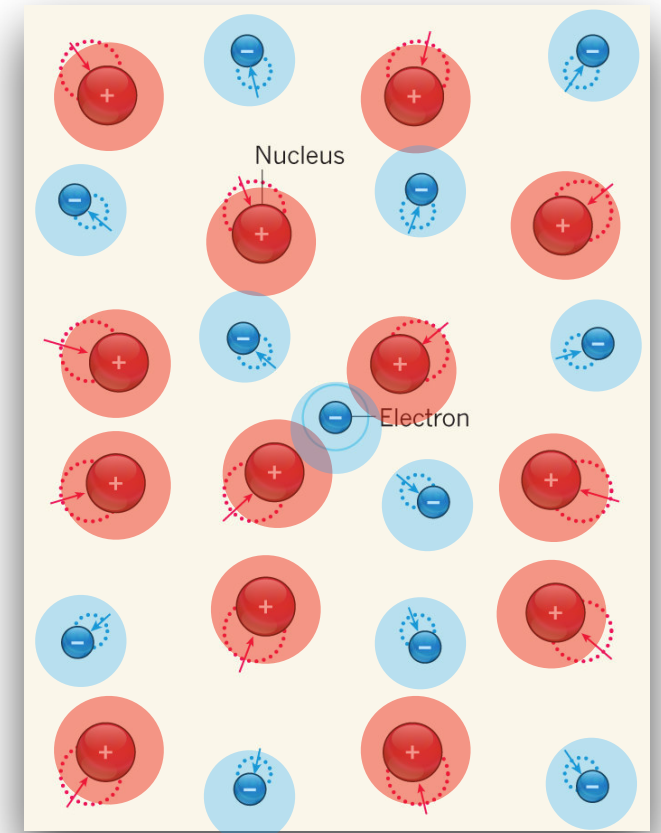
Electrons

$$G^{-1}(\omega, k) = G_0^{-1}(\omega, k) - \Sigma(\omega, k)$$

Phonons

$$D^{-1}(\omega, Q) = D_0^{-1}(\omega, Q) - \Pi(\omega, Q)$$

Dyson equation



....with Green-functions

$$G(\mathbf{x}t, \mathbf{x}'t') = -\frac{i}{\hbar} \langle N | \hat{T} \hat{\psi}(\mathbf{x}t) \hat{\psi}^\dagger(\mathbf{x}'t') | N \rangle$$

Electrons

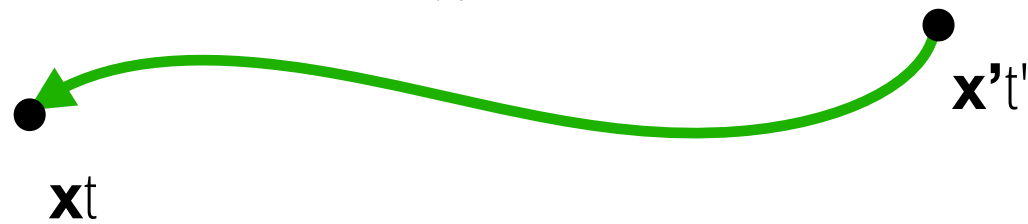
$$\mathbf{D}_{\kappa\kappa'}(tt') = -\frac{i}{\hbar} \langle \hat{T} \Delta \hat{\tau}_\kappa(t) \Delta \hat{\tau}_{\kappa'}^T(t') \rangle$$

Phonons

Dyson equation

$$G^{-1}(\omega, k) = G_0^{-1}(\omega, k) - \Sigma(\omega, k)$$

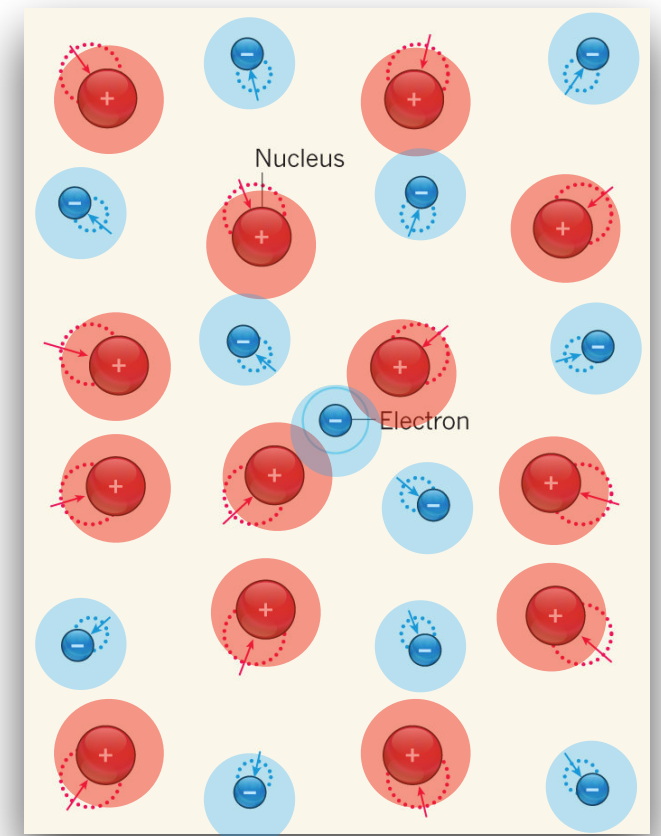
$$D^{-1}(\omega, Q) = D_0^{-1}(\omega, Q) - \Pi(\omega, Q)$$



The pairing is included considering the field operator in the Nambu notation

$$\psi_k = \begin{pmatrix} c_{k\uparrow} \\ c_{-k\downarrow}^\dagger \end{pmatrix}$$

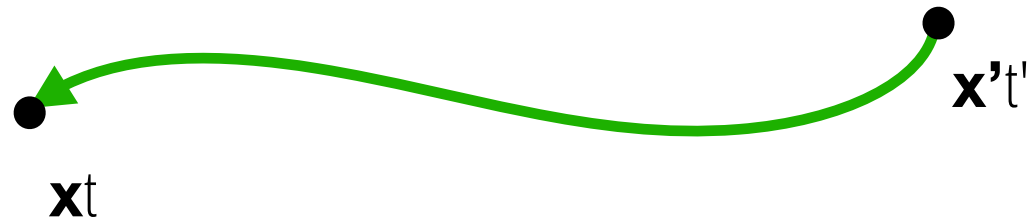
$$\psi_k^\dagger = (c_{k\uparrow}^\dagger, c_{-k\downarrow})$$



....with Green-functions

$$G(\mathbf{x}t, \mathbf{x}'t') = -\frac{i}{\hbar} \langle N | \hat{T} \hat{\psi}(\mathbf{x}t) \hat{\psi}^\dagger(\mathbf{x}'t') | N \rangle$$

$$\mathbf{D}_{\kappa\kappa'}(tt') = -\frac{i}{\hbar} \langle \hat{T} \Delta \hat{\tau}_\kappa(t) \Delta \hat{\tau}_{\kappa'}^T(t') \rangle$$



The pairing is included considering the field operator in the Nambu notation

$$\psi_k = \begin{pmatrix} c_{k\uparrow} \\ c_{-k\downarrow}^\dagger \end{pmatrix}$$

$$\psi_k^\dagger = (c_{k\uparrow}^\dagger, c_{-k\downarrow})$$

$$G(k, \tau) = - \langle T \psi_k(\tau) \psi_k^\dagger(0) \rangle = - \begin{pmatrix} \langle c_{k\uparrow}(\tau) c_{k\uparrow}^\dagger(0) \rangle & \langle c_{k\uparrow}(\tau) c_{-k\downarrow}(0) \rangle \\ \langle c_{-k\downarrow}^\dagger(\tau) c_{k\uparrow}^\dagger(0) \rangle & \langle c_{-k\downarrow}^\dagger(\tau) c_{-k\downarrow}(0) \rangle \end{pmatrix}$$

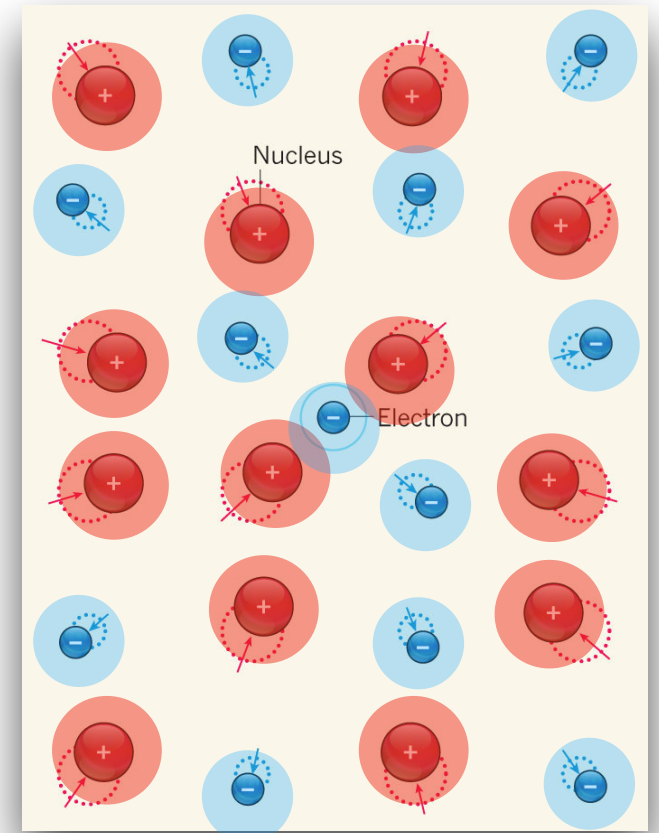
Dyson equation

Electrons

$$G^{-1}(\omega, k) = G_0^{-1}(\omega, k) - \Sigma(\omega, k)$$

Phonons

$$D^{-1}(\omega, Q) = D_0^{-1}(\omega, Q) - \Pi(\omega, Q)$$



Which is the best superconductor?

Which is the best superconductor?

Neil's (Ashcroft) answer

Which is the best superconductor?

Neil's (Ashcroft) answer

VOLUME 21, NUMBER 26

PHYSICAL REVIEW LETTERS

23 DECEMBER 1968

METALLIC HYDROGEN: A HIGH-TEMPERATURE SUPERCONDUCTOR?

N. W. Ashcroft

Laboratory of Atomic and Solid State Physics, Cornell University, Ithaca, New York 14850

(Received 3 May 1968)

Application of the BCS theory to the proposed metallic modification of hydrogen suggests that it will be a high-temperature superconductor. This prediction has interesting astrophysical consequences, as well as implications for the possible development of a superconductor for use at elevated temperatures.

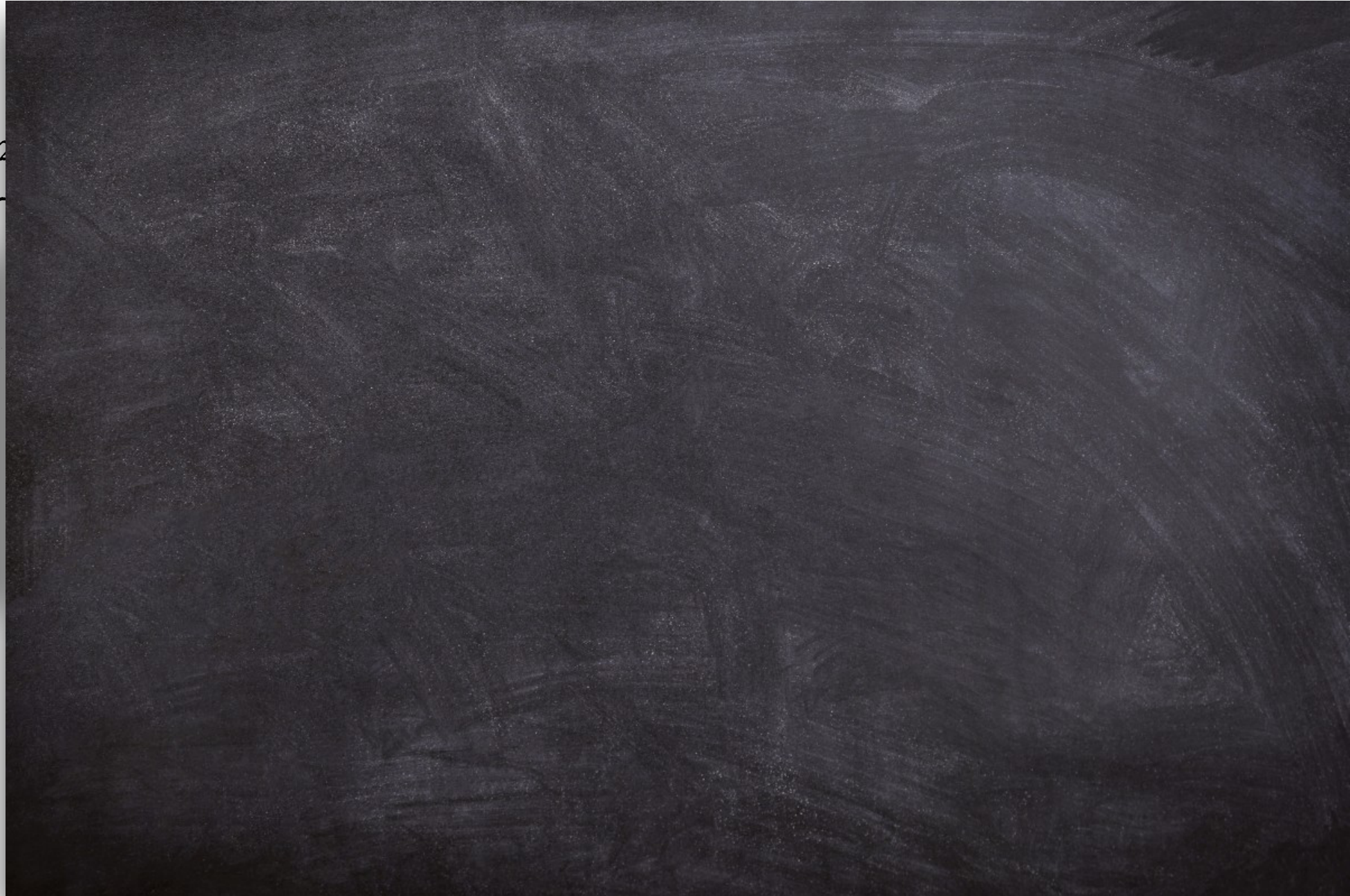


Which is the best superconductor?

Neil's (Ashcroft) answer

VOLUME 2

BER 1968



Which is the best superconductor?

Neil's (Ashcroft) answer

$$T_c = \omega e^{-1/\lambda}$$

VOLUME 2

BER 1968



Which is the best superconductor?

Neil's (Ashcroft) answer

$$T_c = \omega e^{-1/\lambda}$$



$-\omega = \text{sqrt}(K/M)$: low mass, ω large

VOLUME 2

BER 1968



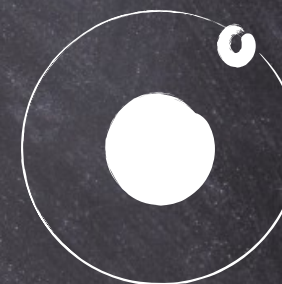
Which is the best superconductor?

Neil's (Ashcroft) answer

$$T_c = \omega e^{-1/\lambda}$$

- $\omega = \sqrt{K/M}$: low mass, ω large

-No screening: the electron-phonon coupling is high



VOLUME 2

BER 1968



Which is the best superconductor?

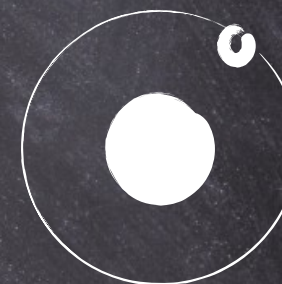
Neil's (Ashcroft) answer

$$T_c = \omega e^{-1/\lambda}$$



- $\omega = \sqrt{K/M}$: low mass, ω large

-No screening: the electron-phonon coupling is high



-High-pressure: $E_{kin} \gg E_{coul}$, metal

VOLUME 2

BER 1968



Which is the best superconductor?

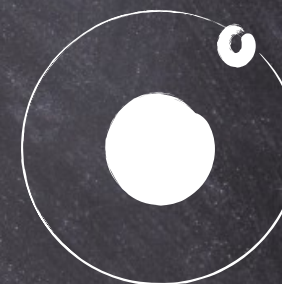
Neil's (Ashcroft) answer

$$T_c = \omega e^{-1/\lambda}$$



- $\omega = \sqrt{K/M}$: low mass, ω large

-No screening: the electron-phonon coupling is high



-High-pressure: $E_{kin} \gg E_{coul}$, metal

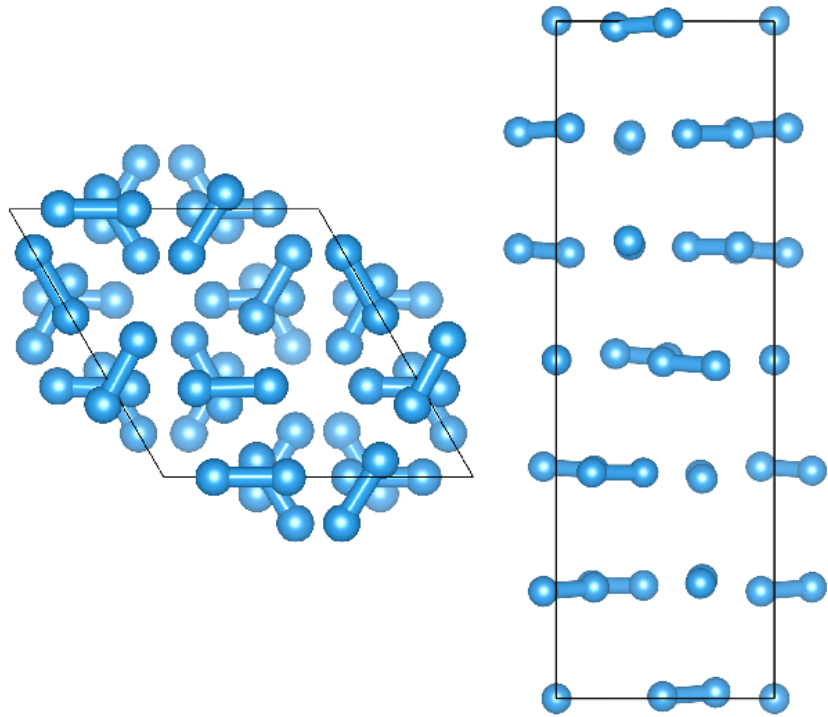
Hydrogen under high pressure is a
(high-T) superconductor

VOLUME 2

BER 1968



**But hydrogen is (always) an insulator
where is the metal?**



ON SUPERCONDUCTIVITY AND SUPERFLUIDITY

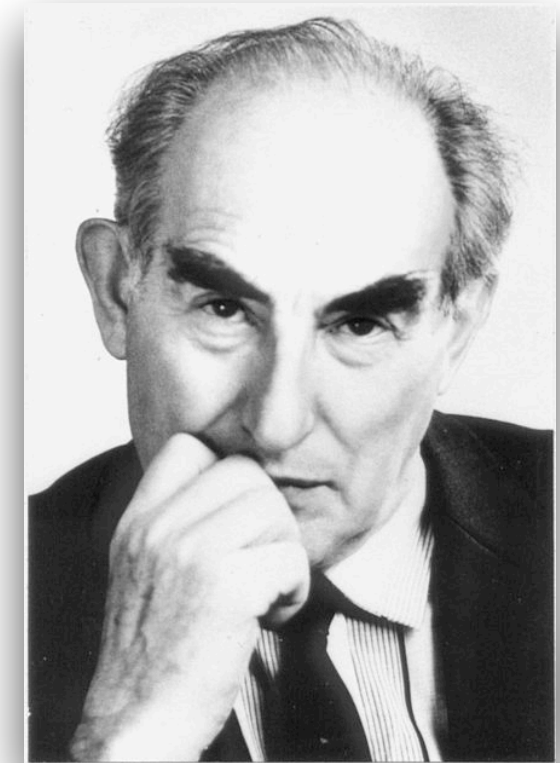
Nobel Lecture, December 8, 2003

by

VITALY L. GINZBURG

P. N. Lebedev Physics Institute, Russian Academy of Sciences, Moscow, Russia.

1. Controlled nuclear fusion.
2. High-temperature and room-temperature superconductivity (HTSC and RTSC).
3. Metallic hydrogen. Other exotic substances.
4. Two-dimensional electron liquid (anomalous Hall effect and other effects).
5. Some questions of solid-state physics (heterostructures in semiconductors, quantum wells and dots, metal – dielectric transitions, charge and spin density waves, mesoscopics).
- ...
7. Surface physics. Clusters.
8. Liquid crystals. Ferroelectrics. Ferrotoroids.
9. Fullerenes. Nanotubes.
10. The behavior of matter in superstrong magnetic fields.
11. Nonlinear physics. Turbulence. Solitons. Chaos. Strange attractors.
12. X-ray lasers, gamma-ray lasers, superhigh-power lasers.
13. Superheavy elements. Exotic nuclei.
-
22. Gravitational waves and their detection.
-
- 27 The problem of dark matter (hidden mass) and its detection.



2003



“pioneering contributions to the theory of superconductors and superfluids”

ON SUPERCONDUCTIVITY AND SUPERFLUIDITY

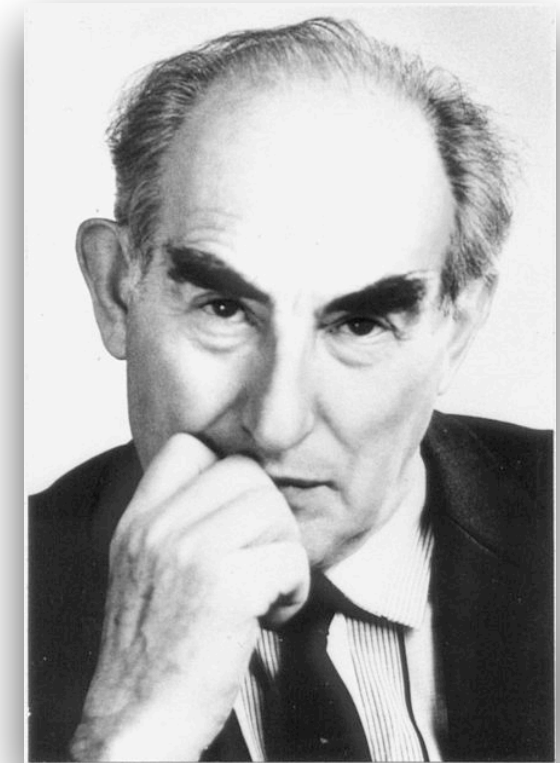
Nobel Lecture, December 8, 2003

by

VITALY L. GINZBURG

P. N. Lebedev Physics Institute, Russian Academy of Sciences, Moscow, Russia.

1. Controlled nuclear fusion.
2. High-temperature and room-temperature superconductivity (HTSC and RTSC).
3. Metallic hydrogen. Other exotic substances.
- ✓ 4. Two-dimensional electron liquid (anomalous Hall effect and other effects).
- ✓ 5. Some questions of solid-state physics (heterostructures in semiconductors, quantum wells and dots, metal – dielectric transitions, charge and spin density waves, mesoscopics).
- ...
- ✓ 7. Surface physics. Clusters.
- ✓ 8. Liquid crystals. Ferroelectrics. Ferrotoroids.
- ✓ 9. Fullerenes. Nanotubes.
- ✓ 10. The behavior of matter in superstrong magnetic fields.
- ✓ 11. Nonlinear physics. Turbulence. Solitons. Chaos. Strange attractors.
- ✓ 12. X-ray lasers, gamma-ray lasers, superhigh-power lasers.
- ✓ 13. Superheavy elements. Exotic nuclei.
-
- ✓ 22. Gravitational waves and their detection.
-
- 27 The problem of dark matter (hidden mass) and its detection.



2003



“pioneering contributions to the theory of superconductors and superfluids”

ON SUPERCONDUCTIVITY AND SUPERFLUIDITY

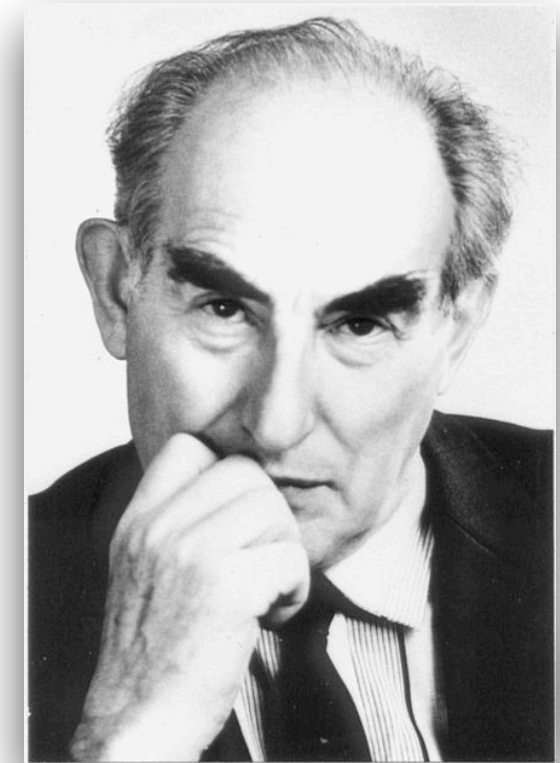
Nobel Lecture, December 8, 2003

by

VITALY L. GINZBURG

P. N. Lebedev Physics Institute, Russian Academy of Sciences, Moscow, Russia.

- ✗ 1. Controlled nuclear fusion.
- ✗ 2. High-temperature and room-temperature superconductivity (HTSC and RTSC).
- ✗ 3. Metallic hydrogen. Other exotic substances.
- ✓ 4. Two-dimensional electron liquid (anomalous Hall effect and other effects).
- ✓ 5. Some questions of solid-state physics (heterostructures in semiconductors, quantum wells and dots, metal – dielectric transitions, charge and spin density waves, mesoscopics).
- ...
- ✓ 7. Surface physics. Clusters.
- ✓ 8. Liquid crystals. Ferroelectrics. Ferrotoroids.
- ✓ 9. Fullerenes. Nanotubes.
- ✓ 10. The behavior of matter in superstrong magnetic fields.
- ✓ 11. Nonlinear physics. Turbulence. Solitons. Chaos. Strange attractors.
- ✓ 12. X-ray lasers, gamma-ray lasers, superhigh-power lasers.
- ✓ 13. Superheavy elements. Exotic nuclei.
-
- ✓ 22. Gravitational waves and their detection.
-
- ✗ 27 The problem of dark matter (hidden mass) and its detection.



2003



“pioneering contributions to the theory of superconductors and superfluids”

ON SUPERCONDUCTIVITY AND SUPERFLUIDITY

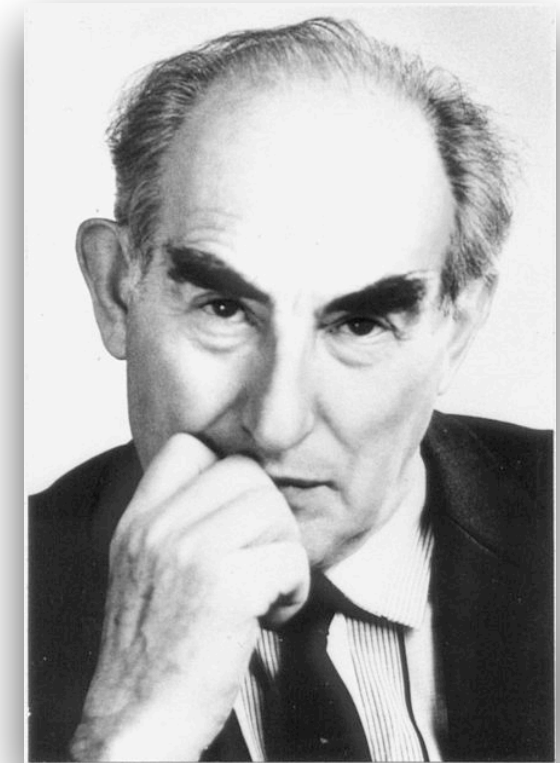
Nobel Lecture, December 8, 2003

by

VITALY L. GINZBURG

P. N. Lebedev Physics Institute, Russian Academy of Sciences, Moscow, Russia.

- ✗ 1. Controlled nuclear fusion.
- ✗ 2. High-temperature and room-temperature superconductivity (HTSC and RTSC).
- ✗ 3. Metallic hydrogen. Other exotic substances.
- ✓ 4. Two-dimensional electron liquid (anomalous Hall effect and other effects).
- ✓ 5. Some questions of solid-state physics (heterostructures in semiconductors, quantum wells and dots, metal – dielectric transitions, charge and spin density waves, mesoscopics).
- ...
- ✓ 7. Surface physics. Clusters.
- ✓ 8. Liquid crystals. Ferroelectrics. Ferrotoroids.
- ✓ 9. Fullerenes. Nanotubes.
- ✓ 10. The behavior of matter in superstrong magnetic fields.
- ✓ 11. Nonlinear physics. Turbulence. Solitons. Chaos. Strange attractors.
- ✓ 12. X-ray lasers, gamma-ray lasers, superhigh-power lasers.
- ✓ 13. Superheavy elements. Exotic nuclei.
-
- ✓ 22. Gravitational waves and their detection.
-
- ✗ 27 The problem of dark matter (hidden mass) and its detection.



2003



“pioneering contributions to the theory of superconductors and superfluids”

ON SUPERCONDUCTIVITY AND SUPERFLUIDITY

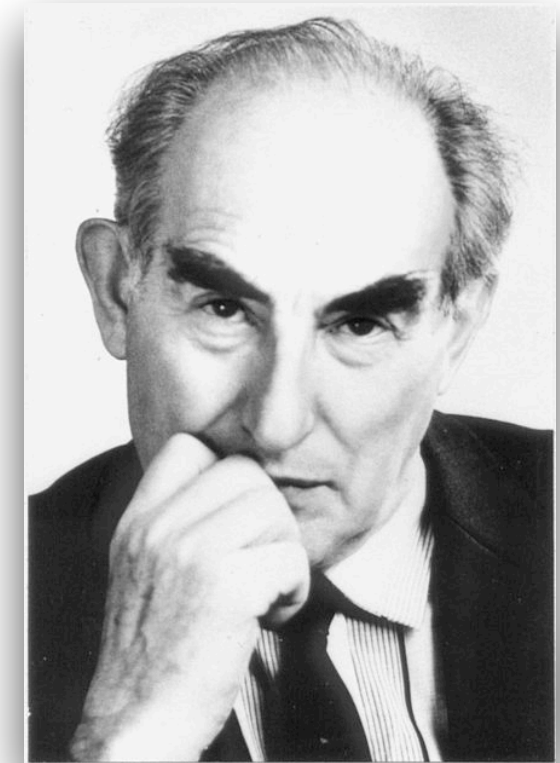
Nobel Lecture, December 8, 2003

by

VITALY L. GINZBURG

P. N. Lebedev Physics Institute, Russian Academy of Sciences, Moscow, Russia.

- ✗ 1. Controlled nuclear fusion.
- ✗ 2. High-temperature and room-temperature superconductivity (HTSC and RTSC).
- ✗ 3. Metallic hydrogen. Other exotic substances.
- ✓ 4. Two-dimensional electron liquid (anomalous Hall effect and other effects).
- ✓ 5. Some questions of solid-state physics (heterostructures in semiconductors, quantum wells and dots, metal – dielectric transitions, charge and spin density waves, mesoscopics).
- ...
- ✓ 7. Surface physics. Clusters.
- ✓ 8. Liquid crystals. Ferroelectrics. Ferrotoroids.
- ✓ 9. Fullerenes. Nanotubes.
- ✓ 10. The behavior of matter in superstrong magnetic fields.
- ✓ 11. Nonlinear physics. Turbulence. Solitons. Chaos. Strange attractors.
- ✓ 12. X-ray lasers, gamma-ray lasers, superhigh-power lasers.
- ✓ 13. Superheavy elements. Exotic nuclei.
-
- ✓ 22. Gravitational waves and their detection.
-
- ✗ 27 The problem of dark matter (hidden mass) and its detection.



2003



“pioneering contributions to the theory of superconductors and superfluids”

Metallic hydrogen: The holy grail of physics

Metallic hydrogen: The holy grail of physics



1899: Dewar produces
solid hydrogen

Metallic hydrogen: The holy grail of physics



1899: Dewar produces solid hydrogen



1935: Wigner predicted metallic hydrogen at 25 GPa

Metallic hydrogen: The holy grail of physics

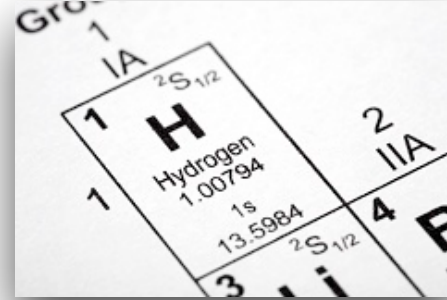


1899: Dewar produces solid hydrogen



1935: Wigner predicted metallic hydrogen at 25 GPa

1968: Ashcroft's proposal



Metallic hydrogen: The holy grail of physics

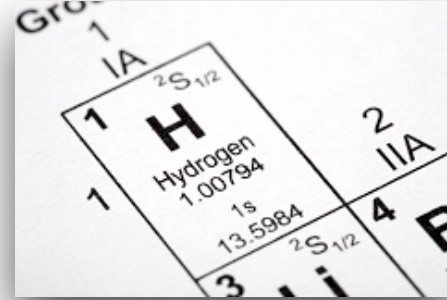


1899: Dewar produces solid hydrogen

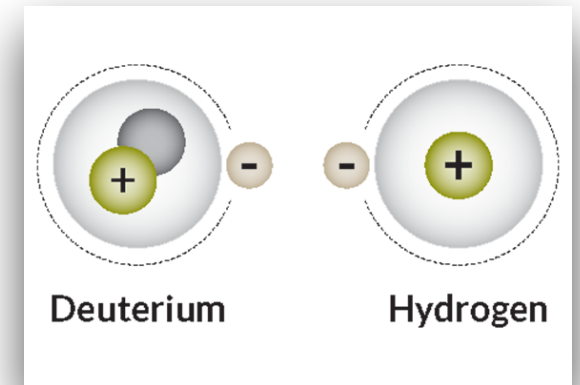


1935: Wigner predicted metallic hydrogen at 25 GPa

1968: Ashcroft's proposal



1981: Phase II discovered



Metallic hydrogen: The holy grail of physics

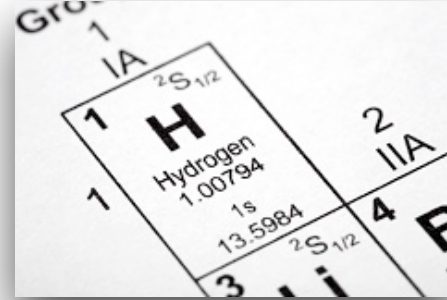


1899: Dewar produces solid hydrogen

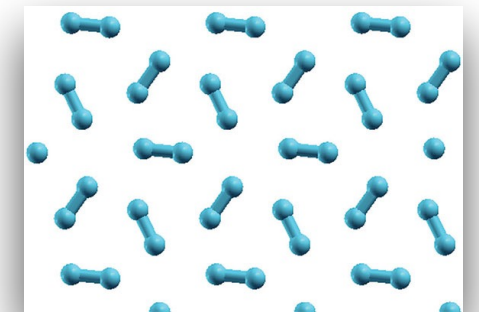
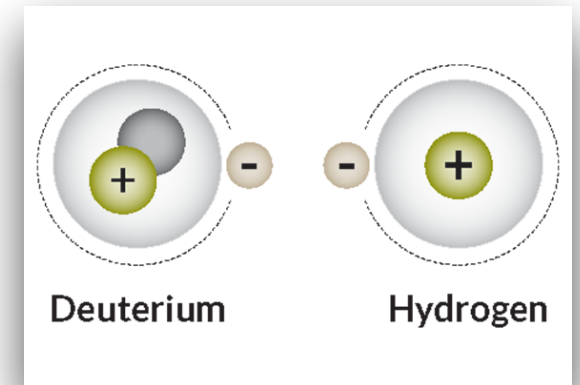


1935: Wigner predicted metallic hydrogen at 25 GPa

1968: Ashcroft's proposal

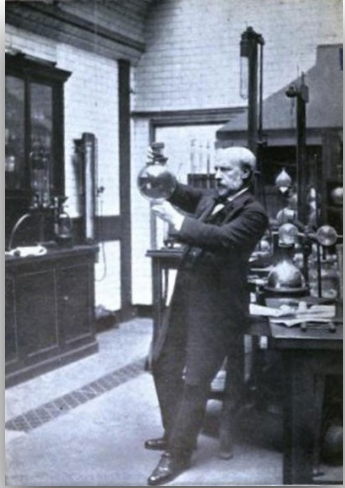


1981: Phase II discovered



1988: Phase III

Metallic hydrogen: The holy grail of physics

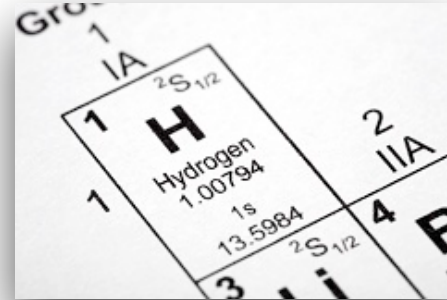


1899: Dewar produces solid hydrogen

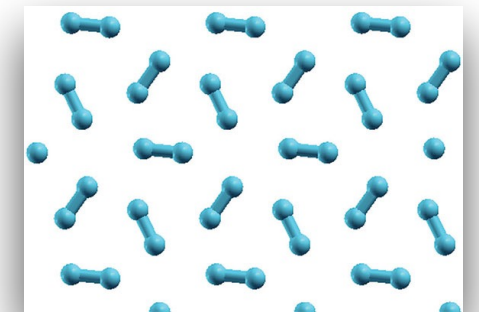
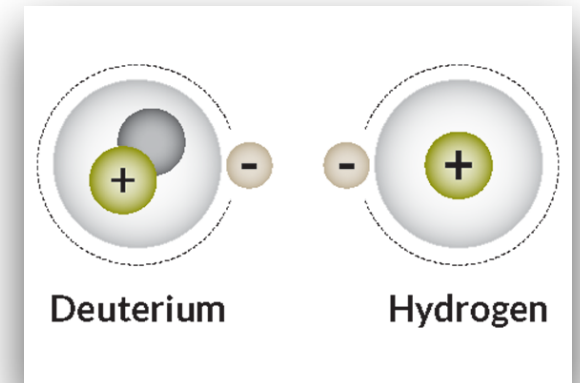


1935: Wigner predicted metallic hydrogen at 25 GPa

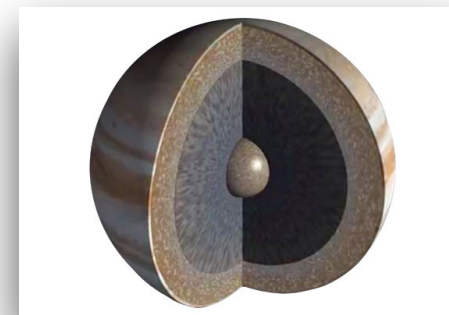
1968: Ashcroft's proposal



1981: Phase II discovered



1988: Phase III



1996: Nellis produces liquid metallic hydrogen (140 GPa and 3000K)

Metallic hydrogen: The holy grail of physics

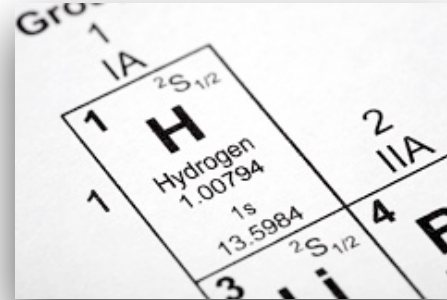


1899: Dewar produces solid hydrogen

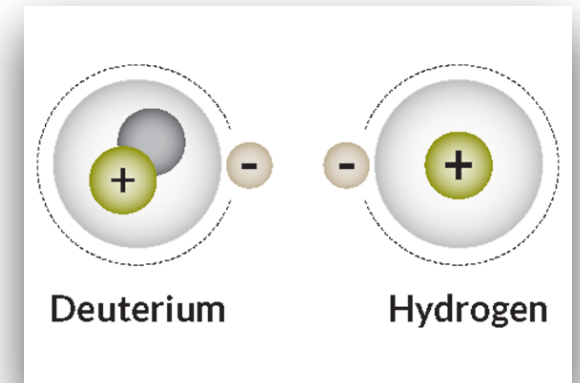


1935: Wigner predicted metallic hydrogen at 25 GPa

1968: Ashcroft's proposal

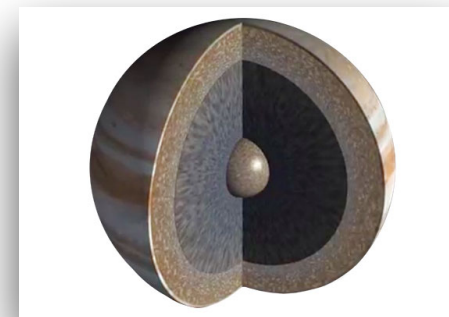


1981: Phase II discovered



1988: Phase III

The pressure is too high, experiments too complicated,
.....theoretical predictions are welcome for both
normal and superconducting properties.



1996: Nellis produces liquid metallic hydrogen (140 GPa and 3000K)

The Density Functional Theory

PHYSICAL REVIEW

VOLUME 136, NUMBER 3B

9 NOVEMBER 1964

Inhomogeneous Electron Gas*

P. HOHENBERG†

École Normale Supérieure, Paris, France

AND

W. KOHN‡

École Normale Supérieure, Paris, France and Faculté des Sciences, Orsay, France

and

University of California at San Diego, La Jolla, California

(Received 18 June 1964)

This paper deals with the ground state of an interacting electron gas in an external potential $v(\mathbf{r})$. It is proved that there exists a universal functional of the density, $F[n(\mathbf{r})]$, independent of $v(\mathbf{r})$, such that the expression $E \equiv \int v(\mathbf{r})n(\mathbf{r})d\mathbf{r} + F[n(\mathbf{r})]$ has as its minimum value the correct ground-state energy associated with $v(\mathbf{r})$. The functional $F[n(\mathbf{r})]$ is then discussed for two situations: (1) $n(\mathbf{r}) = n_0 + \tilde{n}(\mathbf{r})$, $\tilde{n}/n_0 \ll 1$, and (2) $n(\mathbf{r}) = \varphi(\mathbf{r}/r_0)$ with φ arbitrary and $r_0 \rightarrow \infty$. In both cases F can be expressed entirely in terms of the correlation energy and linear and higher order electronic polarizabilities of a uniform electron gas. This approach also sheds some light on generalized Thomas-Fermi methods and their limitations. Some new extensions of these methods are presented.

The Density Functional Theory

PHYSICAL REVIEW

VOLUME 136, NUMBER 3B

9 NOVEMBER 1964

Inhomogeneous Electron Gas*

P. HOHENBERG†

École Normale Supérieure, Paris, France

AND

W. KOHN‡

École Normale Supérieure, Paris, France and Faculté des Sciences, Orsay, France

and

University of California at San Diego, La Jolla, California

(Received 18 June 1964)

This paper deals with the ground state of an interacting electron gas in an external potential $v(\mathbf{r})$. It is proved that there exists a universal functional of the density, $F[n(\mathbf{r})]$, independent of $v(\mathbf{r})$, such that the expression $E \equiv \int v(\mathbf{r})n(\mathbf{r})d\mathbf{r} + F[n(\mathbf{r})]$ has as its minimum value the correct ground-state energy associated with $v(\mathbf{r})$. The functional $F[n(\mathbf{r})]$ is then discussed for two situations: (1) $n(\mathbf{r}) = n_0 + \tilde{n}(\mathbf{r})$, $\tilde{n}/n_0 \ll 1$, and (2) $n(\mathbf{r}) = \varphi(\mathbf{r}/r_0)$ with φ arbitrary and $r_0 \rightarrow \infty$. In both cases F can be expressed entirely in terms of the correlation energy and linear and higher order electronic polarizabilities of a uniform electron gas. This approach also sheds some light on generalized Thomas-Fermi methods and their limitations. Some new extensions of these methods are presented.

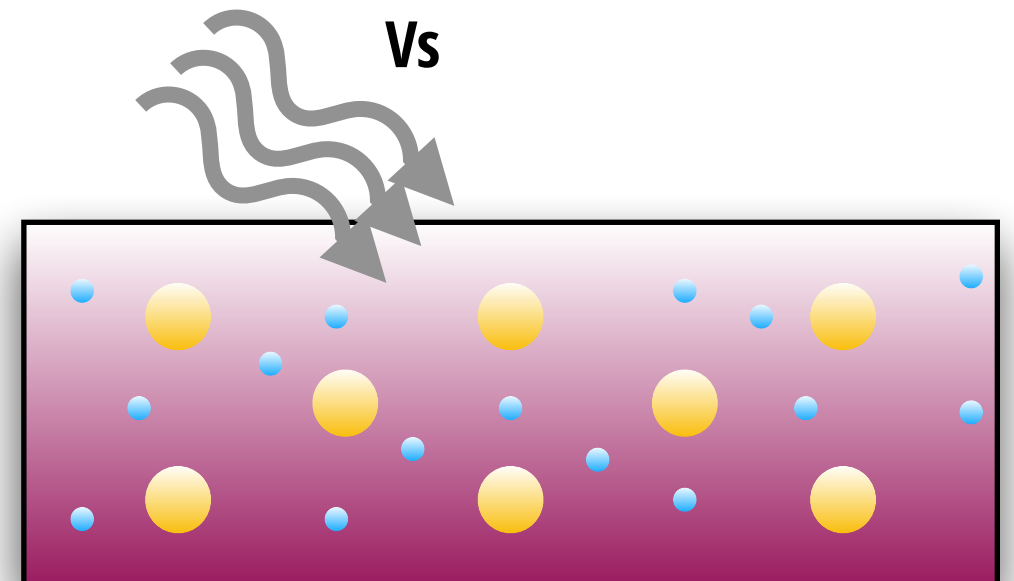
$$n \leftrightarrow V_{ext}$$

$$E[n_0] \leq E[n] = T[n] + U[n] + V[n]$$

$$\left[\frac{\hbar^2 \nabla^2}{2m} + v_s(r) \right] \phi_i(r) = \epsilon_i \phi_i(r)$$

$$v_s(r) = v(r) + v_H(r) + v_{xc}(r)$$

$$n(r) = \sum_i |\phi_i(r)|^2$$



The Density Functional Theory

PHYSICAL REVIEW

VOLUME 136, NUMBER 3B

9 NOVEMBER 1964

Inhomogeneous Electron Gas*

P. HOHENBERG†

École Normale Supérieure, Paris, France

AND

W. KOHN‡

École Normale Supérieure, Paris, France and Faculté des Sciences, Orsay, France

and

University of California at San Diego, La Jolla, California

(Received 18 June 1964)

This paper deals with the ground state of an interacting electron gas in an external potential $v(\mathbf{r})$. It is proved that there exists a universal functional of the density, $F[n(\mathbf{r})]$, independent of $v(\mathbf{r})$, such that the expression $E \equiv \int v(\mathbf{r})n(\mathbf{r})d\mathbf{r} + F[n(\mathbf{r})]$ has as its minimum value the correct ground-state energy associated with $v(\mathbf{r})$. The functional $F[n(\mathbf{r})]$ is then discussed for two situations: (1) $n(\mathbf{r}) = n_0 + \tilde{n}(\mathbf{r})$, $\tilde{n}/n_0 \ll 1$, and (2) $n(\mathbf{r}) = \varphi(\mathbf{r}/r_0)$ with φ arbitrary and $r_0 \rightarrow \infty$. In both cases F can be expressed entirely in terms of the correlation energy and linear and higher order electronic polarizabilities of a uniform electron gas. This approach also sheds some light on generalized Thomas-Fermi methods and their limitations. Some new extensions of these methods are presented.

$$n \leftrightarrow V_{ext}$$

$$E[n_0] \leq E[n] = T[n] + U[n] + V[n]$$

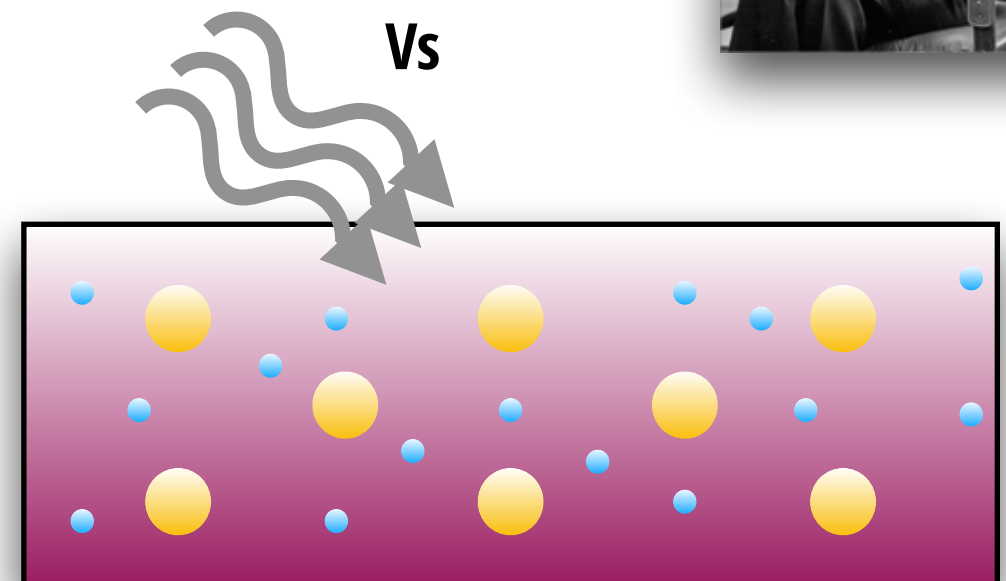
$$\left[\frac{\hbar^2 \nabla^2}{2m} + v_s(r) \right] \phi_i(r) = \epsilon_i \phi_i(r)$$

$$v_s(r) = v(r) + v_H(r) + v_{xc}(r)$$

$$n(r) = \sum_i |\phi_i(r)|^2$$



1998



Super Conducting Density Functional Theory (2005)

Kohn-Sham system for superconductor

$$H = H_e + H_{en} + H_n + H_{ext}$$

$$\rho(\mathbf{r}) = \text{Tr} \left[\varrho_0 \sum_{\sigma} \psi_{\sigma}^{\dagger}(\mathbf{r}) \psi_{\sigma}(\mathbf{r}) \right]$$

$$\chi(\mathbf{r}, \mathbf{r}') = \text{Tr} [\varrho_0 \psi_{\uparrow}(\mathbf{r}) \psi_{\downarrow}(\mathbf{r}')]]$$

$$\Gamma(\{\mathbf{R}_i\}) = \text{Tr} \left[\varrho_0 \prod_j \Phi^{\dagger}(\mathbf{R}_j) \Phi(\mathbf{R}_j) \right]$$



Super Conducting Density Functional Theory (2005)

Kohn-Sham system for superconductor

$$H = H_e + H_{en} + H_n + H_{ext}$$

$$\rho(\mathbf{r}) = \text{Tr} \left[\rho_0 \sum_{\sigma} \psi_{\sigma}^{\dagger}(\mathbf{r}) \psi_{\sigma}(\mathbf{r}) \right]$$

$$\chi(\mathbf{r}, \mathbf{r}') = \text{Tr} [\rho_0 \psi_{\uparrow}(\mathbf{r}) \psi_{\downarrow}(\mathbf{r}')]]$$

$$\Gamma(\{\mathbf{R}_i\}) = \text{Tr} \left[\rho_0 \prod_j \Phi^{\dagger}(\mathbf{R}_j) \Phi(\mathbf{R}_j) \right]$$

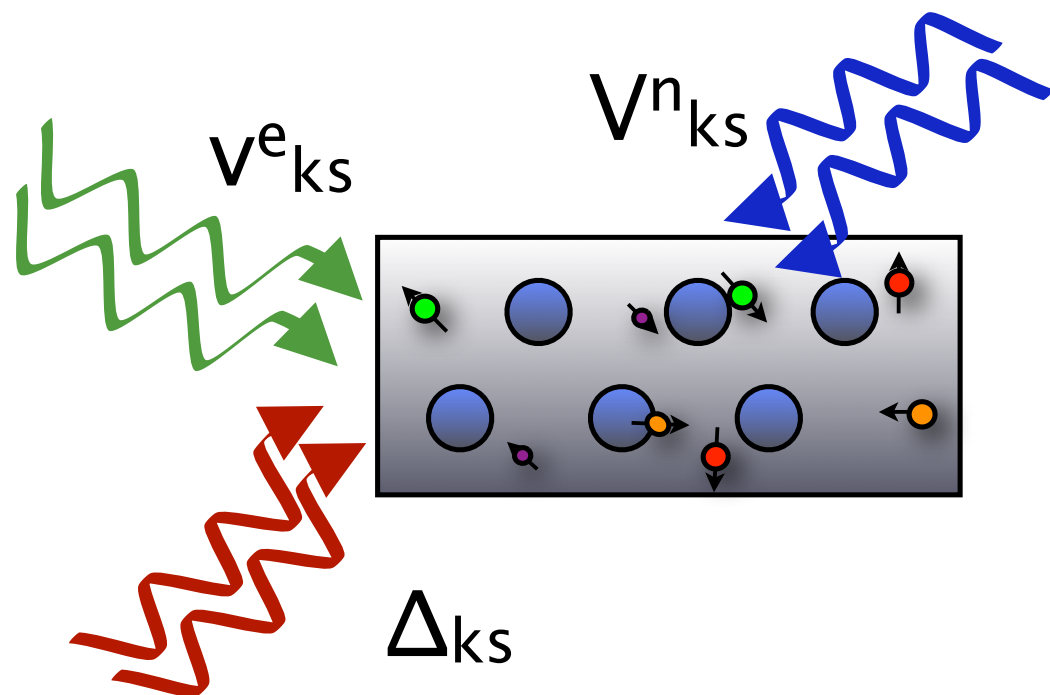


PHYSICAL REVIEW B 72, 024545 (2005)

Ab initio theory of superconductivity. I. Density functional formalism and approximate functionals

M. Lüders,^{1,2} M. A. L. Marques,^{2,3} N. N. Lathiotakis,^{2,3} A. Floris,^{3,4} G. Profeta,⁵ L. Fast,^{2,6} A. Continenza,⁵ S. Massidda,^{4,*} and E. K. U. Gross^{2,3}

An approach to the description of superconductors in thermal equilibrium is developed within a formally exact density functional framework. The theory is formulated in terms of three “densities:” the ordinary electron density, the superconducting order parameter, and the diagonal of the nuclear N -body density matrix. The electron density and the order parameter are determined by Kohn-Sham equations that resemble the Bogoliubov–de Gennes equations. The nuclear density matrix follows from a Schrödinger equation with an effective N -body interaction. These equations are coupled to each other via exchange-correlation potentials which are universal functionals of the three densities. Approximations of these exchange-correlation functionals are derived using the diagrammatic techniques of many-body perturbation theory. The bare Coulomb repulsion between the electrons and the electron-phonon interaction enter this perturbative treatment on the same footing. In this way, a truly *ab initio* description is achieved which does not contain any empirical parameters.



Super Conducting Density Functional Theory (2005)

$$\Sigma \approx \text{[Diagram: wavy line labeled } W \text{ on a horizontal line]} + \text{[Diagram: semi-circular dashed line labeled } \Lambda^{\text{Ph}} \text{ above a horizontal line labeled } \bar{G}^{\text{KS}} \text{]}.$$

Interactions from first-principles

$$\bar{\Sigma}_k(\omega_n) \approx \sum_m \sum_{k'} W_{kk'}(\omega_n - \omega_m) \bar{G}_{k'}^{\text{KS}}(\omega_m) + \sum_m \sum_{k'} \Lambda_{kk'}^{\text{Ph}}(\omega_n - \omega_m) \bar{G}_{k'}^{\text{KS}}(\omega_m),$$

$$\Lambda_{kk'}^{\text{Ph}}(\omega_n) = -\frac{1}{\pi} \int_0^\infty d\omega \frac{2\omega}{\omega_n^2 + \omega^2} \Im[\Lambda_{kk'}^{\text{Ph}}(\omega)]$$

$$\Im[\Lambda_{kk'}^{\text{Ph}}(\omega)] = -\pi \sum_{\lambda \mathbf{q}} |g_{\lambda \mathbf{q}}^{kk'}|^2 \delta(\omega - \Omega_{\lambda \mathbf{q}}).$$

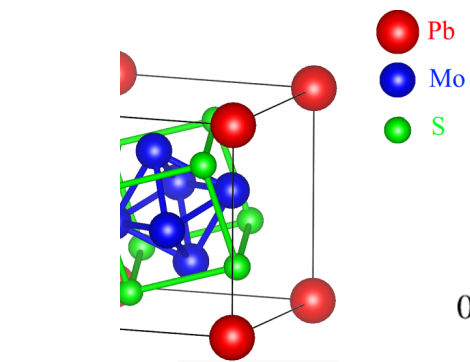
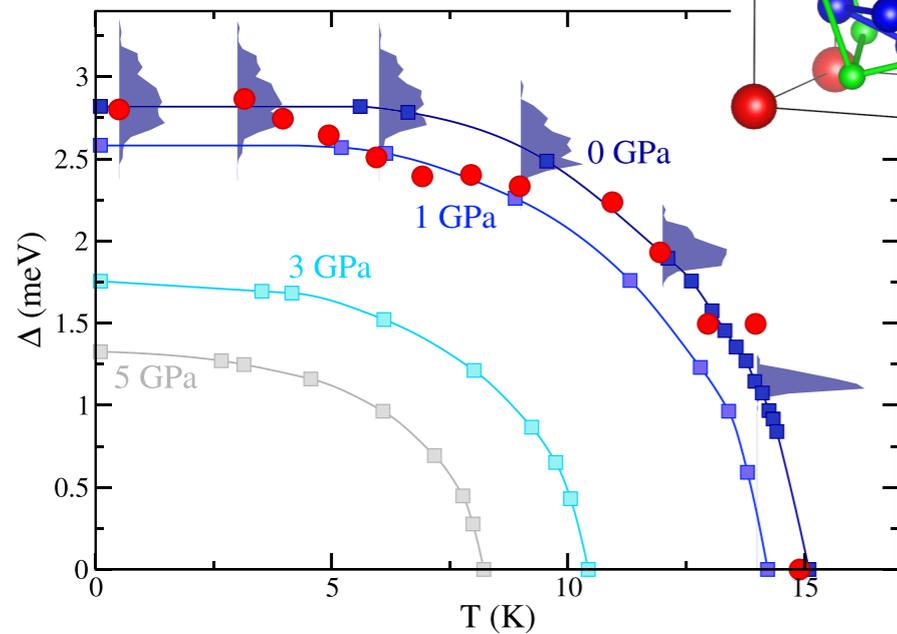
$$W_{k_1 k_2}(\omega_n) = \sum_{k'} \epsilon_{k_1 k'}^{-1}(\omega_n) v_{k' k_2}$$

$$\bar{G}_k(\omega_n) = \tau^z \begin{pmatrix} G_k(\omega_n) & F_k(\omega_n) \\ F_k^\dagger(\omega_n) & G_k^\dagger(\omega_n) \end{pmatrix}$$

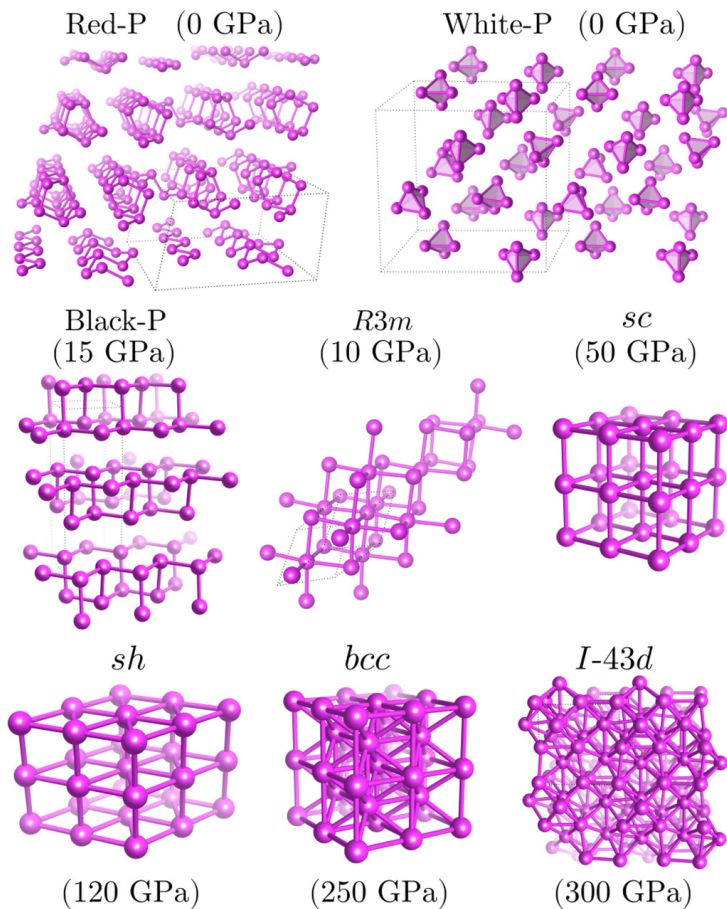
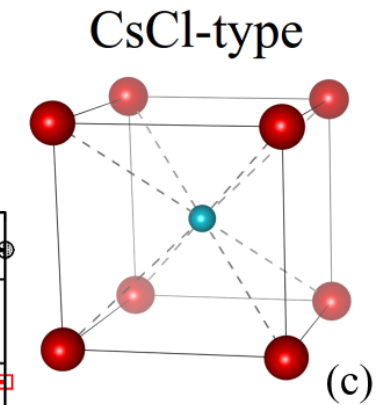
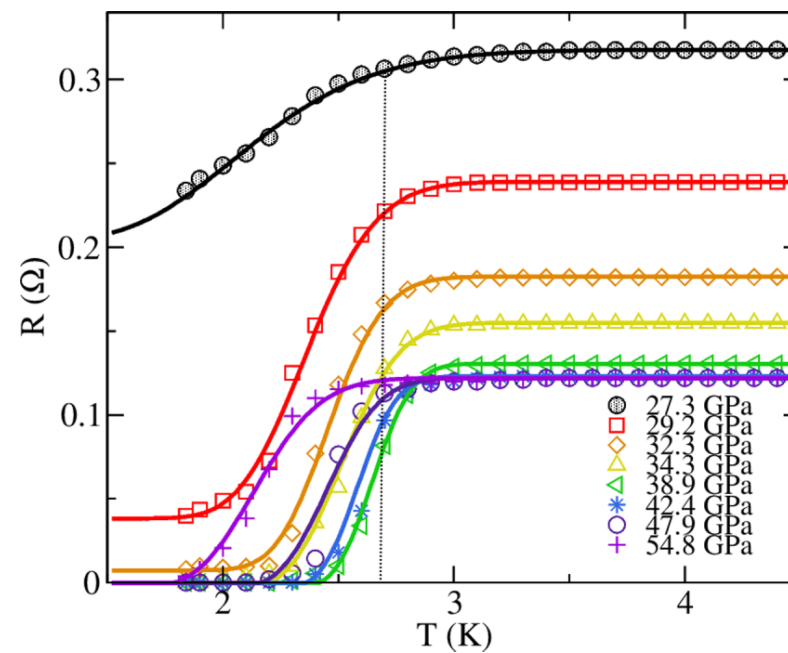
$$\Delta_k^{\text{xc}} = -\Delta_k^{\text{xc}} \mathcal{Z}_k^{\text{D}} - \sum_{k'} \mathcal{K}_{kk'}^{\text{C}} \frac{\tanh\left(\frac{\beta E_{k'}}{2}\right)}{2E_{k'}} \Delta_{k'}^{\text{xc}}$$

It works

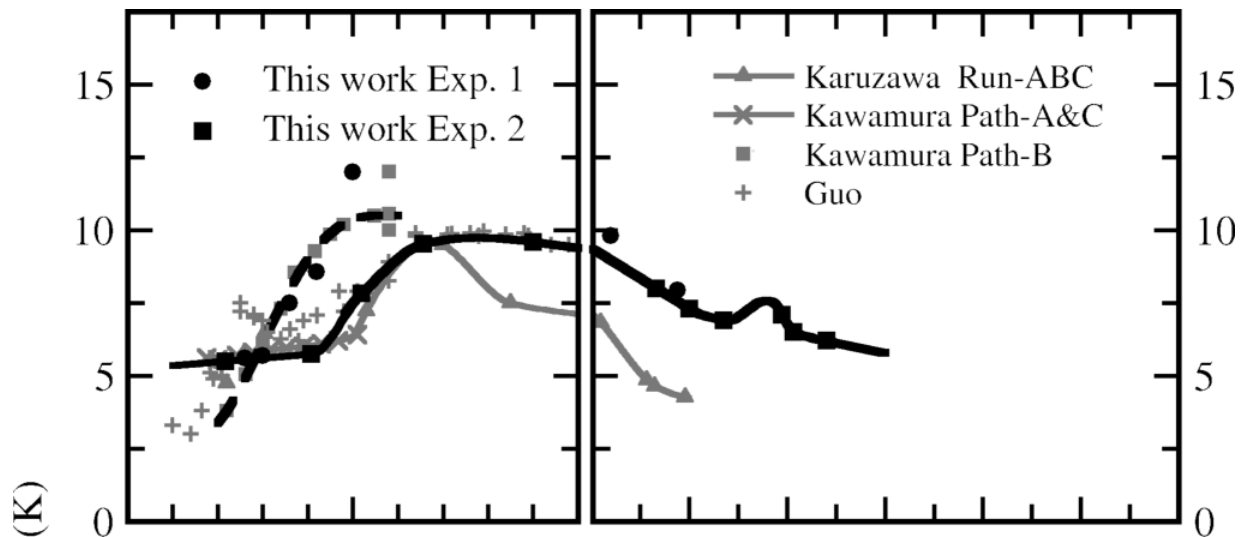
Chevrel phases, PbMo_6S_8



Tin-selenide, SnSe

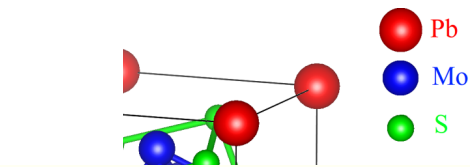


The many phases of phosphorus under pressure

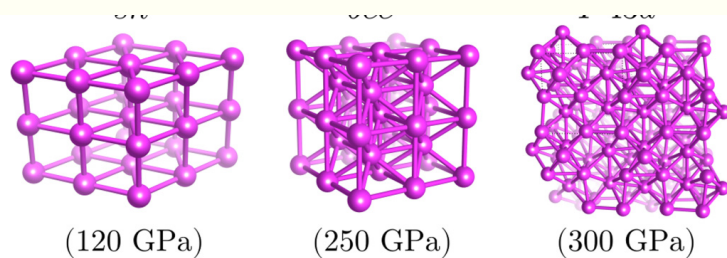
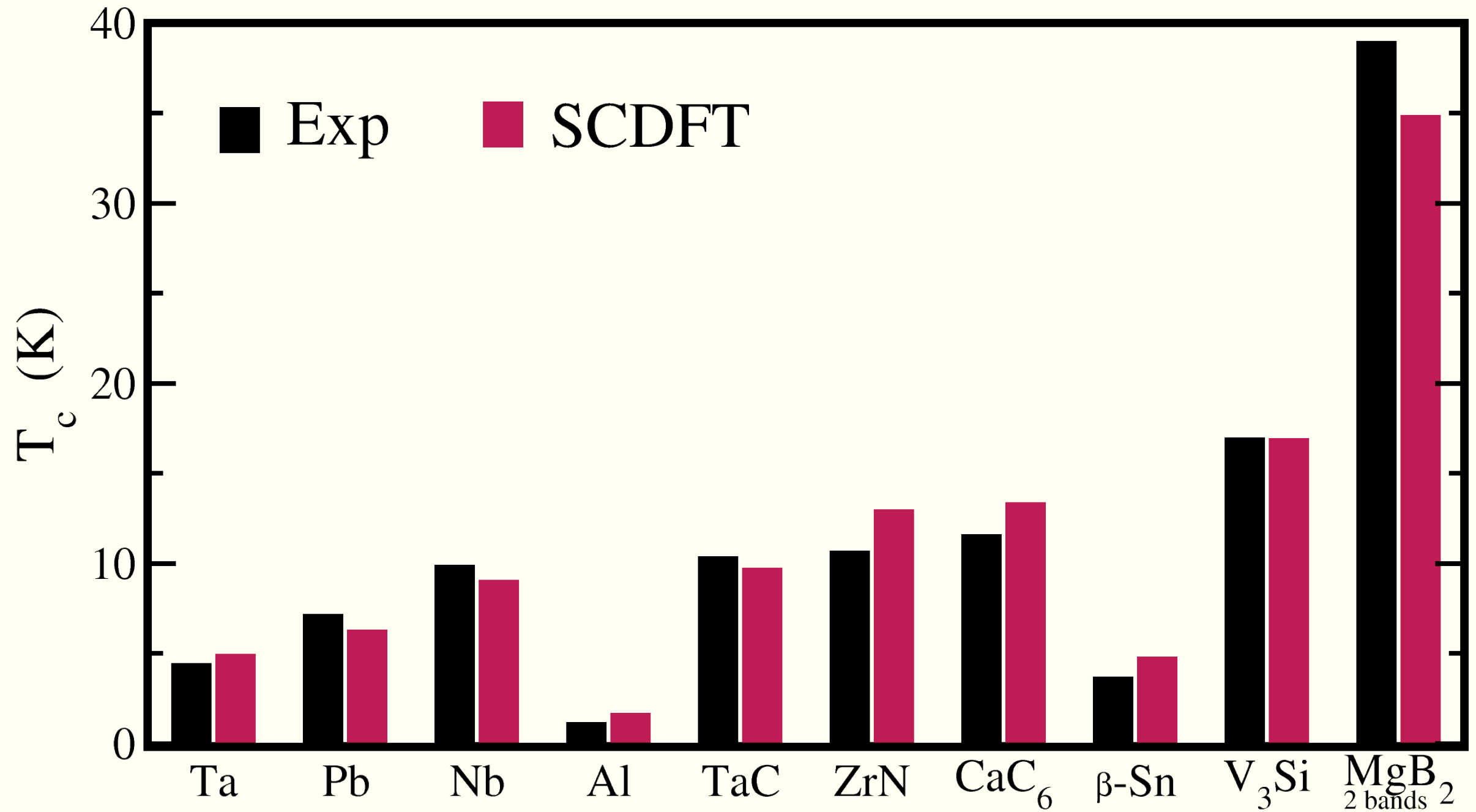
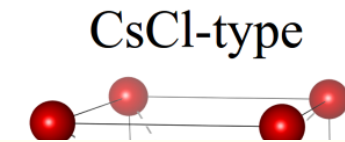


It works

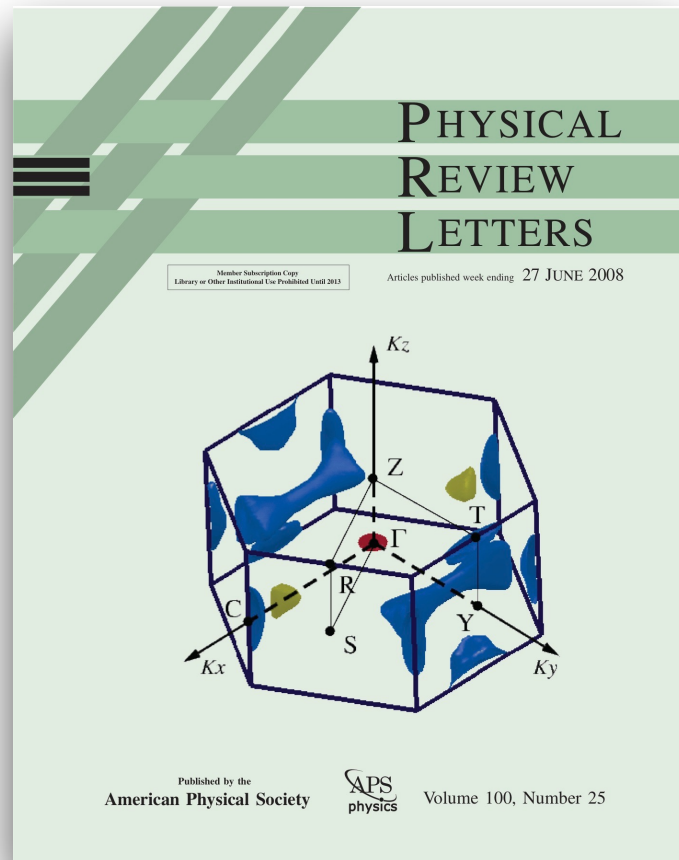
Chevrel phases, PbMo_6S_8



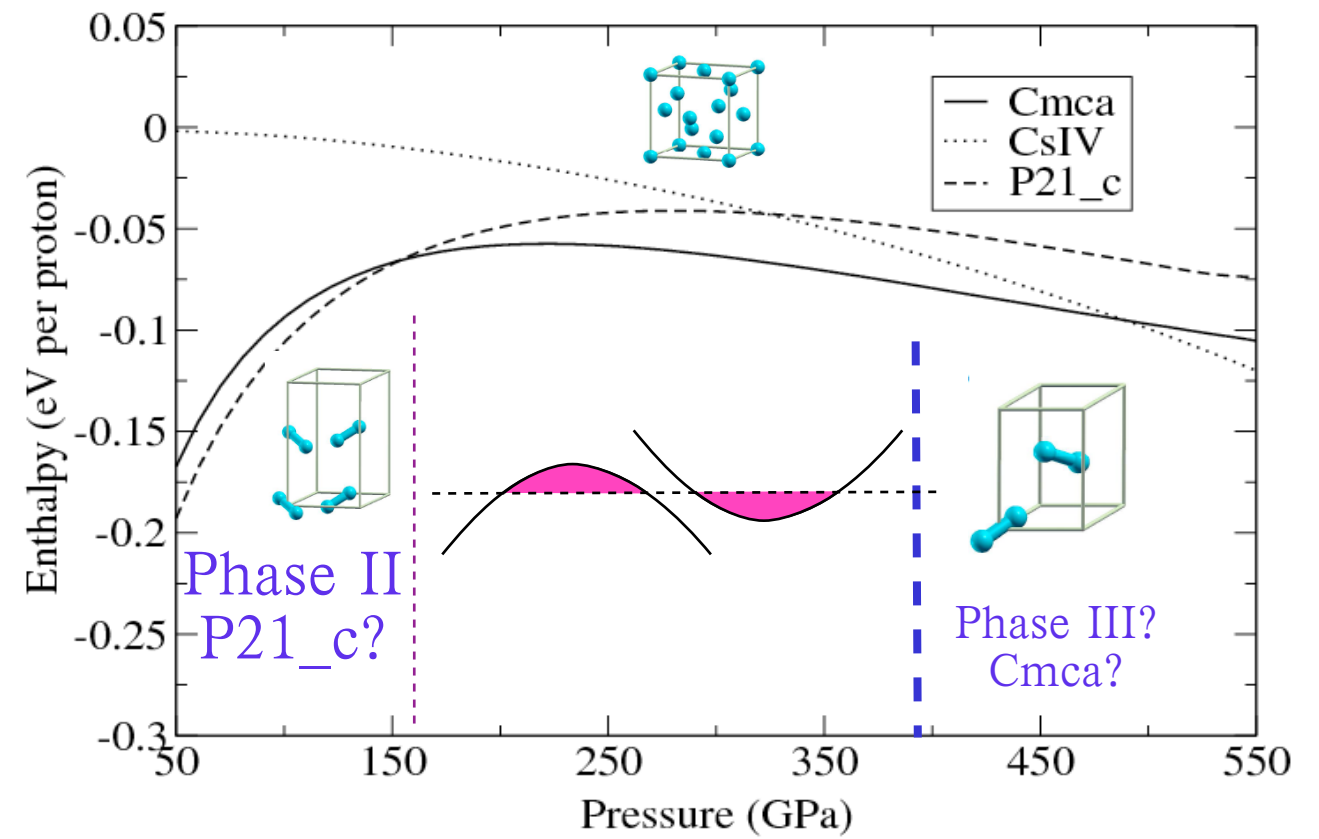
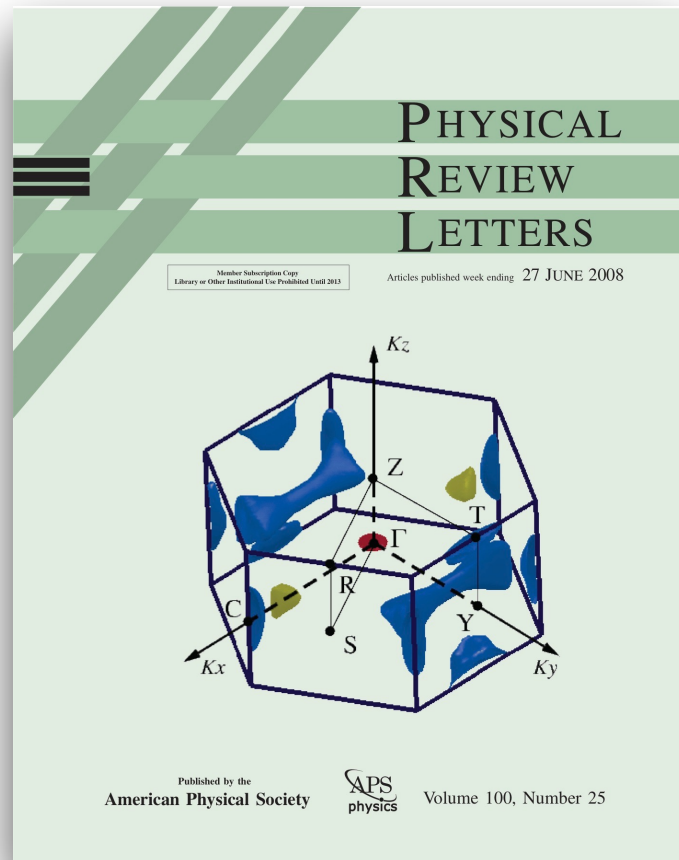
Tin-selenide, SnSe



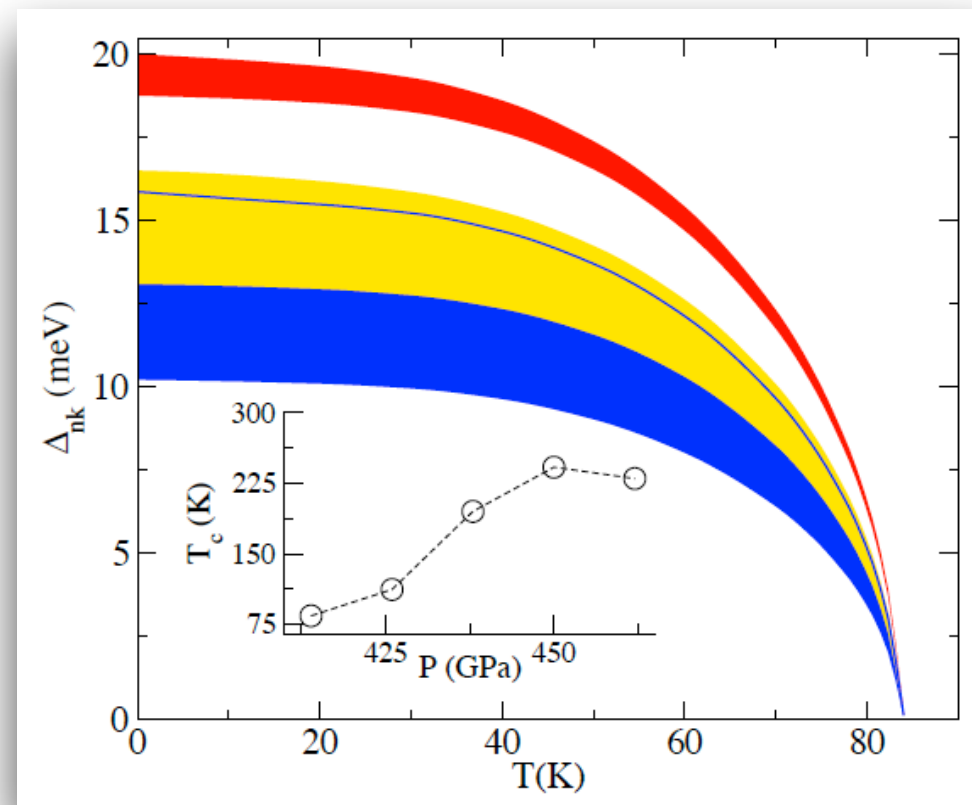
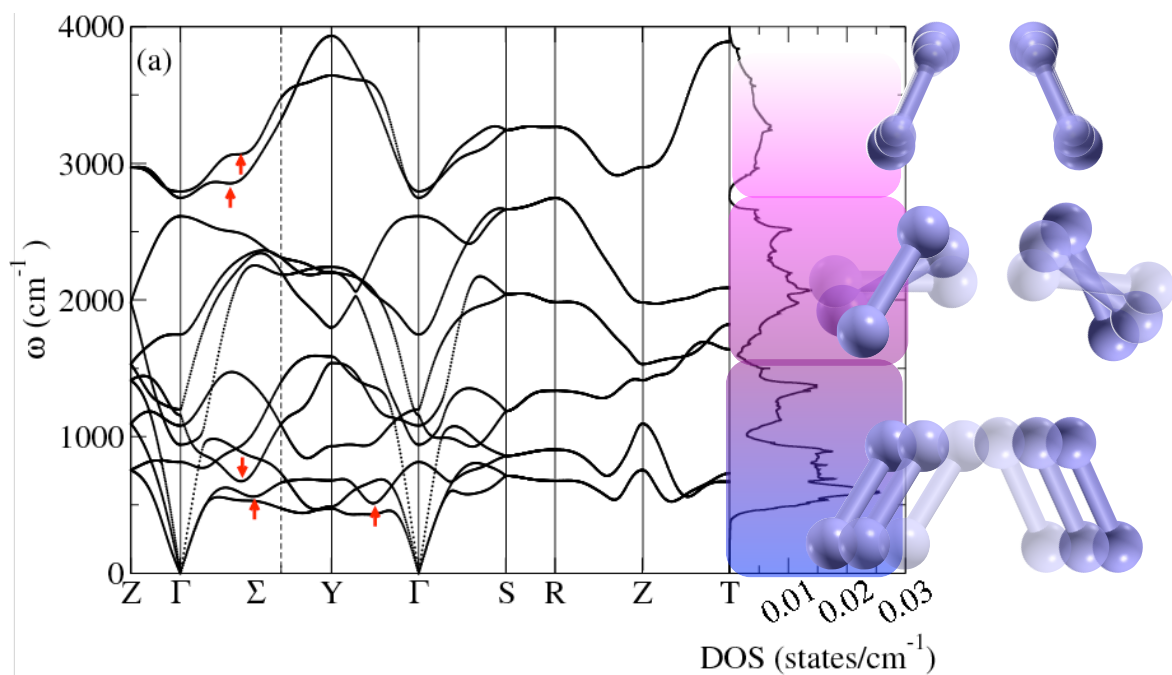
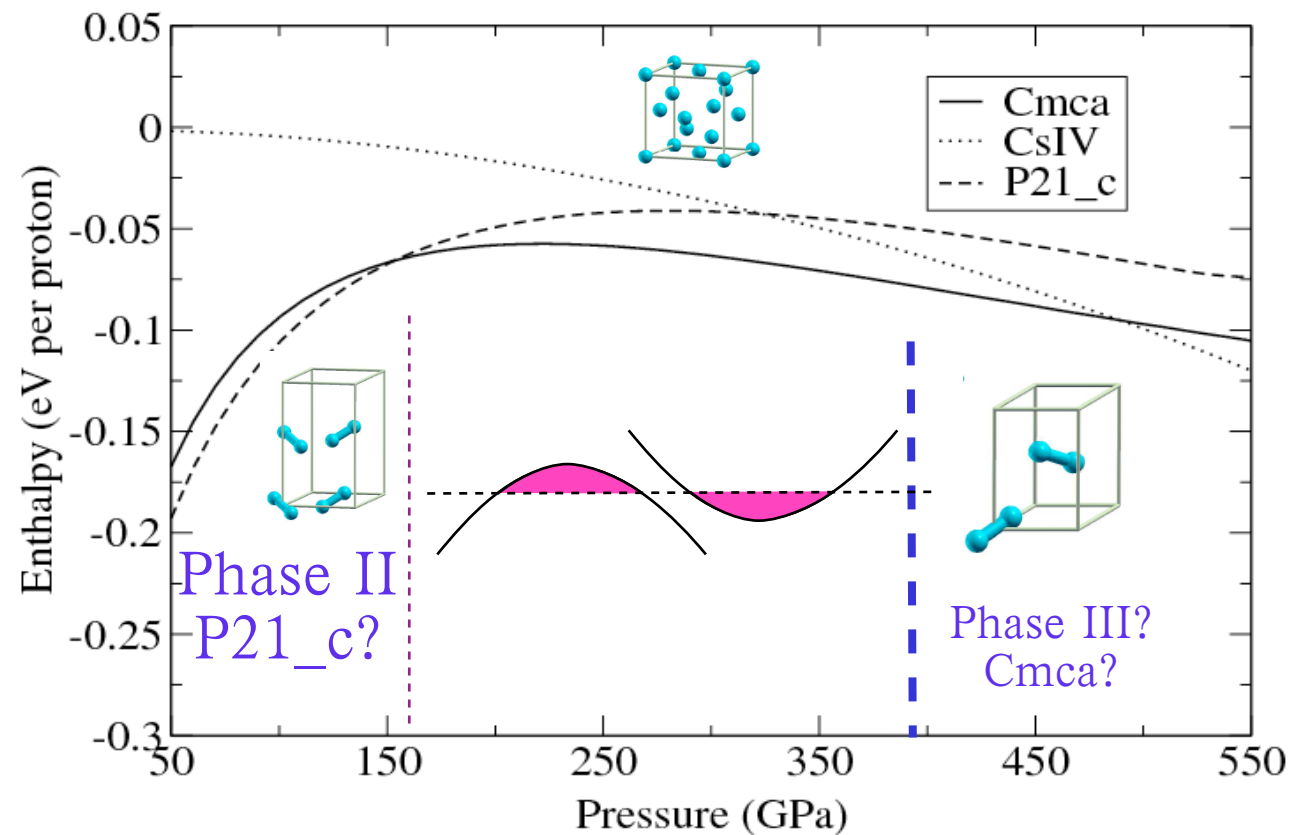
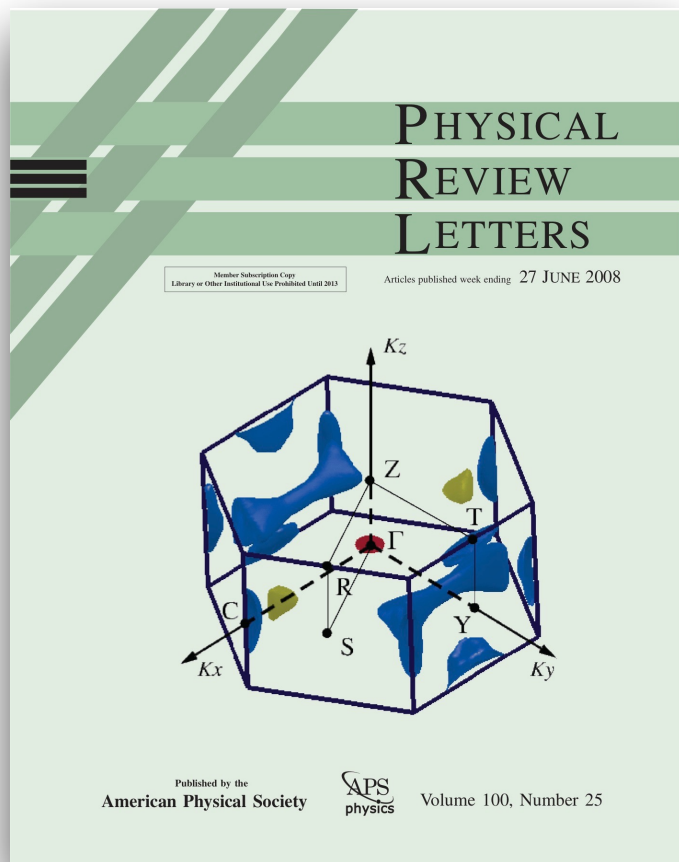
High-temperature superconducting phase in hydrogen phase III (2008)



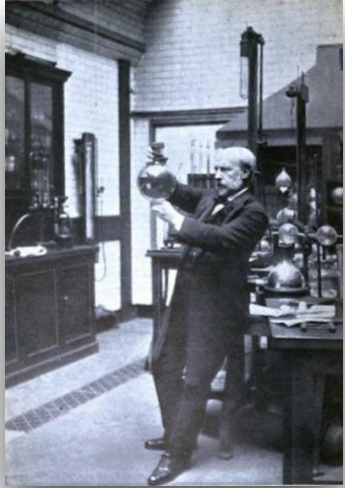
High-temperature superconducting phase in hydrogen phase III (2008)



High-temperature superconducting phase in hydrogen phase III (2008)



Metallic hydrogen: The holy grail of physics

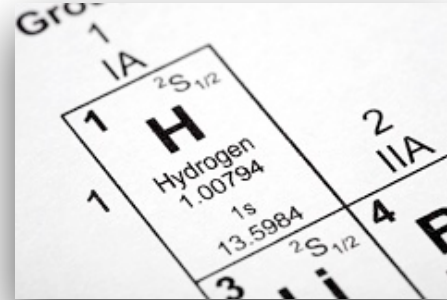


1899: Dewar produces solid hydrogen

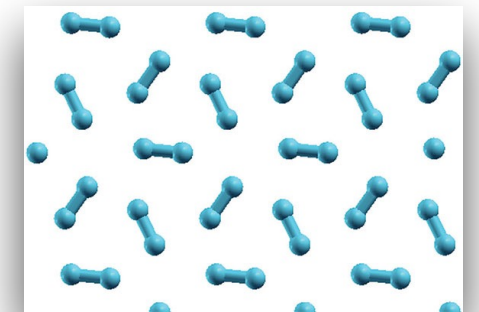
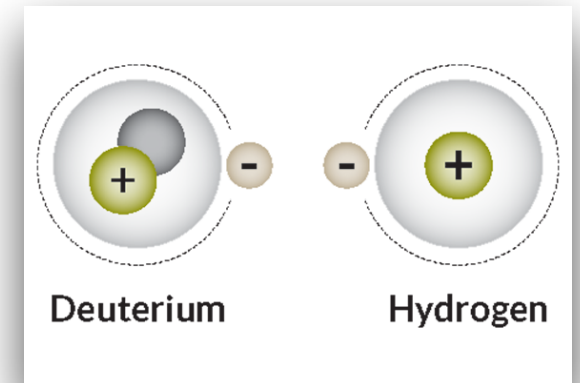


1935: Wigner predicted metallic hydrogen at 25 GPa

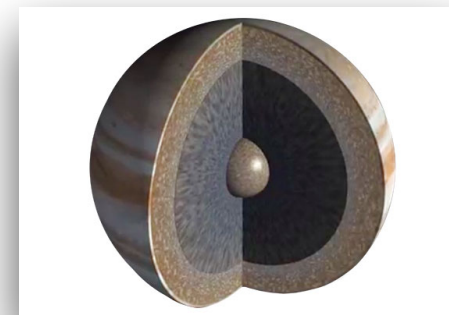
1968: Ashcroft's proposal



1981: Phase II discovered



1988: Phase III



1996: Nellis produces liquid metallic hydrogen (140 GPa and 3000K)

Metallic hydrogen: The holy grail of physics

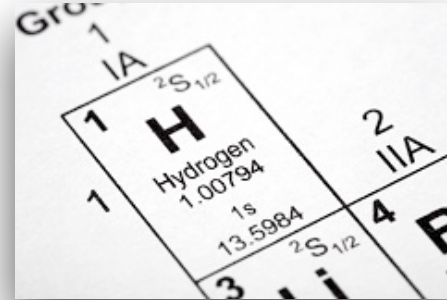


1899: Dewar produces solid hydrogen

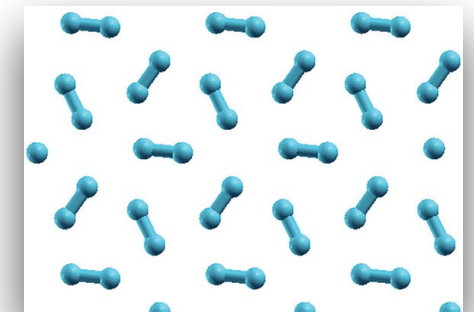
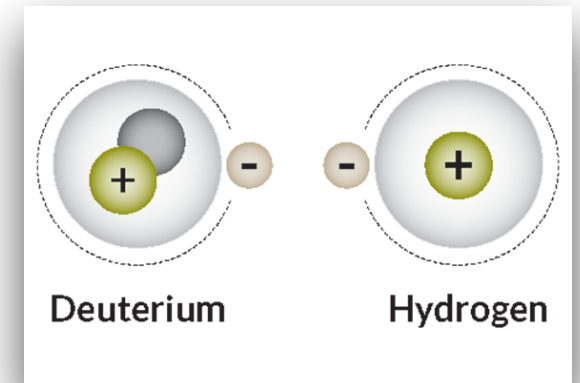


1935: Wigner predicted metallic hydrogen at 25 GPa

1968: Ashcroft's proposal

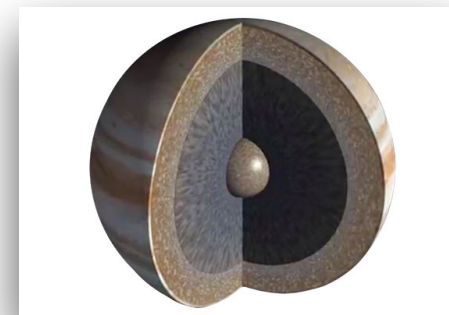
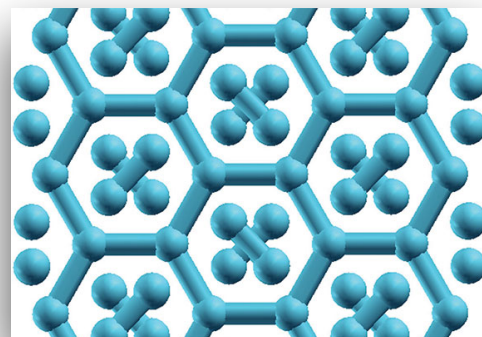


1981: Phase II discovered



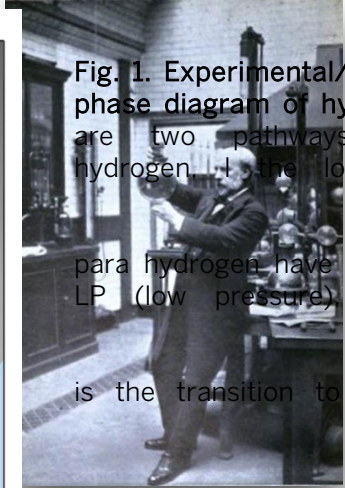
1988: Phase III

2011: Eremets discovers solid Phase IV (220 GPa)



1996: Nellis produces liquid metallic hydrogen (140 GPa and 3000K)

Metallic hydrogen: The holy grail of physics

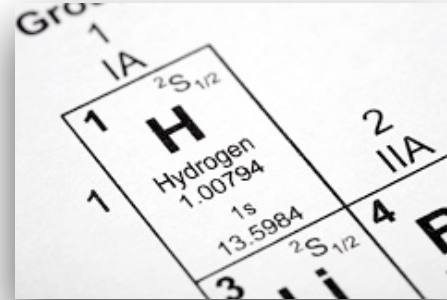


1899: Dewar produces solid hydrogen

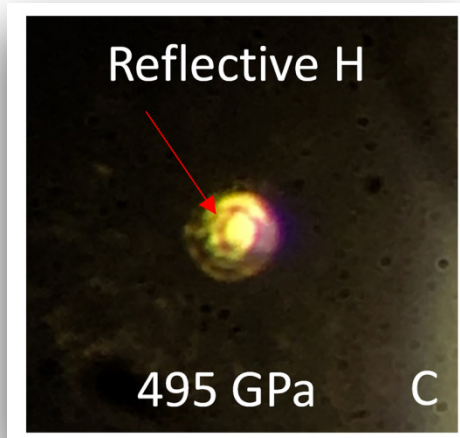
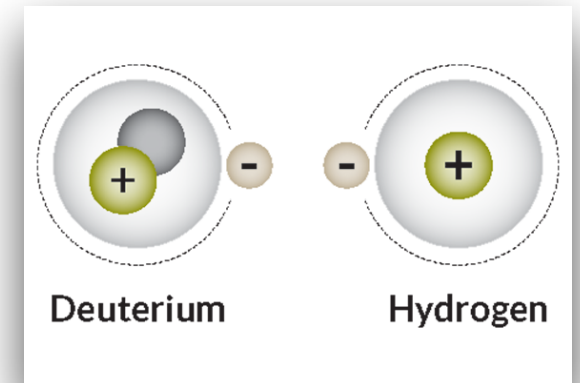


1935: Wigner predicted metallic hydrogen at 25 GPa

1968: Ashcroft's proposal

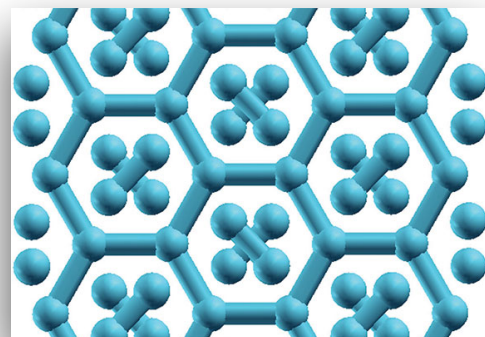


1981: Phase II discovered

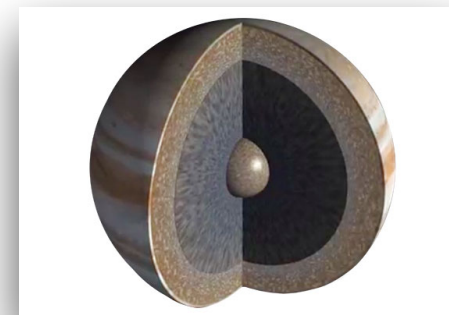


2017: Metallic hydrogen discovered by Silveira at 500 GPa (?)

2011: Eremets discovers solid Phase IV (220 GPa)

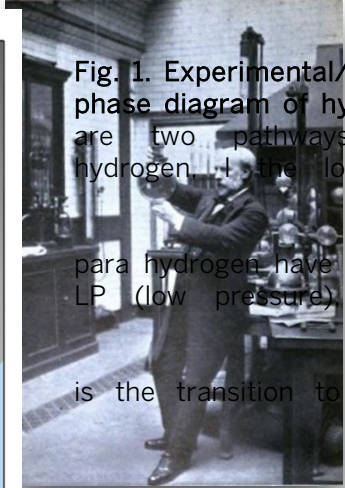


1988: Phase III



1996: Nellis produces liquid metallic hydrogen (140 GPa and 3000K)

Metallic hydrogen: The holy grail of physics

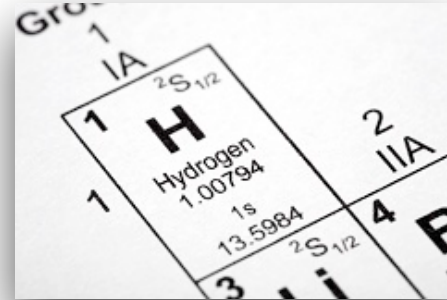


1899: Dewar produces solid hydrogen



1935: Wigner predicted metallic hydrogen at 25 GPa

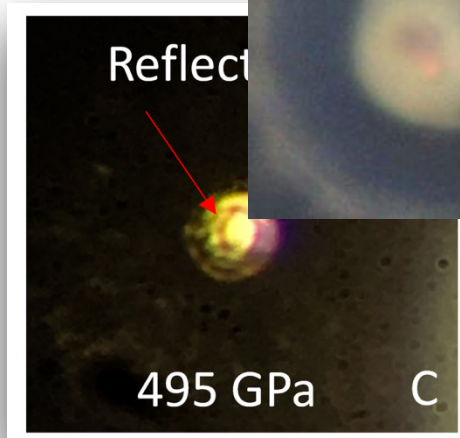
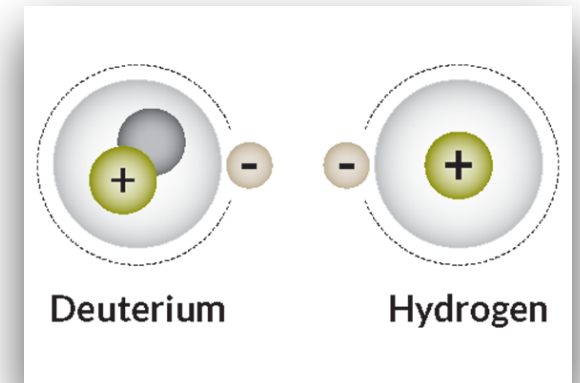
1968: Ashcroft's proposal



2020: Loubeyre: (Probable) Metallic hydrogen

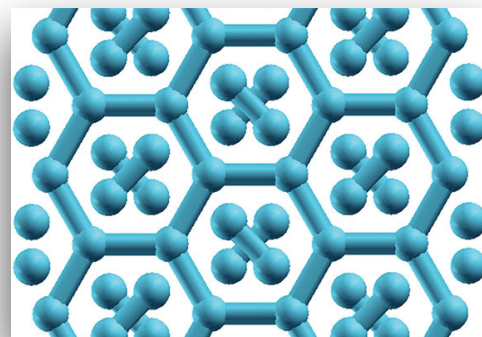


1981: Phase II discovered

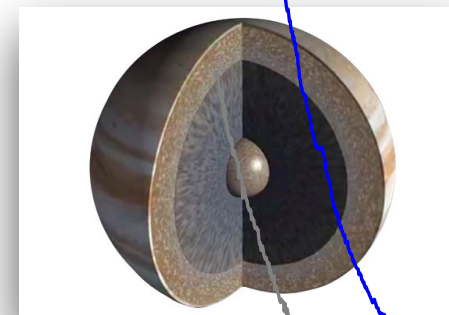


2017: Metallic hydrogen discovered by Silveira at 500 GPa (?)

2011: Eremets discovers solid Phase IV (220 GPa)



1988: Phase III

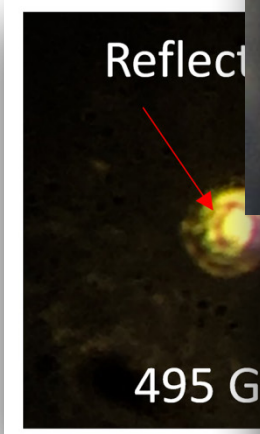


1996: Nellis produces liquid metallic hydrogen (140 GPa and 3000K)

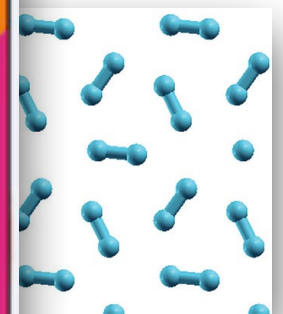
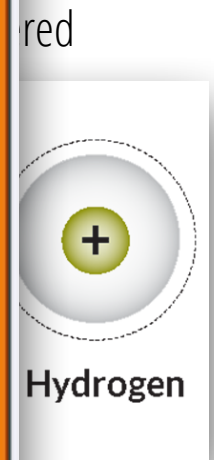
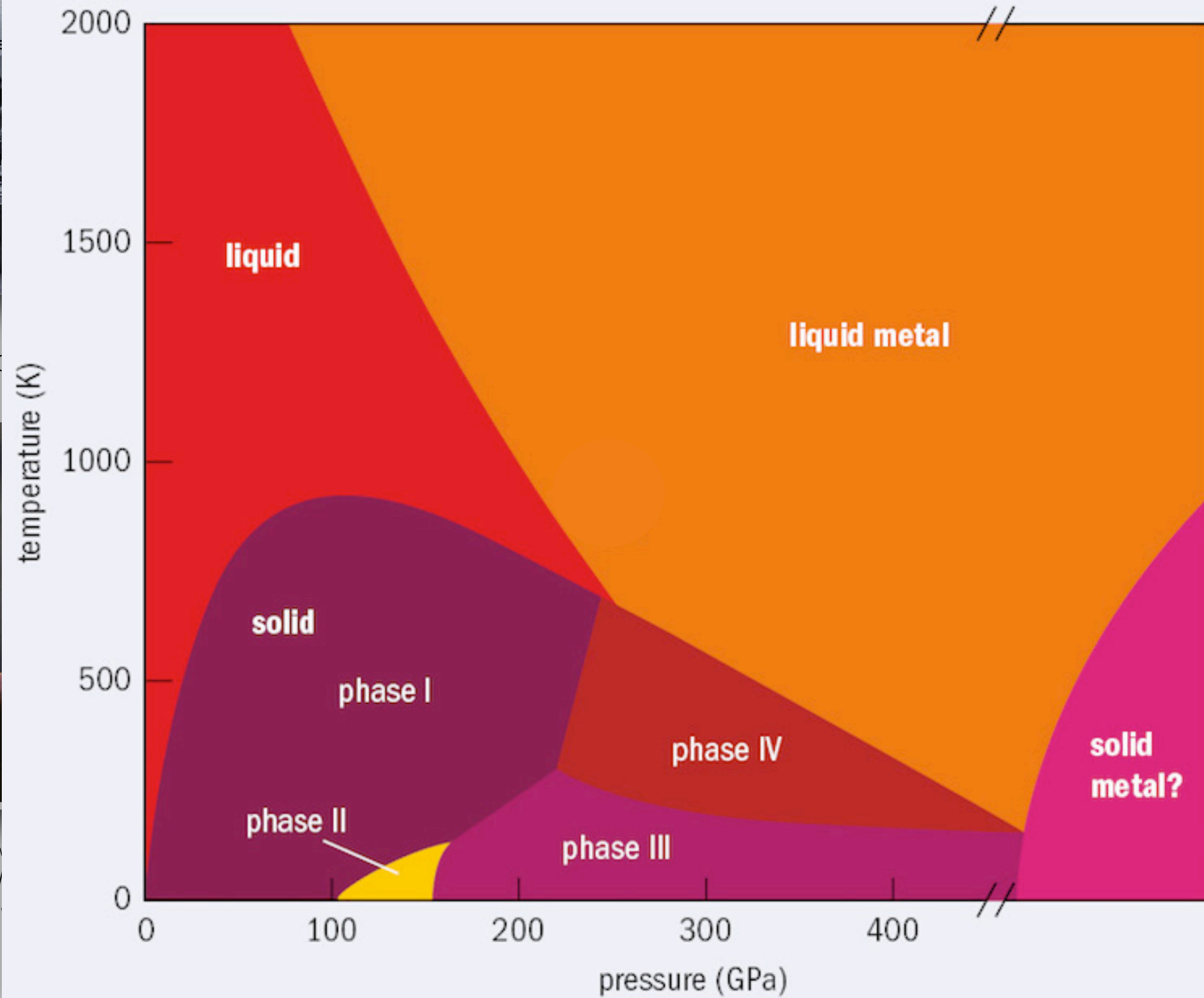
Metallic hydrogen: The holy grail of physics



1899: Dewar produces solid hydrogen



2017: Metallic hydrogen discovered by Shimizu et al. at 500 GPa (?)

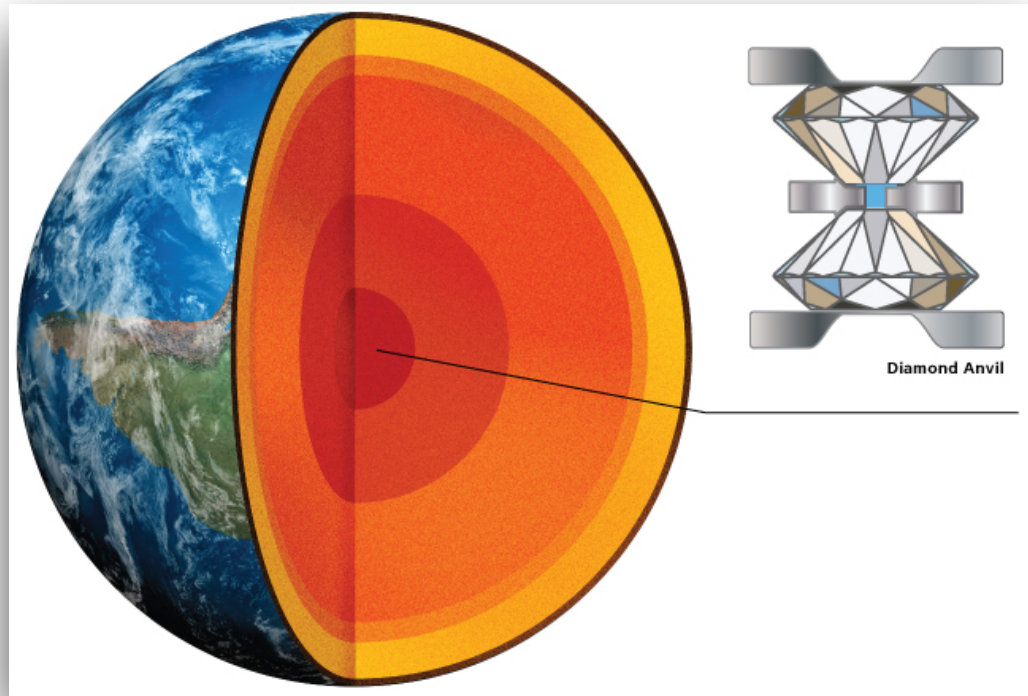


phase III



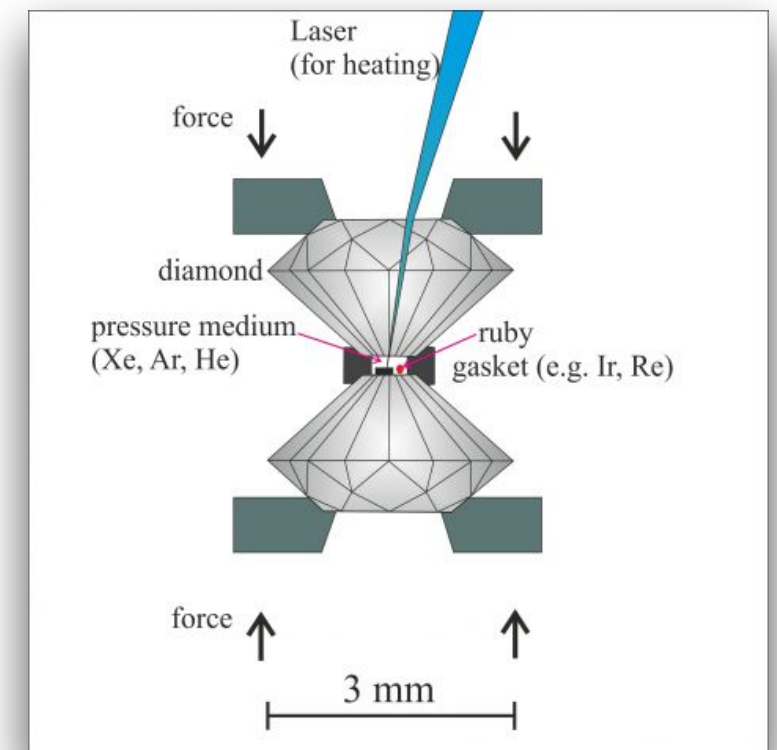
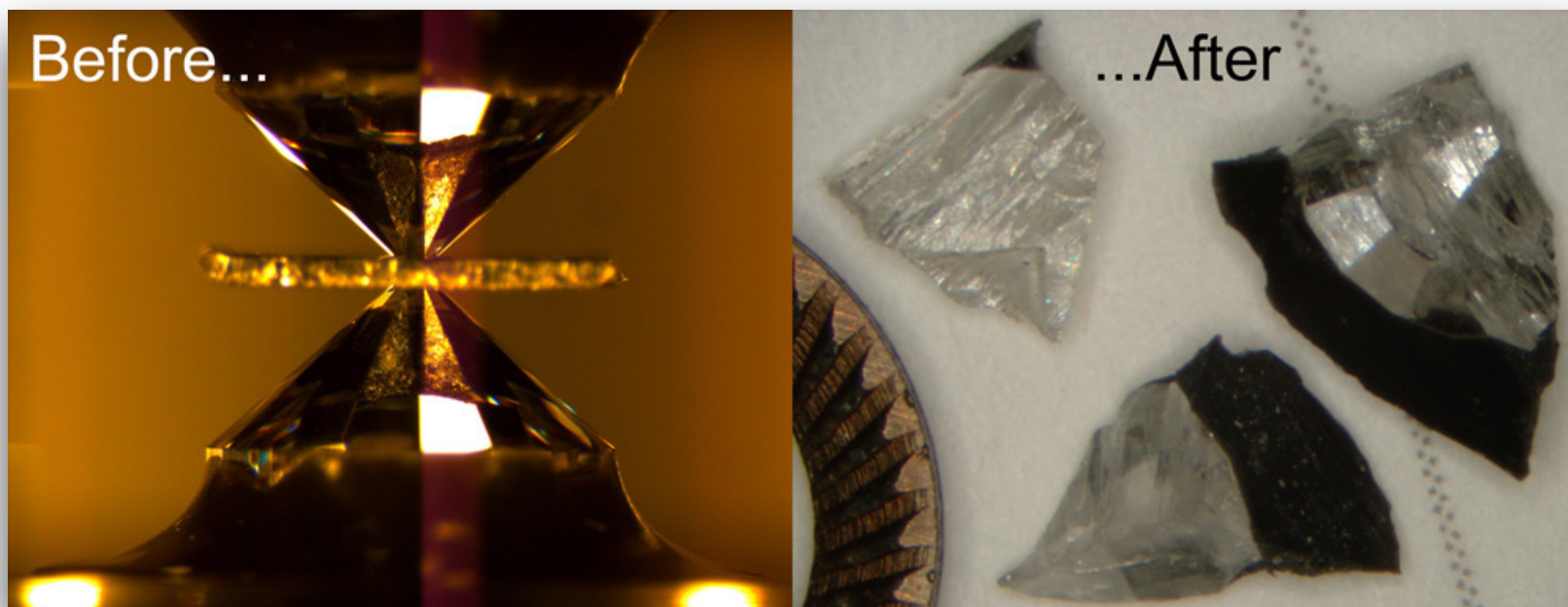
1996: Neilsen produces liquid metallic hydrogen (140 GPa and 3000K)

Hydrogen metallization: $P > 450$ GPa



Modern anvil cell reaches 350 GPa

Pressure in the inner core of earth is about 330 GPa!



Better call Ashcroft

VOLUME 92, NUMBER 18

PHYSICAL REVIEW LETTERS

week ending
7 MAY 2004

Hydrogen Dominant Metallic Alloys: High Temperature Superconductors?

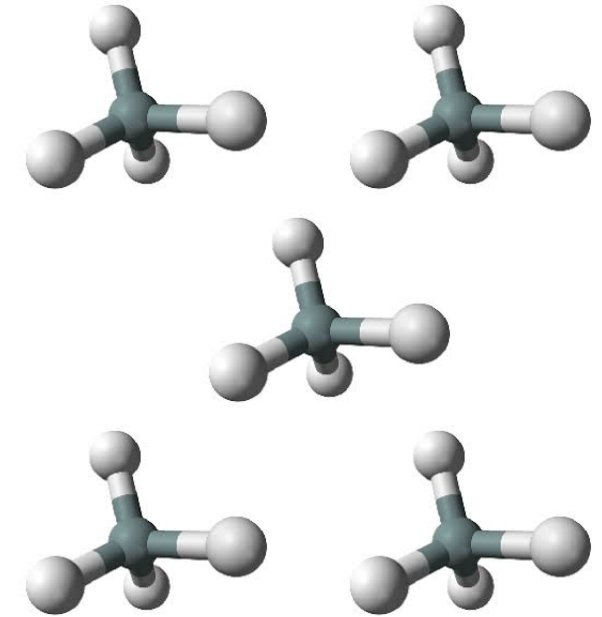
N.W. Ashcroft

Laboratory of Atomic and Solid State Physics, Cornell University, Ithaca, New York 14853-2501, USA

Donostia International Physics Center, San Sebastian, Spain

(Received 29 December 2003; published 6 May 2004)

The arguments suggesting that metallic hydrogen, either as a monatomic or paired metal, should be a candidate for high temperature superconductivity are shown to apply with comparable weight to alloys of metallic hydrogen where hydrogen is a dominant constituent, for example, in the dense group IVa hydrides. The attainment of metallic states should be well within current capabilities of diamond anvil cells, but at pressures considerably lower than may be necessary for hydrogen.



Better call Ashcroft

VOLUME 92, NUMBER 18

PHYSICAL REVIEW LETTERS

week ending
7 MAY 2004

Hydrogen Dominant Metallic Alloys: High Temperature Superconductors?

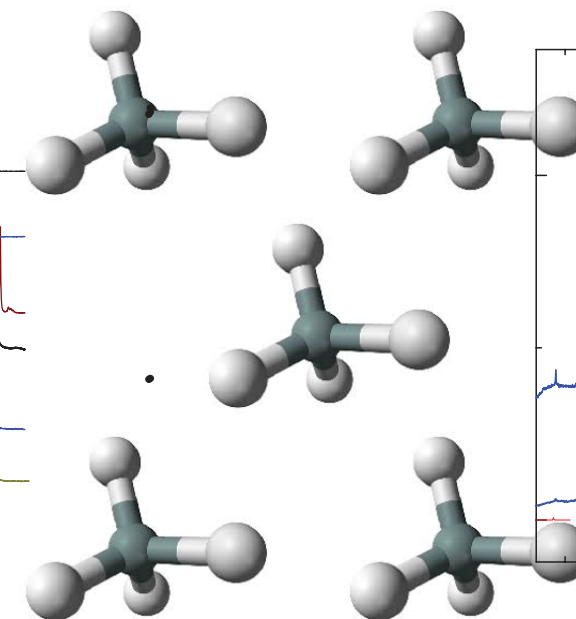
N.W. Ashcroft

Laboratory of Atomic and Solid State Physics, Cornell University, Ithaca, New York 14853-2501, USA

Donostia International Physics Center, San Sebastian, Spain

(Received 29 December 2003; published 6 May 2004)

The arguments suggesting that metallic hydrogen, either as a monatomic or paired metal, should be a candidate for high temperature superconductivity are shown to apply with comparable weight to alloys of metallic hydrogen where hydrogen is a dominant constituent, for example, in the dense group IVa hydrides. The attainment of metallic states should be well within current capabilities of diamond anvil cells, but at pressures considerably lower than may be necessary for hydrogen.

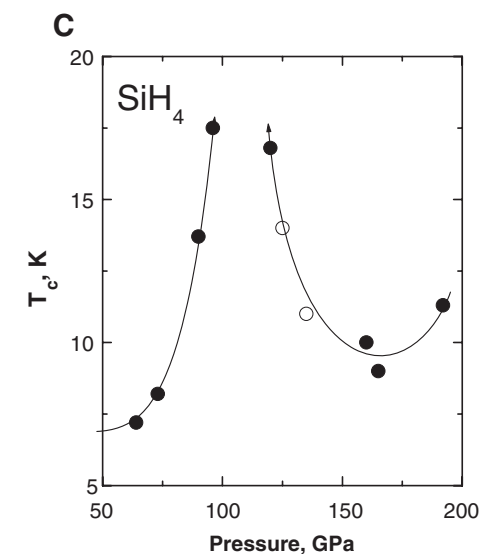
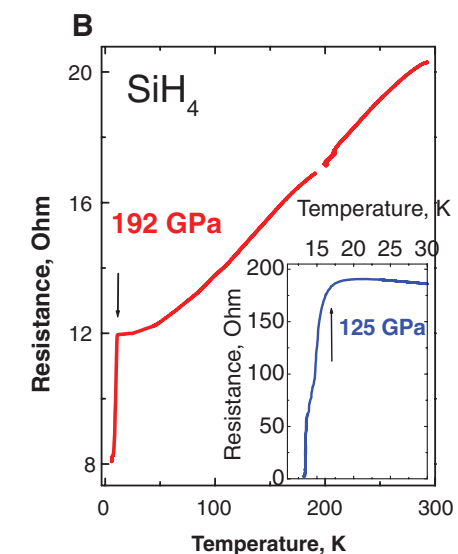
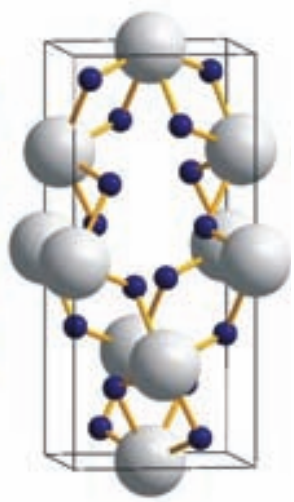


2008

Superconductivity in Hydrogen Dominant Materials: Silane

M. I. Eremets,^{1*} I. A. Trojan,^{1†} S. A. Medvedev,¹ J. S. Tse,² Y. Yao²

The metallization of hydrogen directly would require pressure in excess of 400 gigapascals (GPa), out of the reach of present experimental techniques. The dense group IVa hydrides attract considerable attention because hydrogen in these compounds is chemically precompressed and a metallic state is expected to be achievable at experimentally accessible pressures. We report the transformation of insulating molecular silane to a metal at 50 GPa, becoming superconducting at a transition temperature of $T_c = 17$ kelvin at 96 and 120 GPa. The metallic phase has a hexagonal close-packed structure with a high density of atomic hydrogen, creating a three-dimensional conducting network. These experimental findings support the idea of modeling metallic hydrogen with hydrogen-rich alloy.



17 K is much lower than the predicted Tc

Hydrides at high pressure: search by computers

NATURE VOL. 335 15 SEPTEMBER 1988

NEWS AND VIEWS

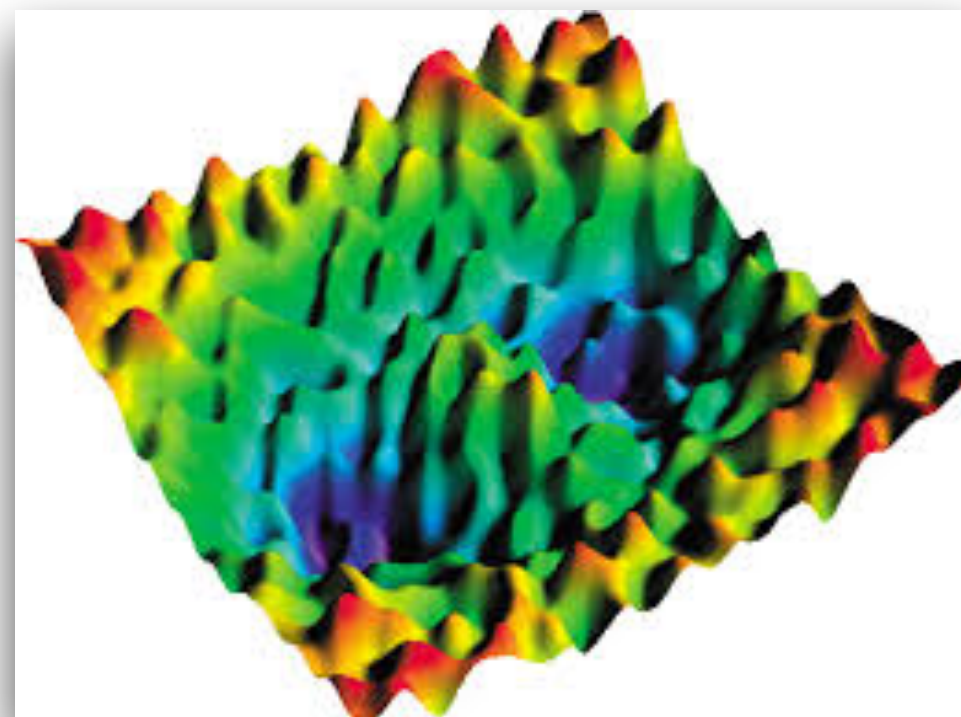
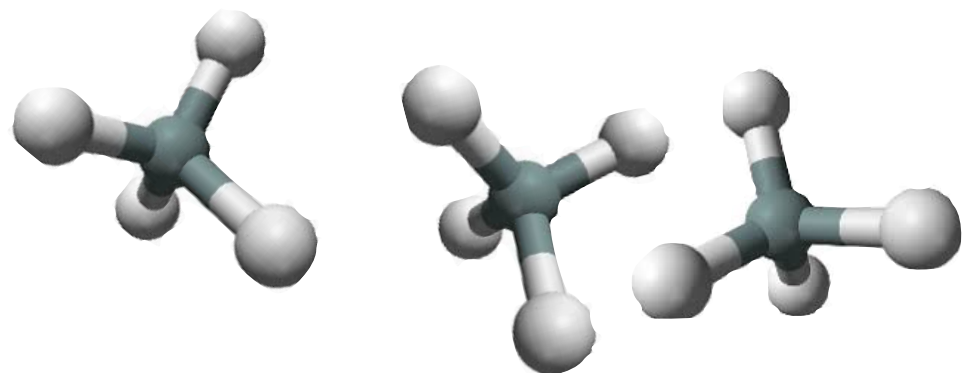
201

Crystals from first principles

by J. Maddox

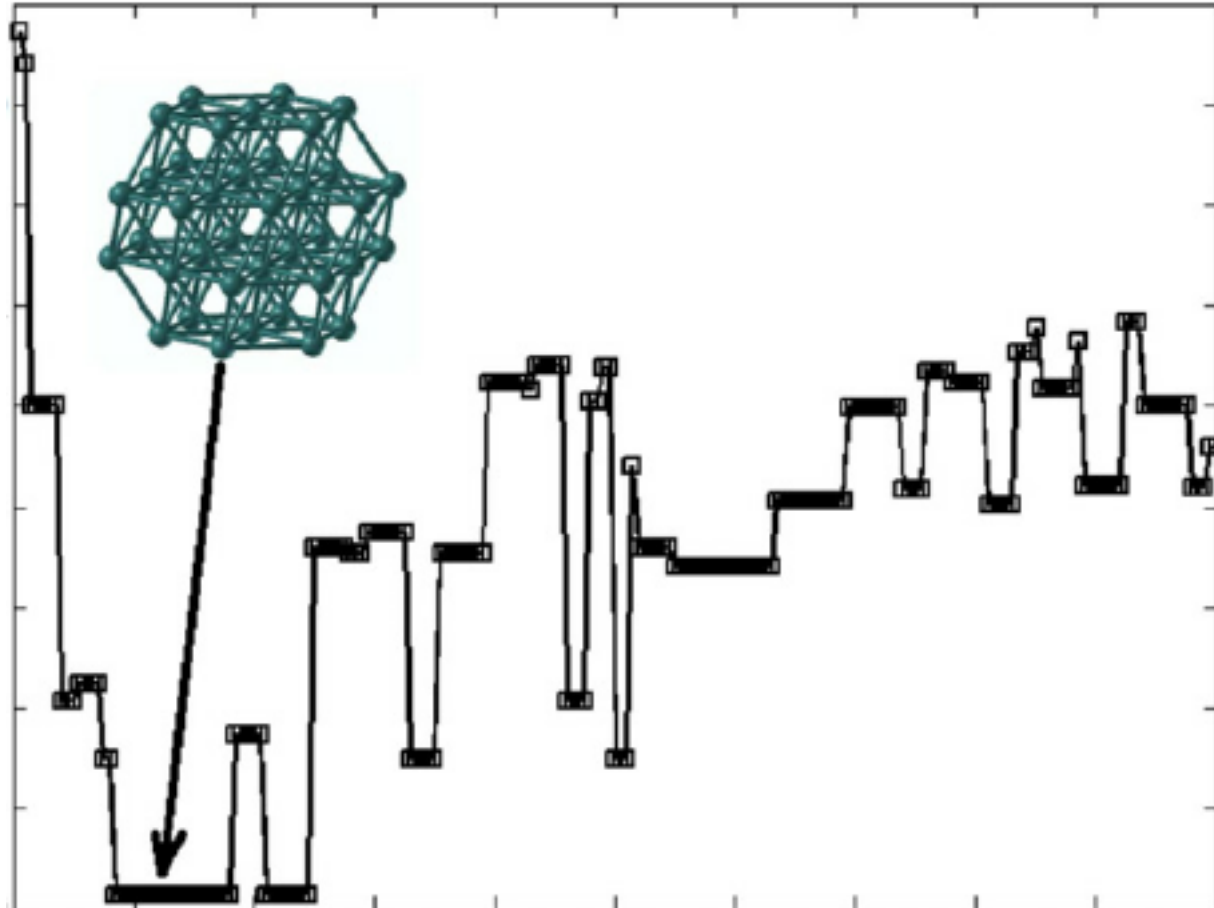
ONE of the continuing scandals in the physical sciences is that it remains in general impossible to predict the structure of even the simplest crystalline solids from a knowledge of their chemical composition. Who, for example, would guess that graphite, not diamond, is the thermodynamically stable allotrope of carbon at ordinary temperature and pressure? Solids such as crystalline water (ice) are still thought to lie beyond mortals' ken.

Yet one would have thought that, by now, it should be possible to equip a sufficiently large computer with a sufficiently large program, type in the formula of the chemical and obtain, as output, the atomic coordinates of the atoms in a unit cell.

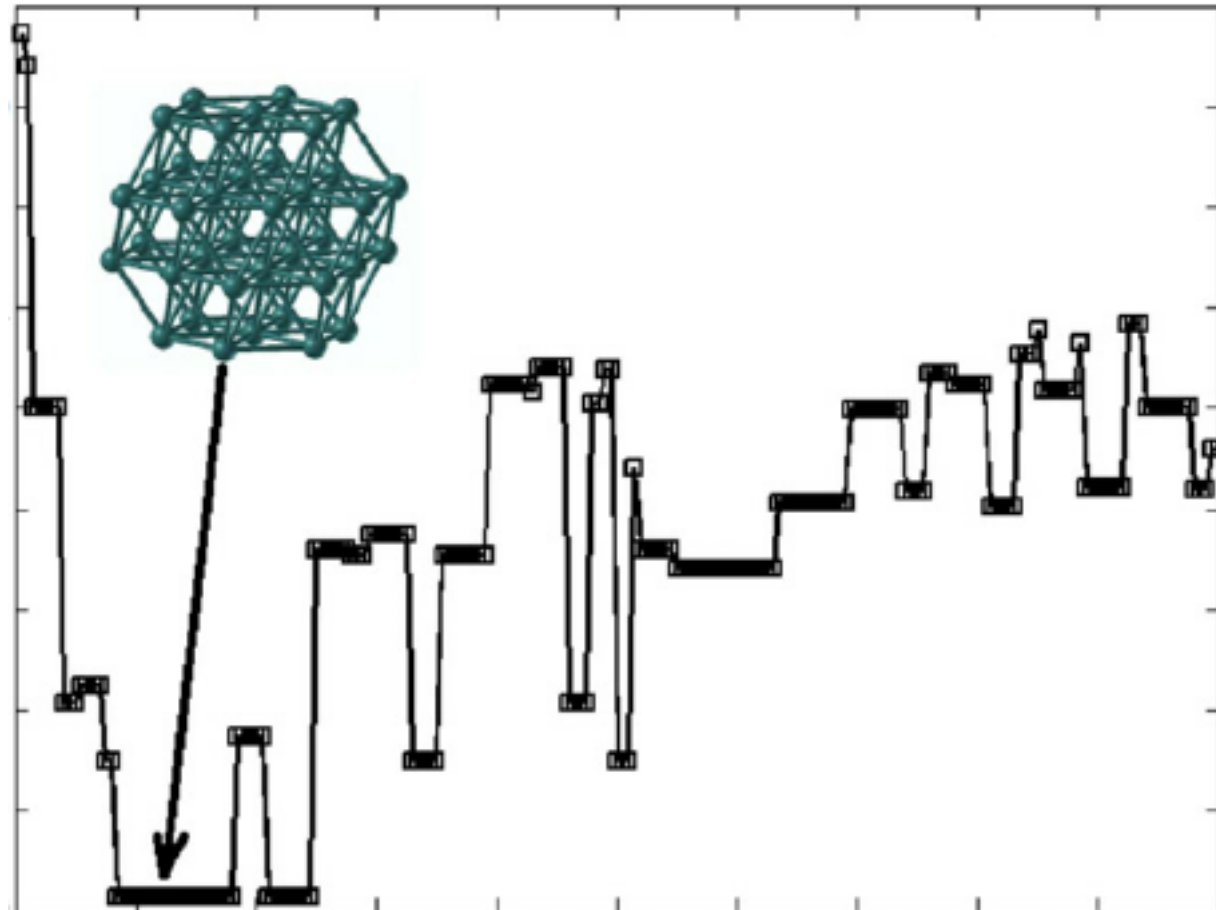


Genetic Algorithms

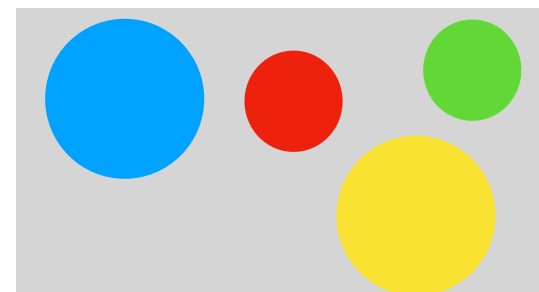
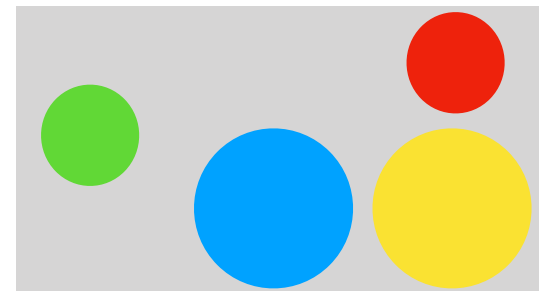
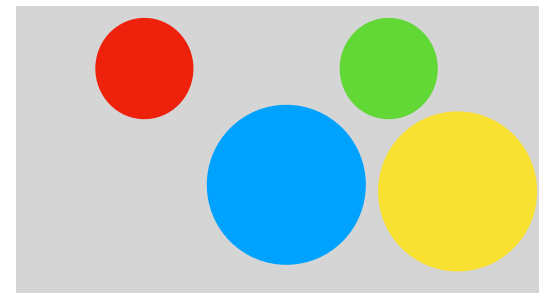
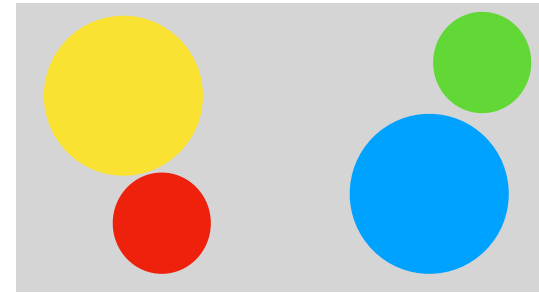
Ab-initio random structure searching (The Columbus egg)



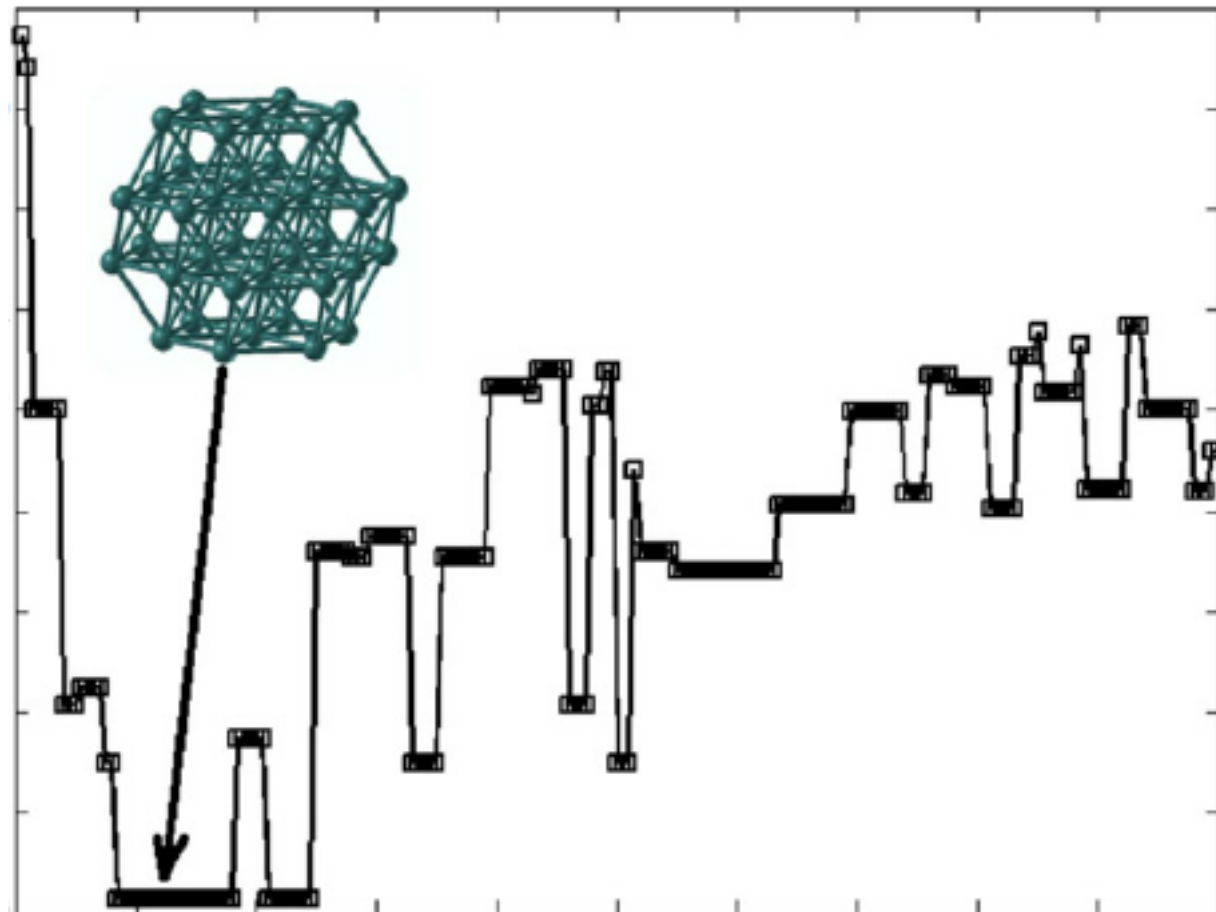
Ab-initio random structure searching (The Columbus egg)



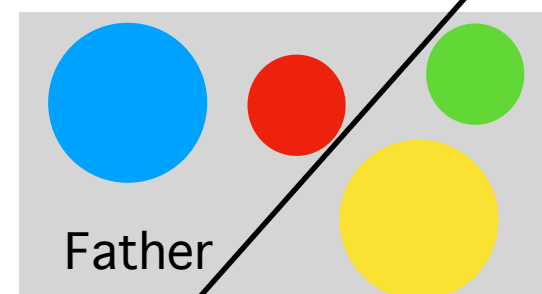
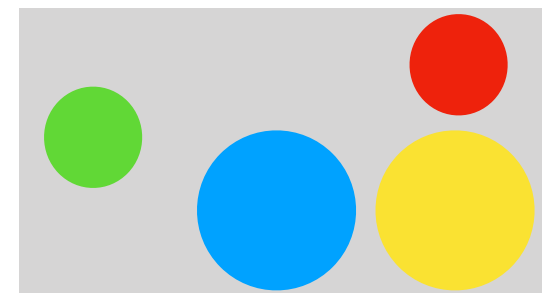
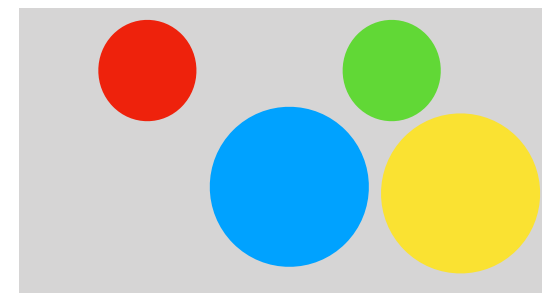
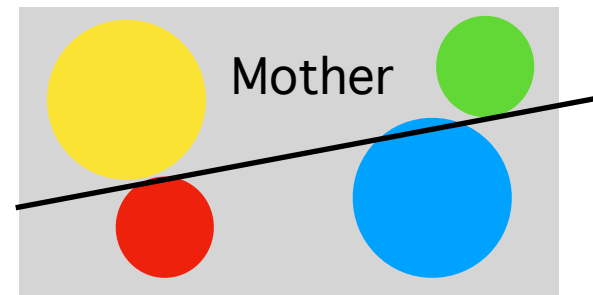
Genetic Algorithms



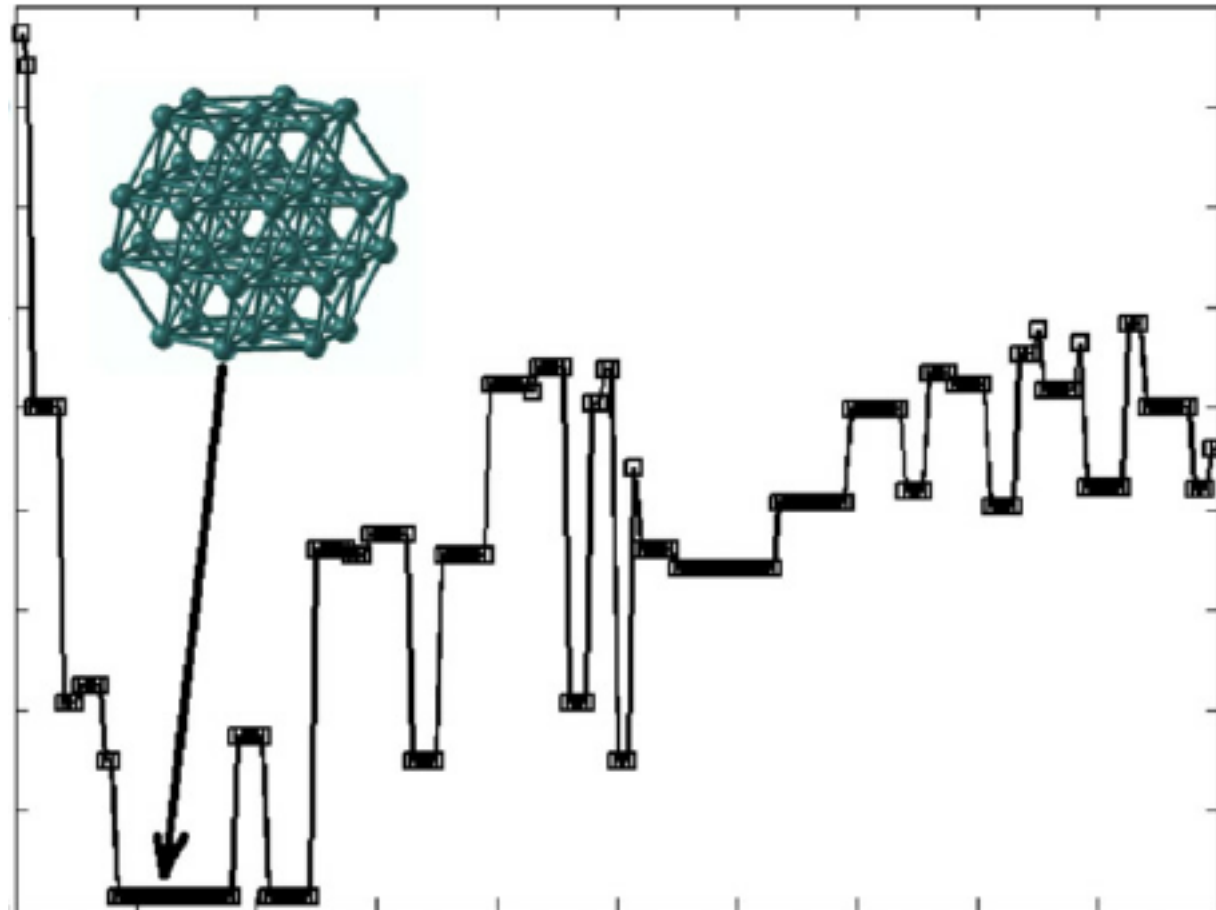
Ab-initio random structure searching (The Columbus egg)



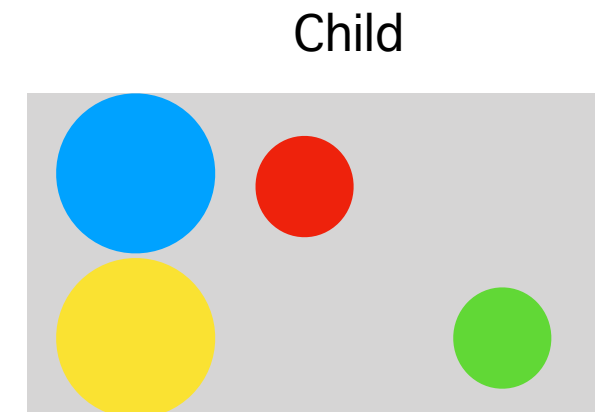
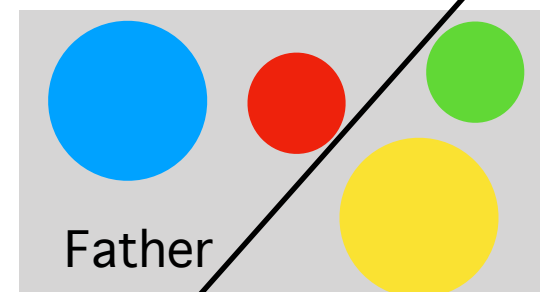
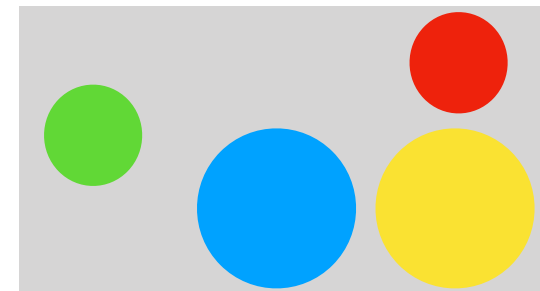
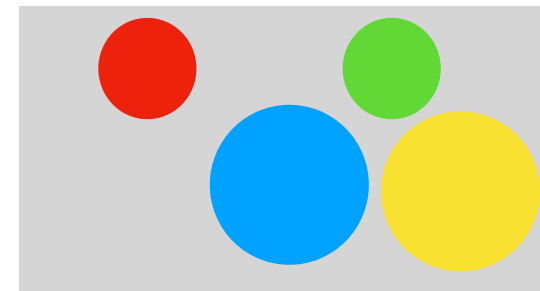
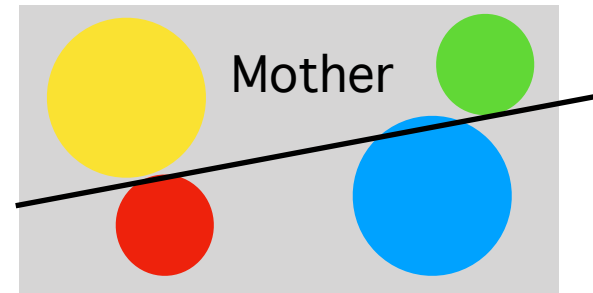
Genetic Algorithms



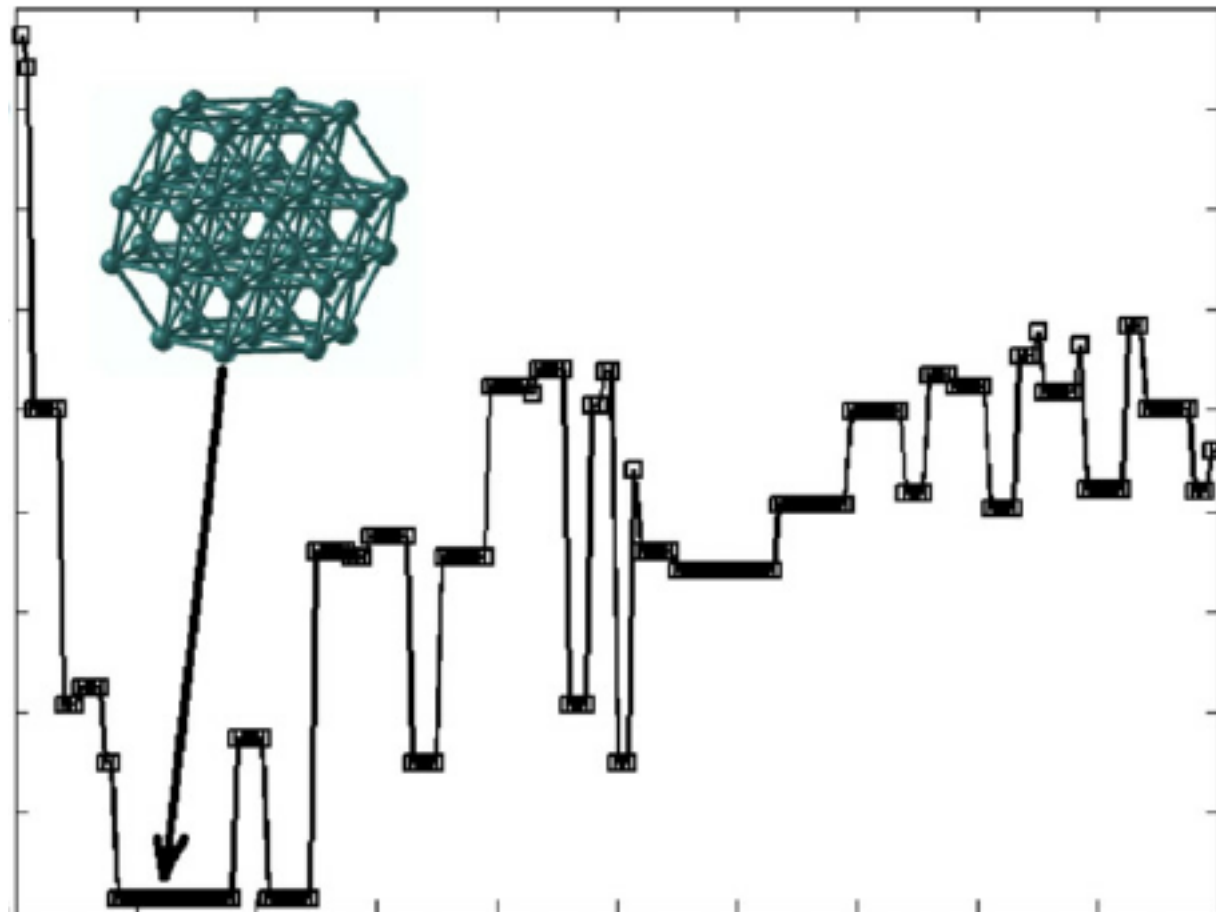
Ab-initio random structure searching (The Columbus egg)



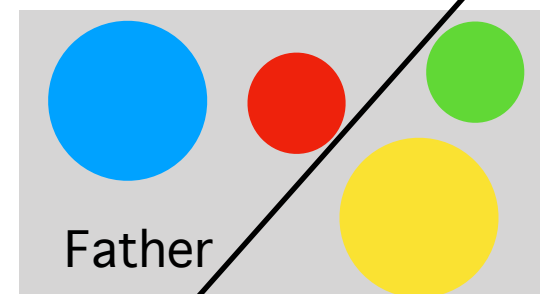
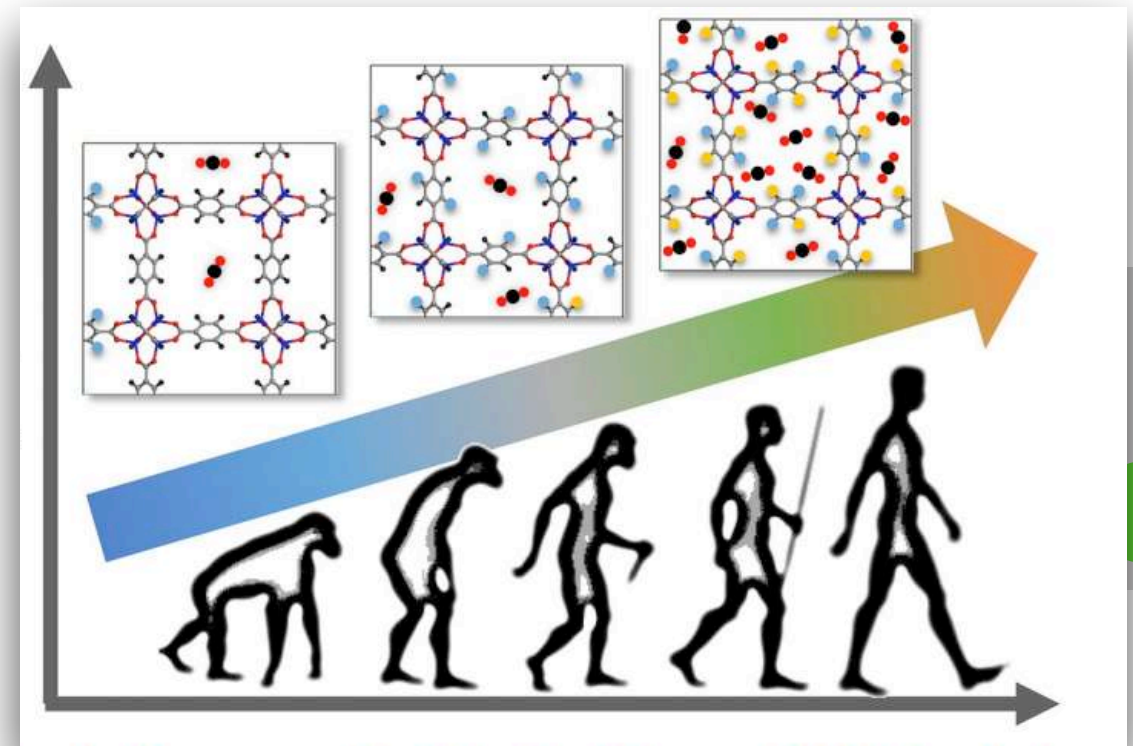
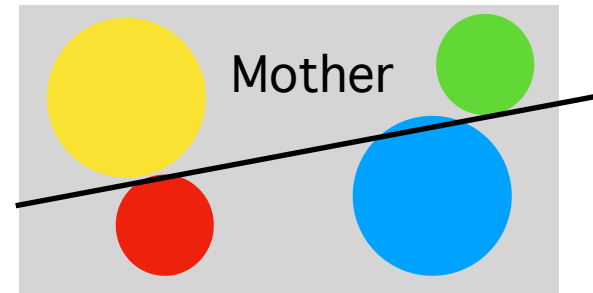
Genetic Algorithms



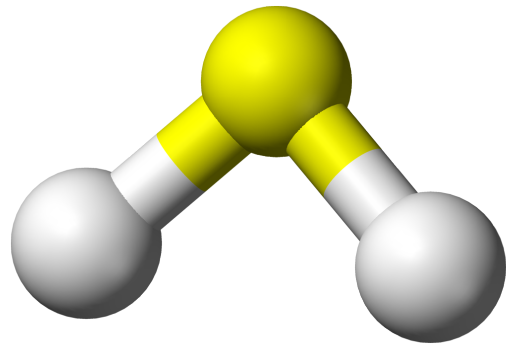
Ab-initio random structure searching (The Columbus egg)



Genetic Algorithms



Hydrogen sulfide: the chemistry changes



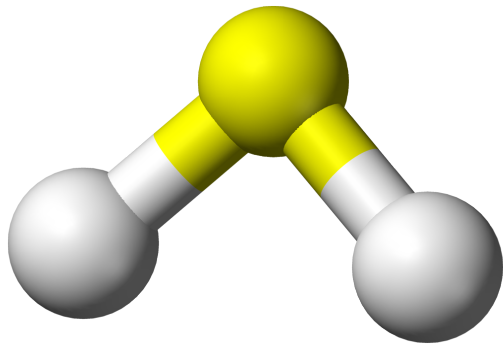
Discovered in 1777

It is a colorless gas with the characteristic foul odor of rotten eggs.

It is very poisonous, corrosive, and flammable, explosive



Hydrogen sulfide: the chemistry changes



Discovered in 1777

It is a colorless gas with the characteristic foul odor of rotten eggs.

It is very poisonous, corrosive, and flammable, explosive



THE JOURNAL OF CHEMICAL PHYSICS **140**, 174712 (2014)



The metallization and superconductivity of dense hydrogen sulfide

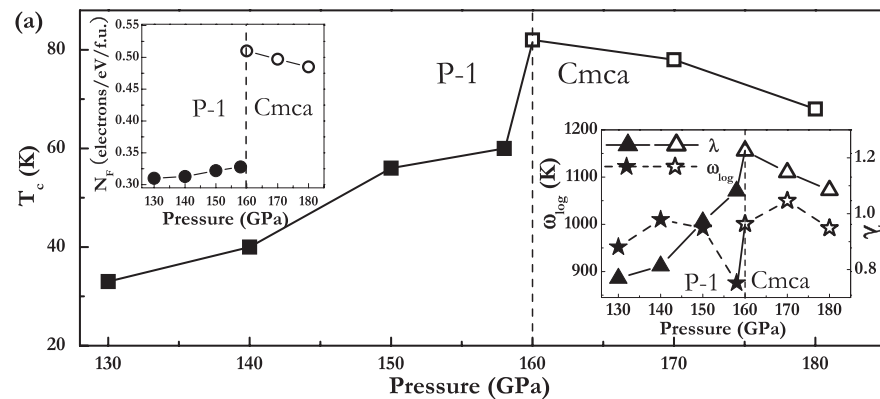
Yinwei Li,^{1,a)} Jian Hao,¹ Hanyu Liu,² Yanling Li,¹ and Yanming Ma^{3,b)}

¹School of Physics and Electronic Engineering, Jiangsu Normal University, Xuzhou 221116, People's Republic of China

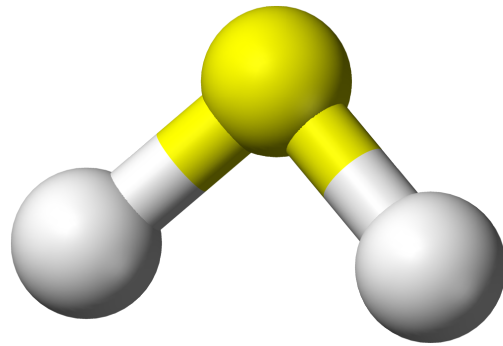
²Department of Physics and Engineering Physics, University of Saskatchewan, Saskatchewan S7N 5E2, Canada

³State Key Laboratory of Superhard Materials, Jilin University, Changchun 130012, People's Republic of China

(Received 20 March 2014; accepted 18 April 2014; published online 7 May 2014)



Hydrogen sulfide: the chemistry changes



Discovered in 1777

It is a colorless gas with the characteristic foul odor of rotten eggs.

It is very poisonous, corrosive, and flammable, explosive



THE JOURNAL OF CHEMICAL PHYSICS **140**, 174712 (2014)



The metallization and superconductivity of dense hydrogen sulfide

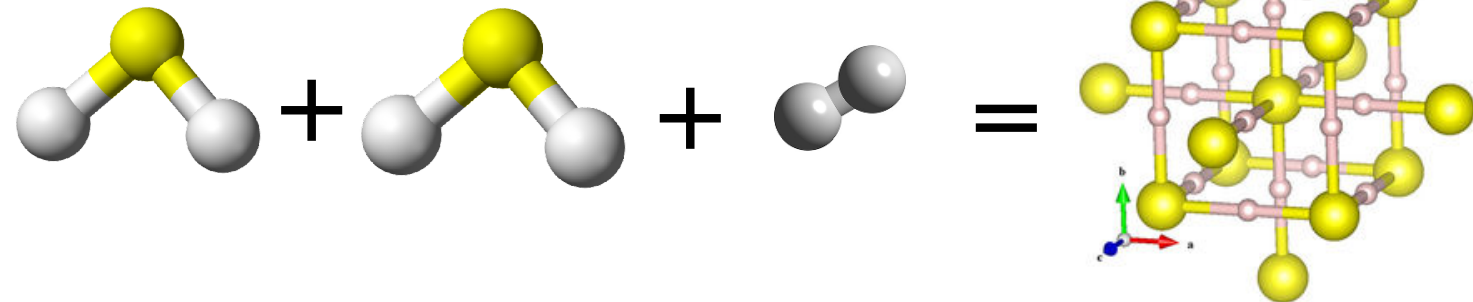
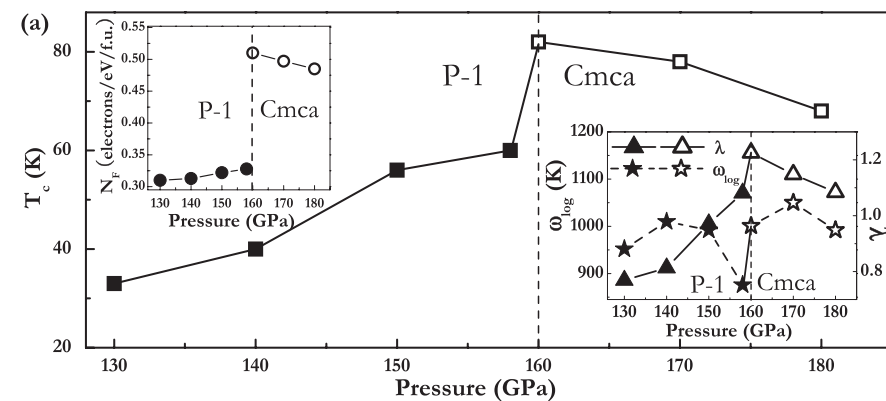
Yinwei Li,^{1,a)} Jian Hao,¹ Hanyu Liu,² Yanling Li,¹ and Yanming Ma^{3,b)}

¹School of Physics and Electronic Engineering, Jiangsu Normal University, Xuzhou 221116, People's Republic of China

²Department of Physics and Engineering Physics, University of Saskatchewan, Saskatchewan S7N 5E2, Canada

³State Key Laboratory of Superhard Materials, Jilin University, Changchun 130012, People's Republic of China

(Received 20 March 2014; accepted 18 April 2014; published online 7 May 2014)



SCIENTIFIC
REPORTS



OPEN

Pressure-induced metallization of dense $(\text{H}_2\text{S})_2\text{H}_2$ with high- T_c superconductivity

SUBJECT AREAS:
THEORY AND
COMPUTATION
CONDENSED-MATTER PHYSICS

Defang Duan^{1,2}, Yunxian Liu¹, Fubo Tian¹, Da Li¹, Xiaoli Huang¹, Zhonglong Zhao¹, Hongyu Yu¹, Bingbing Liu¹, Wenjing Tian² & Tian Cui¹

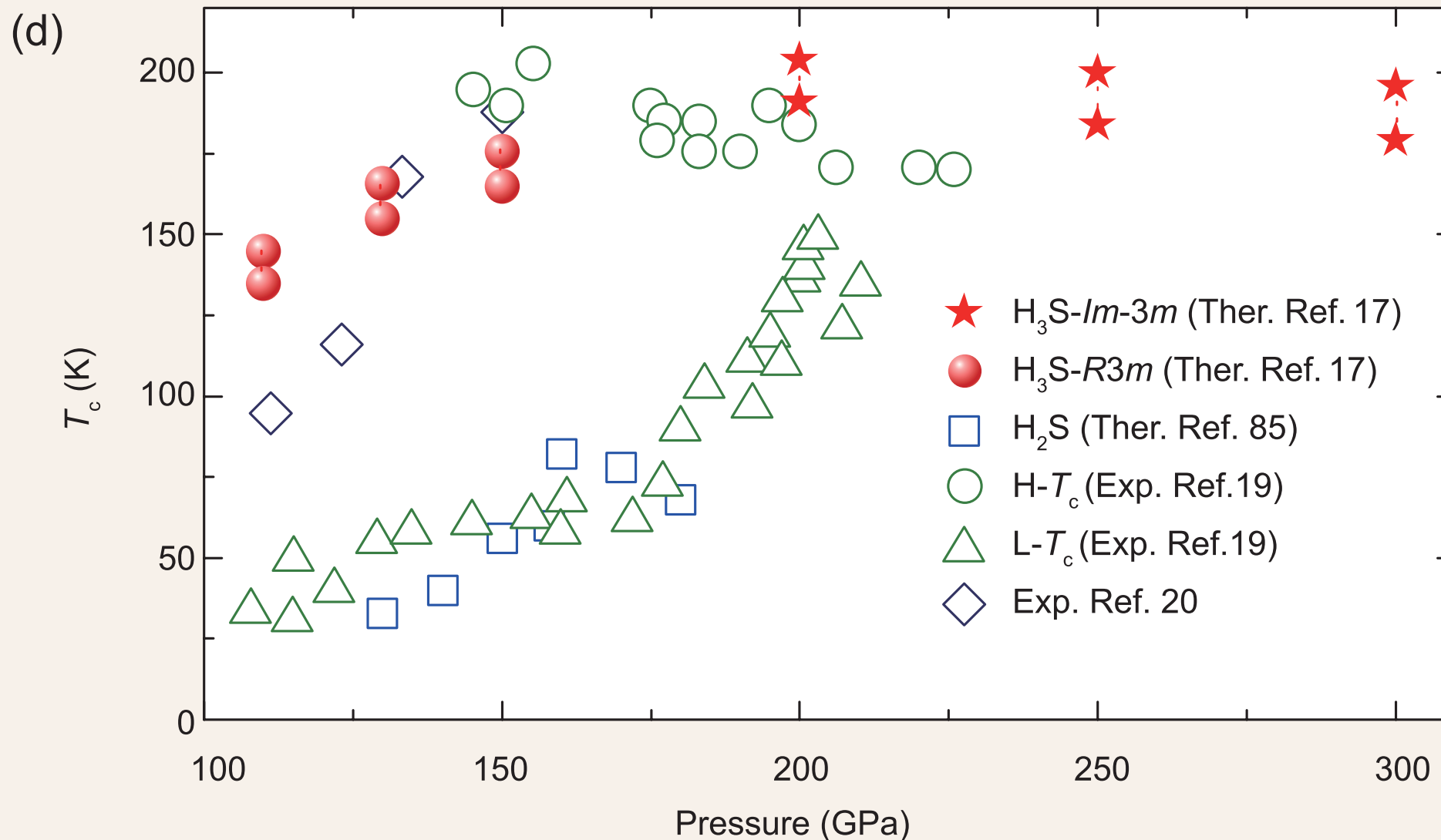
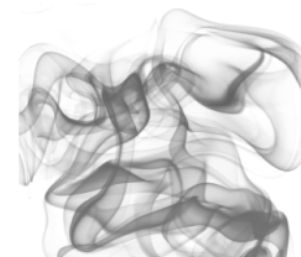
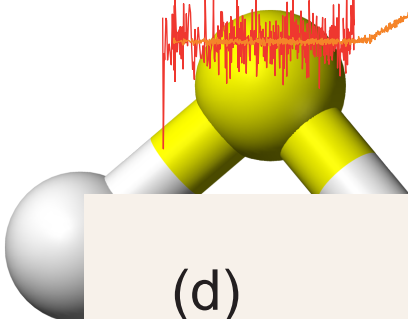
Received
7 July 2014

¹State Key Laboratory of Superhard Materials, College of physics, Jilin University, Changchun, 130012, P. R. China, ²State Key Laboratory of Supramolecular Structure and Materials, Jilin University, Changchun, 130012, P. R. China.

Hydrogen sulfide: the chemistry changes

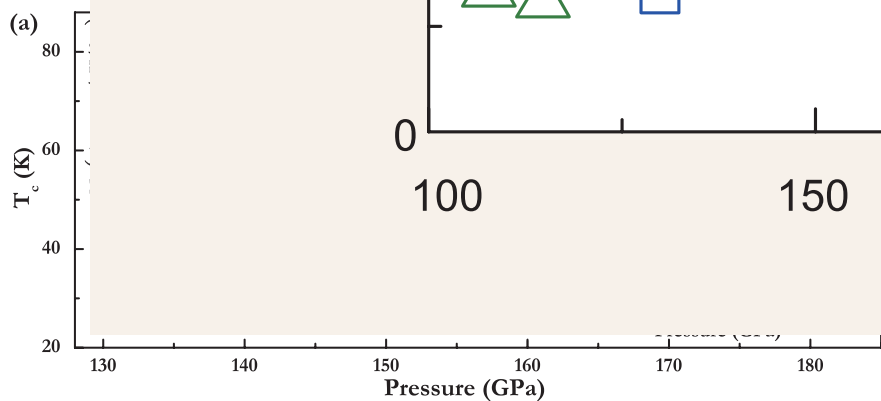
Discovered in 1777

It is a colorless gas with the characteristic foul odor of



The meta

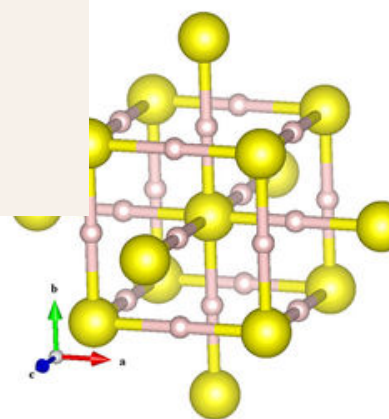
Yinwe
¹School
 People
²Depart
 Saskat
³State
 People
 (Recei



dense
 activity

Hongyu Yu¹,

¹P. R. China, ²State Key



Eremets's experiment

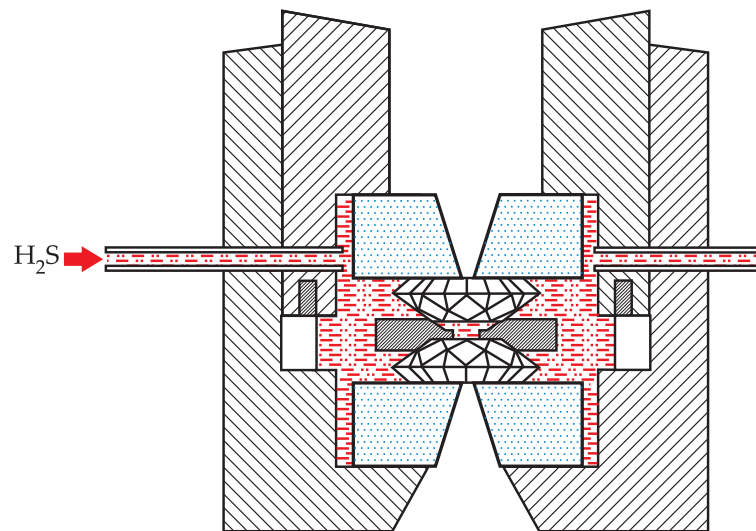
Max-Planck-Institut für Chemie (Mainz), Germany

LETTER

doi:10.1038/nature14964

Conventional superconductivity at 203 kelvin at high pressures in the sulfur hydride system

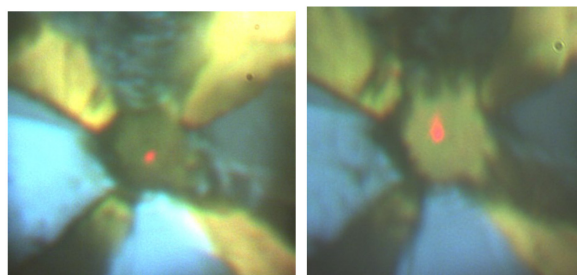
A. P. Drozdov^{1*}, M. I. Eremets^{1*}, I. A. Troyan¹, V. Ksenofontov² & S. I. Shylin²



9 GPa

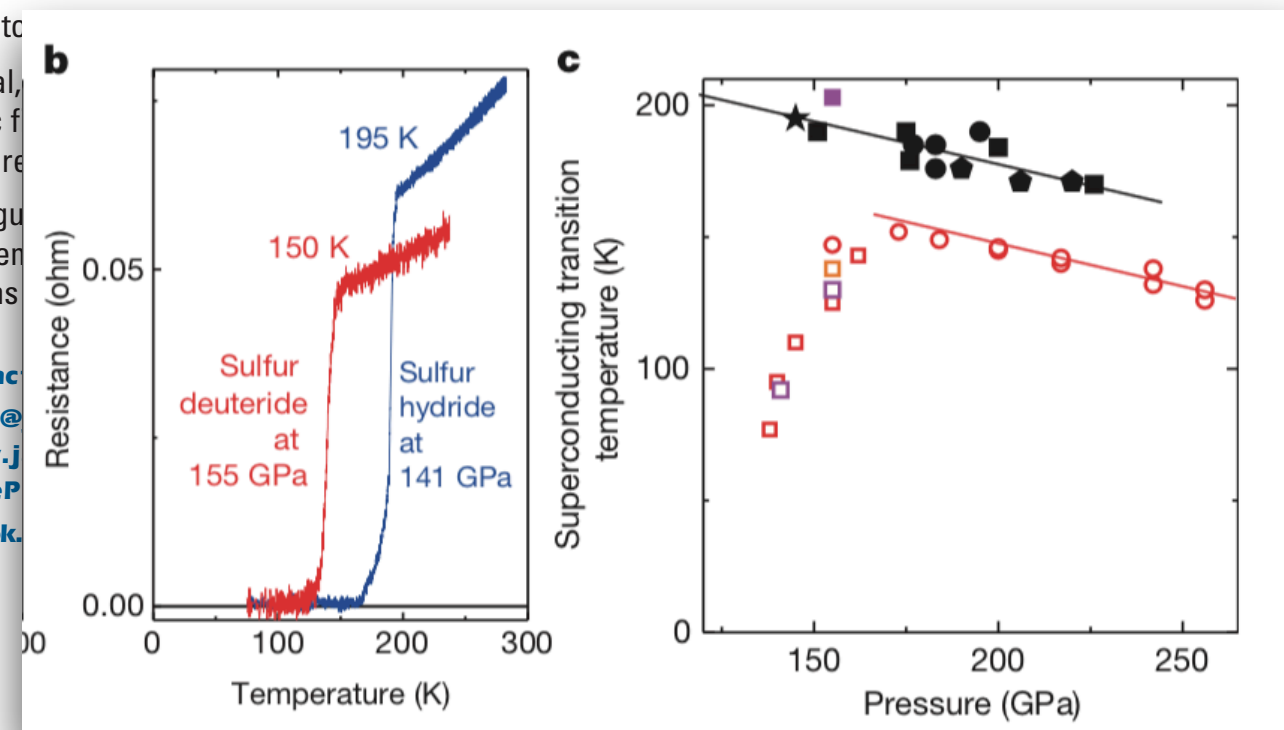
11 GPa

79 GPa



92 GPa

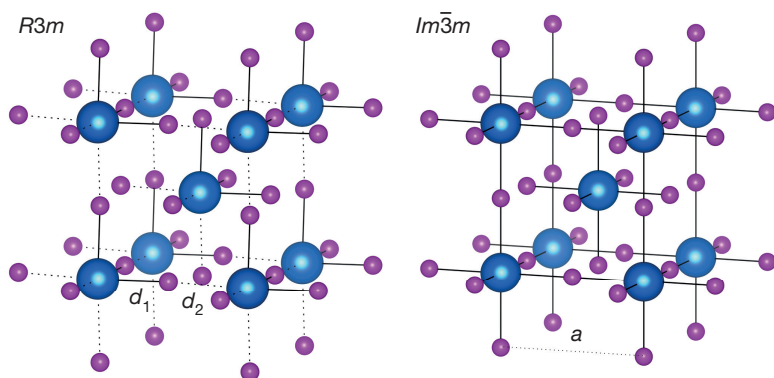
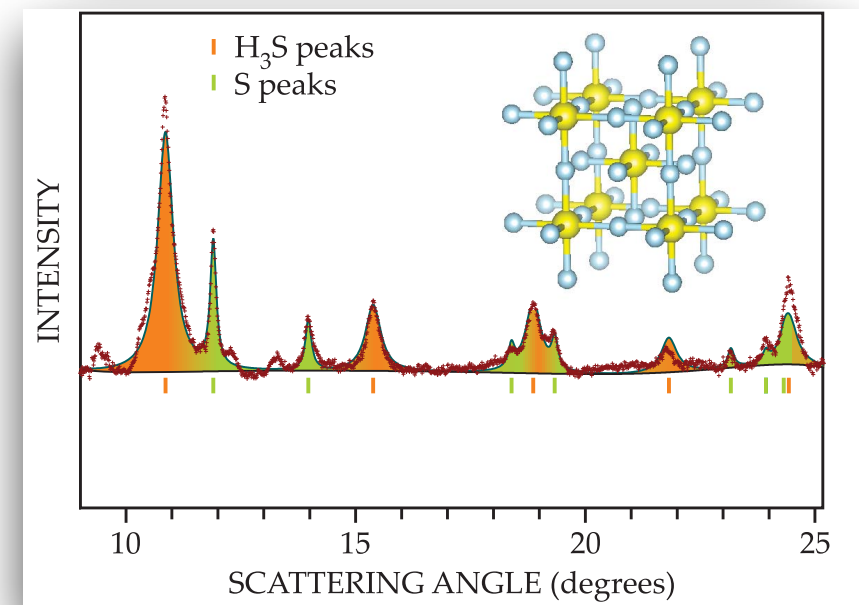
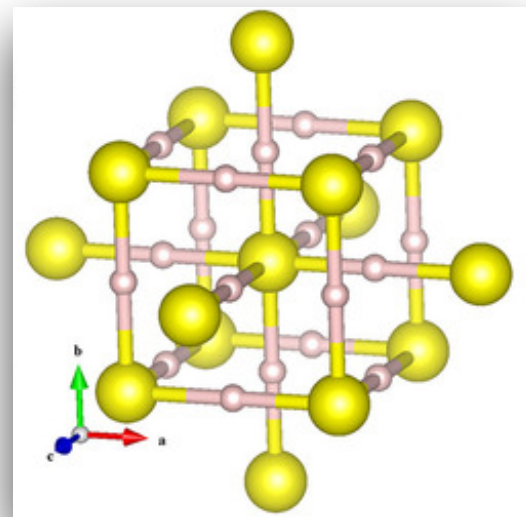
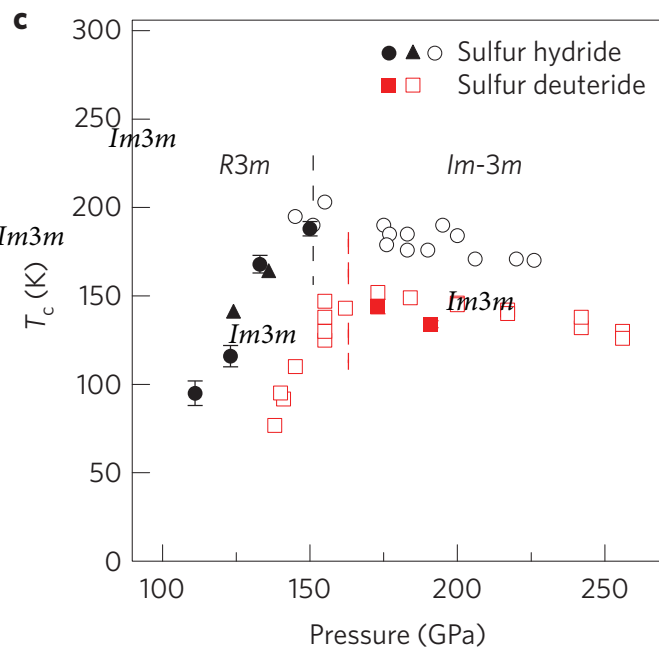
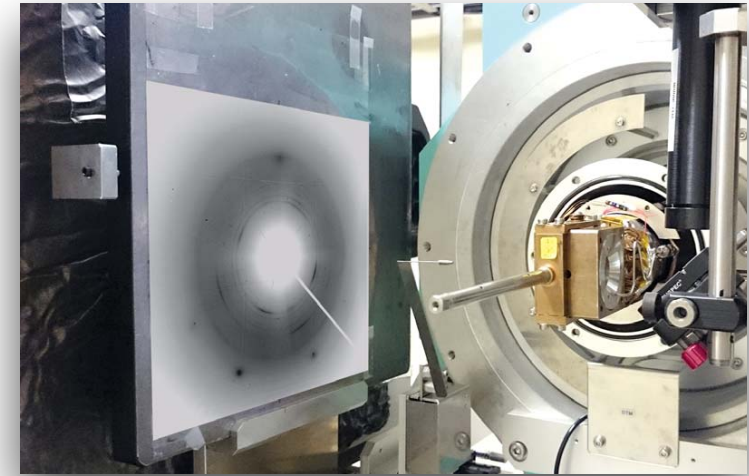
154 GPa



It is true

Crystal structure of the superconducting phase of sulfur hydride

Mari Einaga^{1*}, Masafumi Sakata¹, Takahiro Ishikawa¹, Katsuya Shimizu^{1†}, Mikhail I. Erements^{2†}, Alexander P. Drozdov², Ivan A. Troyan², Naohisa Hirao³ and Yasuo Ohishi³



It is true

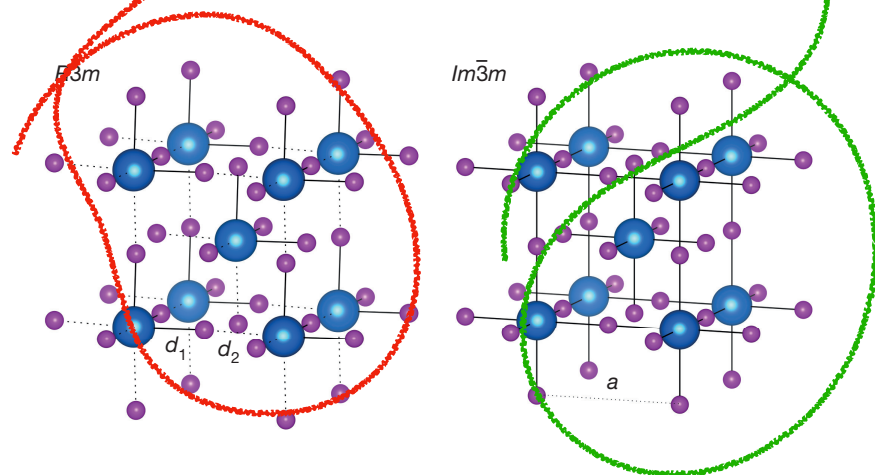
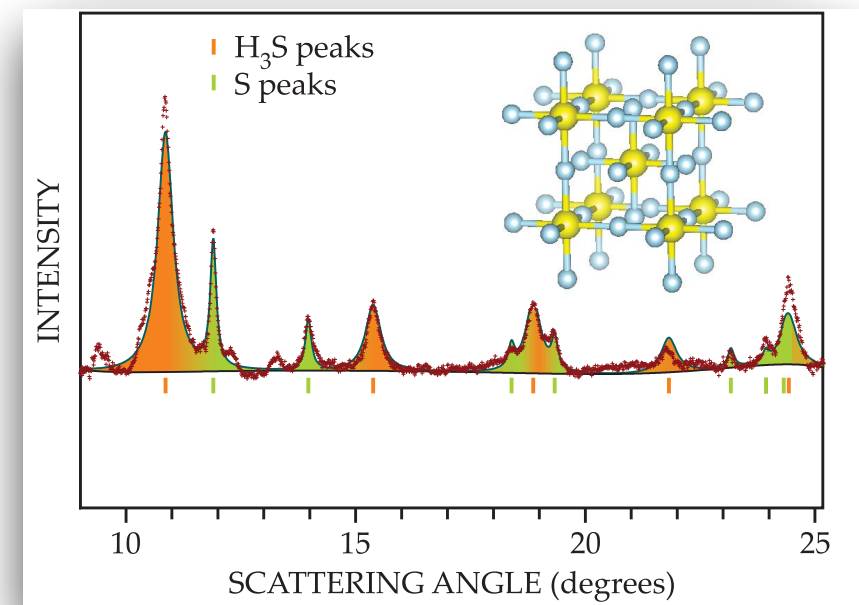
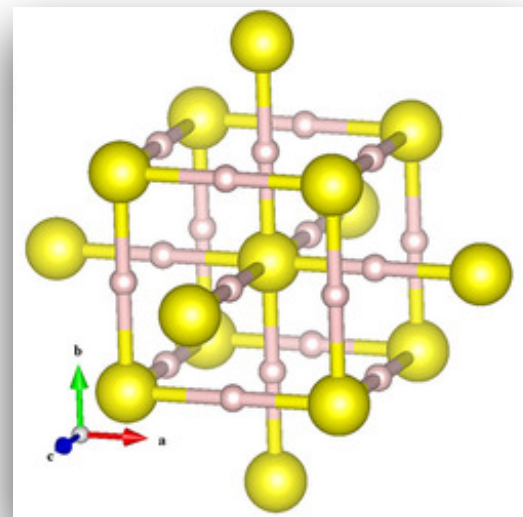
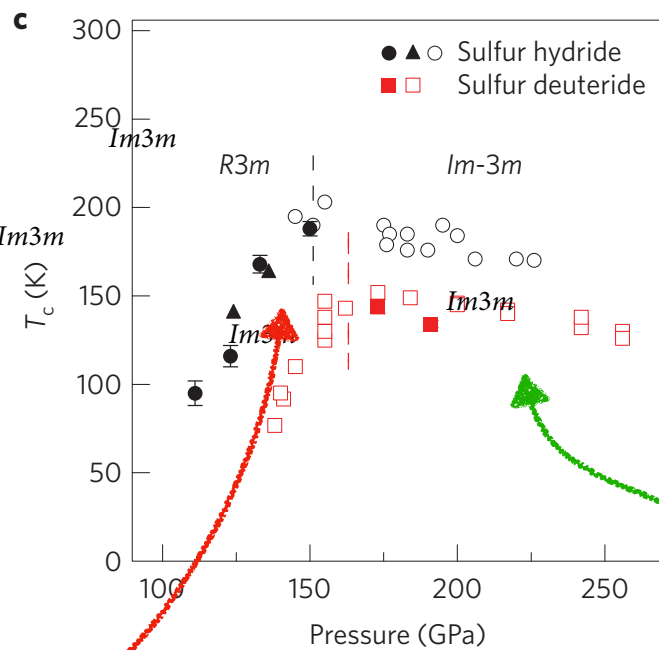
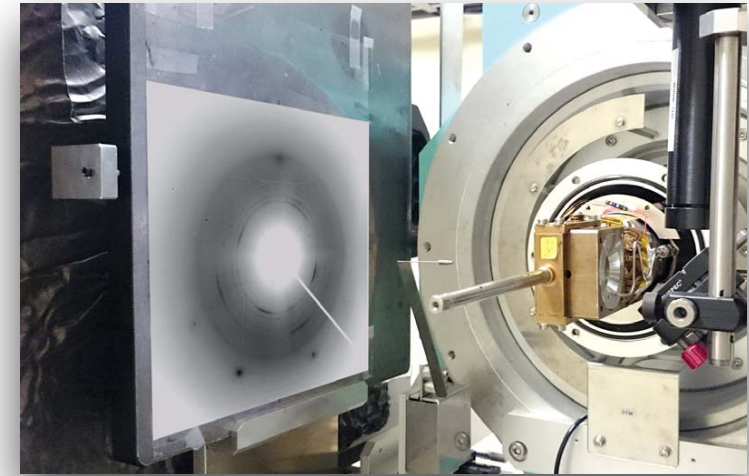
nature
physics

LETTERS

PUBLISHED ONLINE: 9 MAY 2016 | DOI: 10.1038/NPHYS3760

Crystal structure of the superconducting phase of sulfur hydride

Mari Einaga^{1*}, Masafumi Sakata¹, Takahiro Ishikawa¹, Katsuya Shimizu^{1†}, Mikhail I. Erements^{2†}, Alexander P. Drozdov², Ivan A. Troyan², Naohisa Hirao³ and Yasuo Ohishi³



First-principles theories predict the **crystal structure** and **superconducting critical temperature** as a function of the pressure

Room temperature superconductivity? It depends on where the room is.



Vostok base in Antarctica

In 1983 a temperature of $-89.2\text{ }^{\circ}\text{C}$ was registered

Room temperature superconductivity? It depends on where the room is.



Vostok base in Antarctica

In 1983 a temperature of $-89.2\text{ }^{\circ}\text{C}$ was registered

Room temperature superconductivity? It depends on where the room is.



Vostok base in Antarctica

In 1983 a temperature of $-89.2\text{ }^{\circ}\text{C}$ was registered

Flurry of predictions

Periodic table of binary hydride superconductors

H																	He
LiH ₆ 82	BeH ₂ 44											BH 21	C	N	O	F	Ne
Na	MgH ₄ 30	T _c (K) Theoretically predicted										AlH ₅ 140	SiH _x ~20	PH ₂ 87	SH ₃ 204	Cl	Ar
KH ₁₀ 140	CaH ₆ 235	ScH ₉ 233	TiH ₁₄ 54	VH ₈ 72	CrH ₃ 81	Mn	Fe	Co	Ni	Cu	Zn	GaH ₃ 123	GeH ₄ 220	AsH ₄ 90	SeH ₃ 120	BrH ₂ 12	Kr
Rb	SrH ₁₀ 259	YH ₁₀ 326	ZrH ₁₄ 88	NbH ₄ 47	Mo	TcH ₂ 11	RuH ₃ 1.3	RhH 2.5	PdH 5	Ag	Cd	InH ₃ 41	SnH ₁₄ 90	SbH ₄ 95	TeH ₄ 100	IH ₂ 30	XeH 29
Cs	BaH ₆ 38		HfH ₂ 76	TaH ₆ 136	WH ₅ 60	Re	OsH 2	IrH 7	PtH 25	AuH 21	Hg	Tl	PbH ₈ 107	BiH ₅ 110	PoH ₄ 50	At	Rn
FrH ₇ 63	RaH ₁₂ 116		Rf	Db	Sg	Bh	Hs	Mt	Ds	Rg	Cn	Nh	Fl	Mc	Lv	Ts	Og
Lanthanides	LaH ₁₀ 288	CeH ₈ 117	PrH ₈ 31	NdH ₈ 6	Pm	Sm	Eu	Gd	Tb	Dy	HoH ₄ 37	ErH ₁₅ 30	TmH ₈ 21	Yb	LuH ₁₂ 7		
Actinides	AcH ₁₀ 250	ThH ₁₀ 221	PaH ₉ 62	UH ₈ 35	NpH ₇ 10	Pu	AmH ₈ 0.3	CmH ₈ 0.9	Bk	Cf	Es	Fm	Md	No	Lr		

Potential high- T_c superconducting lanthanum and yttrium hydrides at high pressure

Hanyu Liu^a, Ivan I. Naumov^a, Roald Hoffmann^b, N. W. Ashcroft^c, and Russell J. Hemley^{d,e,1}

PRL 119, 107001 (2017)

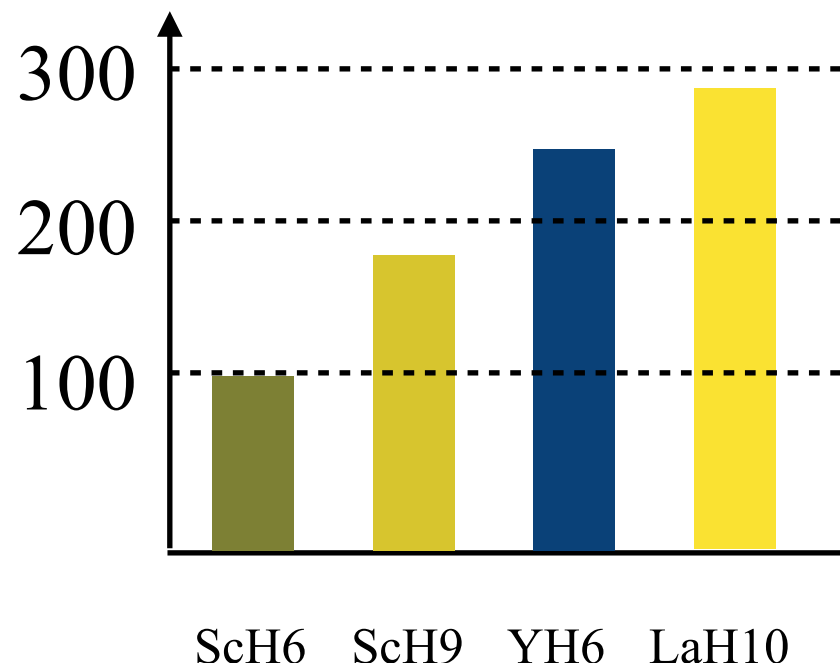
PHYSICAL REVIEW LETTERS

week ending
8 SEPTEMBER 2017

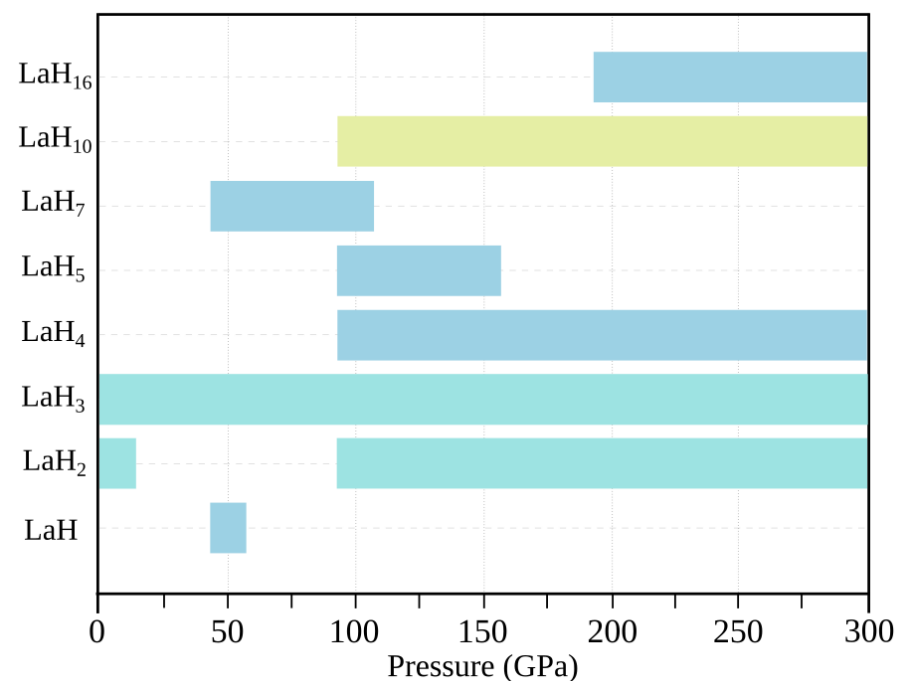
Hydrogen Clathrate Structures in Rare Earth Hydrides at High Pressures: Possible Route to Room-Temperature Superconductivity

Feng Peng,^{1,2,3} Ying Sun,³ Chris J. Pickard,⁴ Richard J. Needs,⁵ Qiang Wu,⁶ and Yanming Ma^{3,7,*}

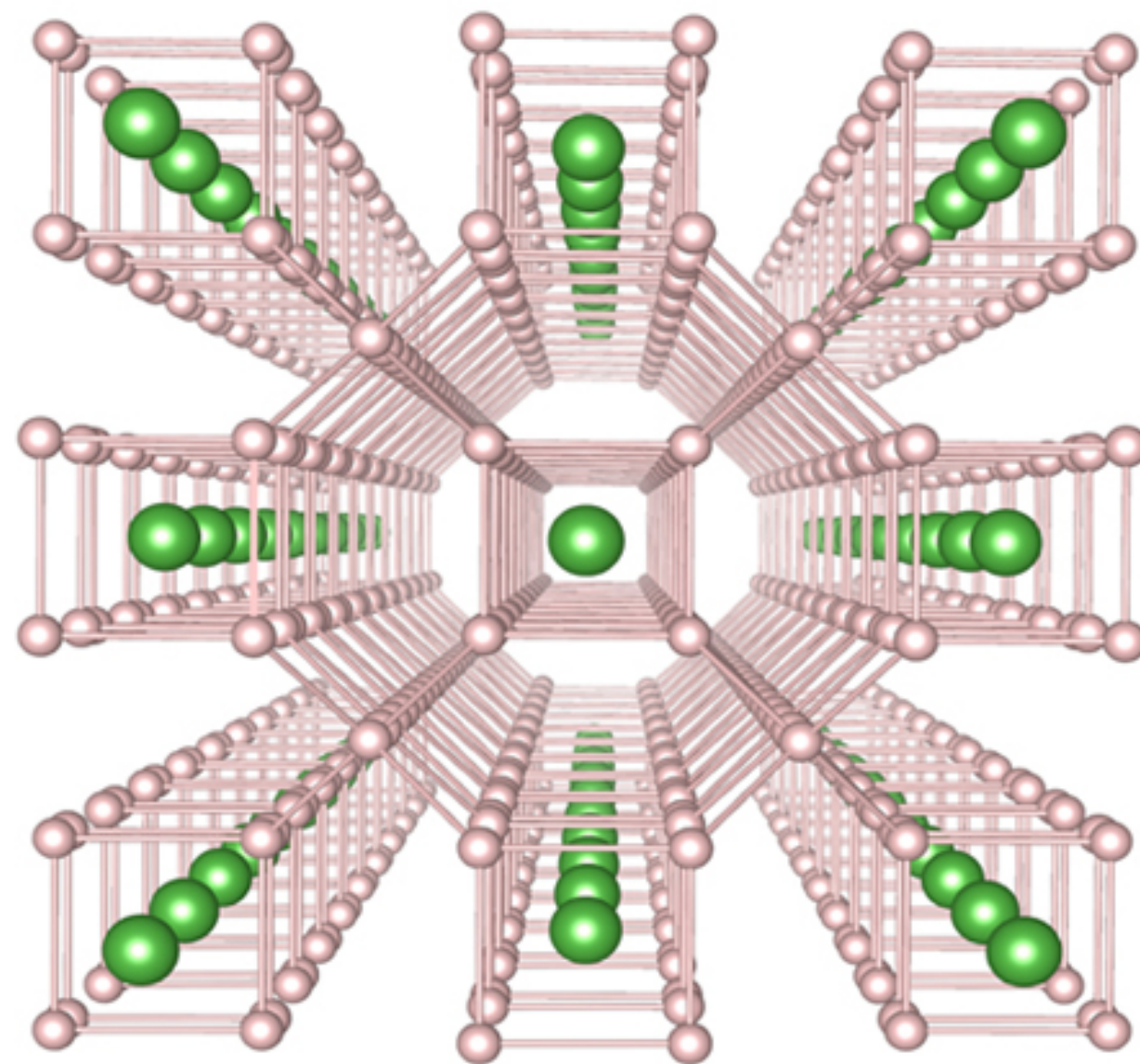
$T_c=260$ K



Stability range

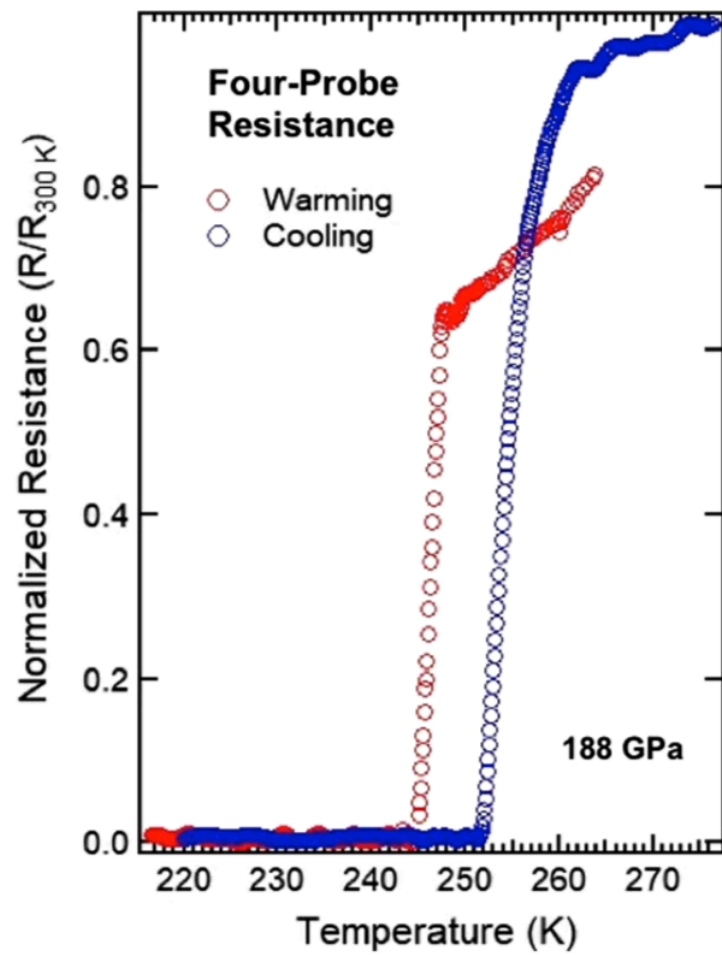
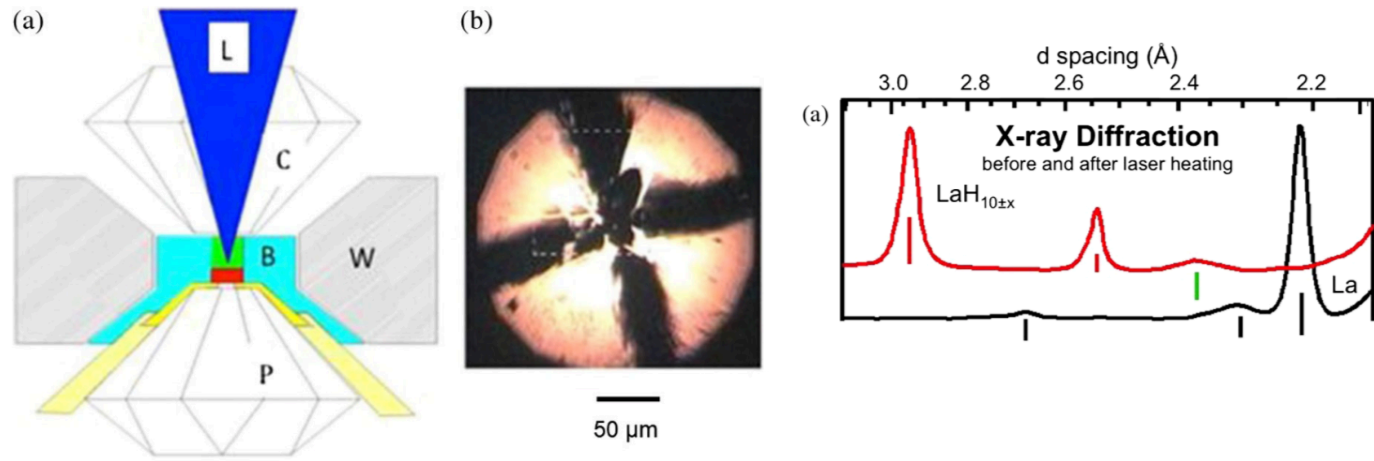


LaH₁₀



Evidence for Superconductivity above 260 K in Lanthanum Superhydride at Megabar Pressures

Maddury Somayazulu,^{1,*} Muhtar Ahart,¹ Ajay K. Mishra,^{2,*} Zachary M. Geballe,² Maria Baldini,^{2,§} Yue Meng,³ Viktor V. Struzhkin,² and Russell J. Hemley^{1,†}



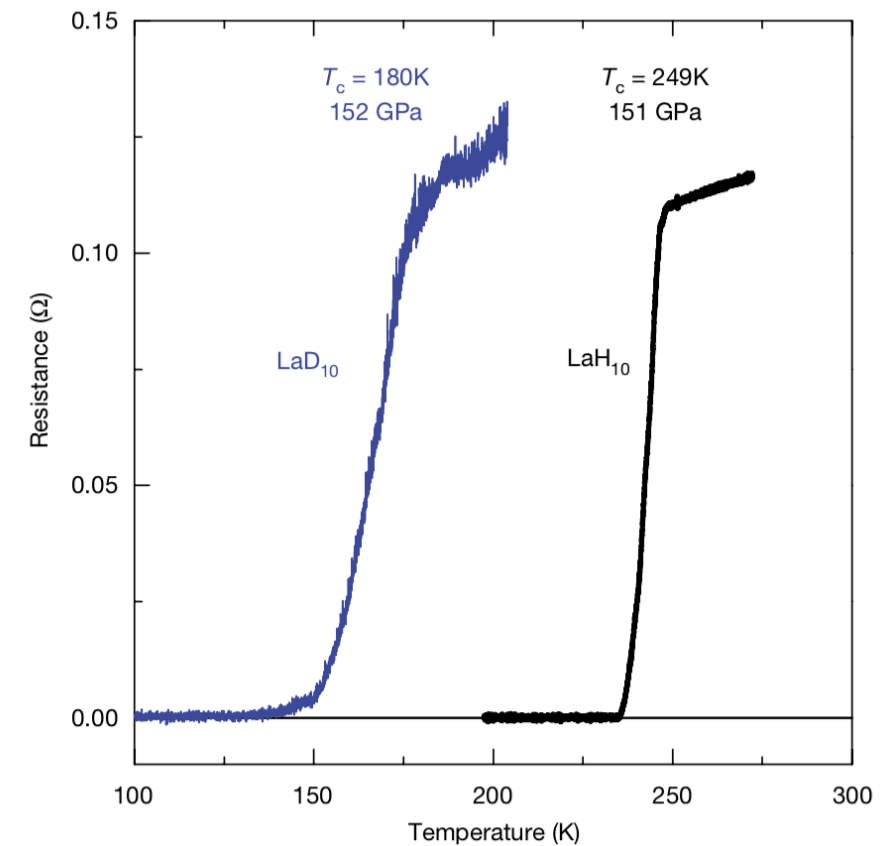
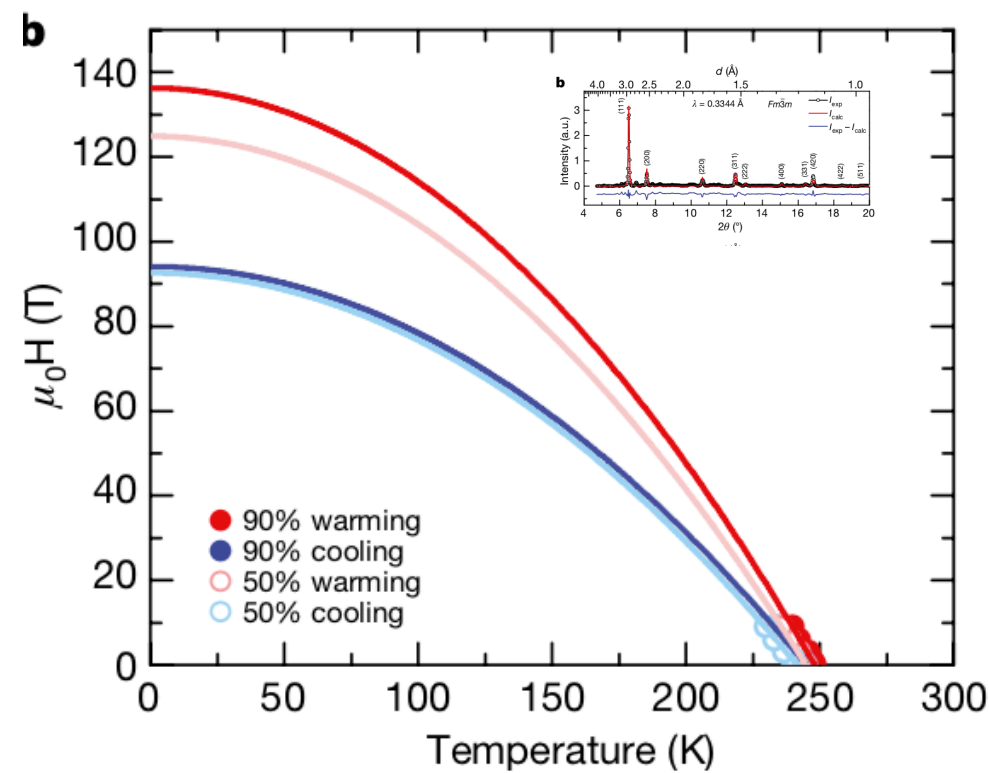
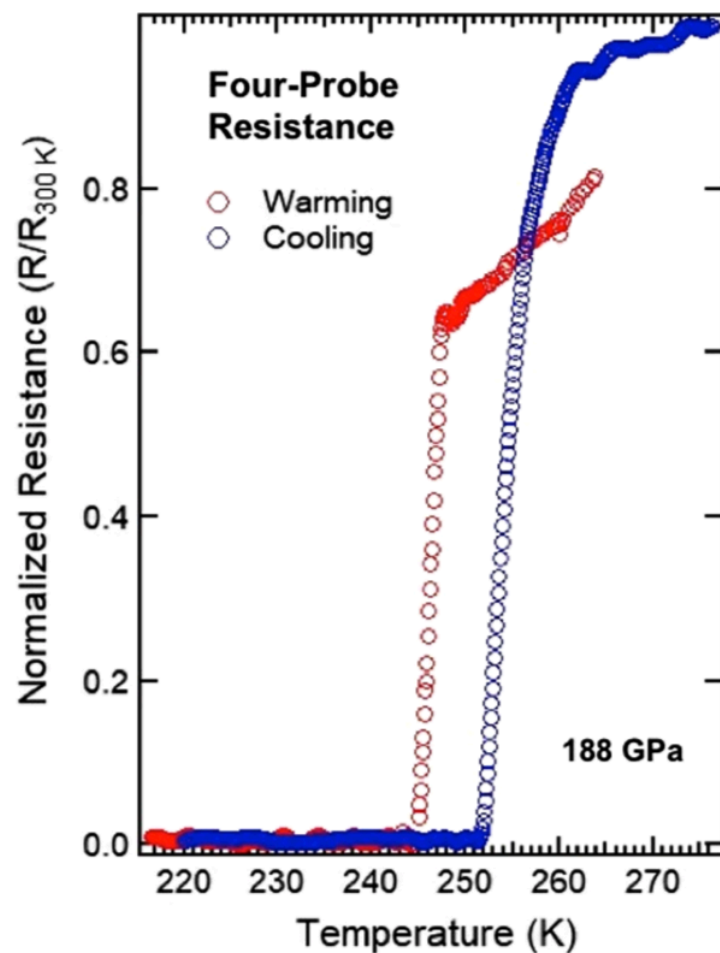
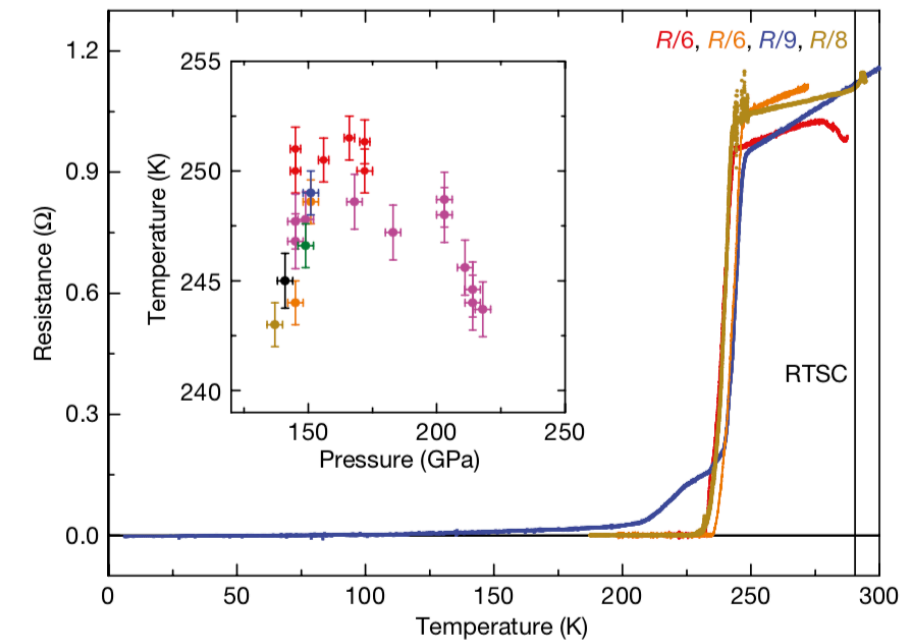
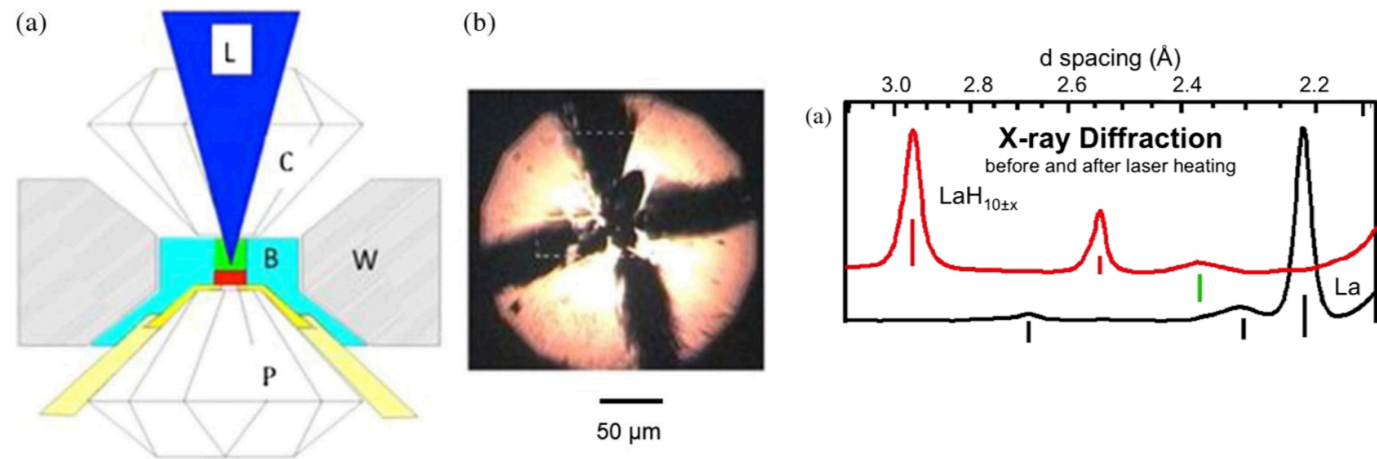
Editors' Suggestion Featured in Physics

Evidence for Superconductivity above 260 K in Lanthanum Superhydride at Megabar Pressures

Maddury Somayazulu,^{1,*} Muhtar Ahart,¹ Ajay K. Mishra,^{2,*} Zachary M. Geballe,² Maria Baldini,^{2,§} Yue Meng,³ Viktor V. Struzhkin,² and Russell J. Hemley^{1,†}

Superconductivity at 250 K in lanthanum hydride under high pressures

A. P. Drozdov^{1,7}, P. P. Kong^{1,7}, V. S. Minkov^{1,7}, S. P. Besedin^{1,7}, M. A. Kuzovnikov^{1,6,7}, S. Mozaffari², L. Balicas², F. F. Balakirev³, D. E. Graf², V. B. Prakapenka⁴, E. Greenberg⁴, D. A. Knyazev¹, M. Tkacz⁵ & M. I. Erements^{1,*}



Quantum crystal structure in the 250-kelvin superconducting lanthanum hydride

<https://doi.org/10.1038/s41586-020-1955-z>

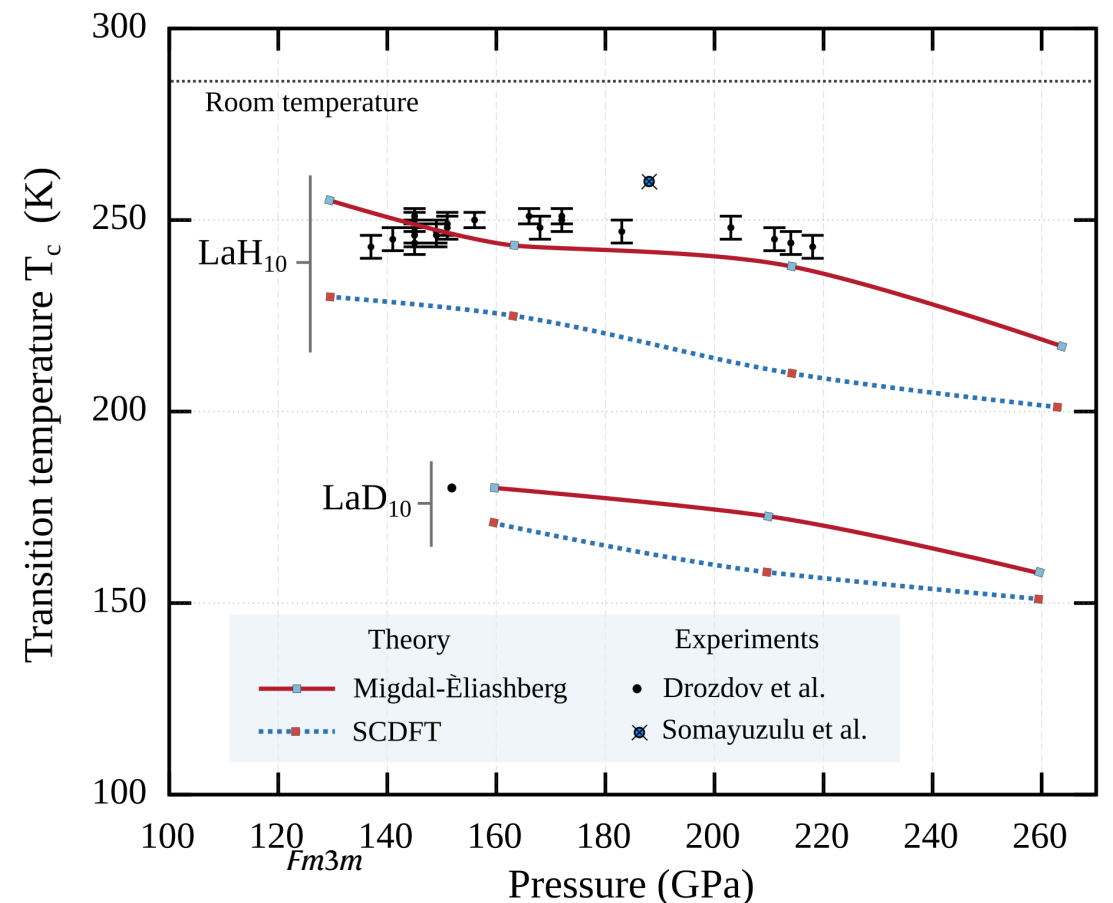
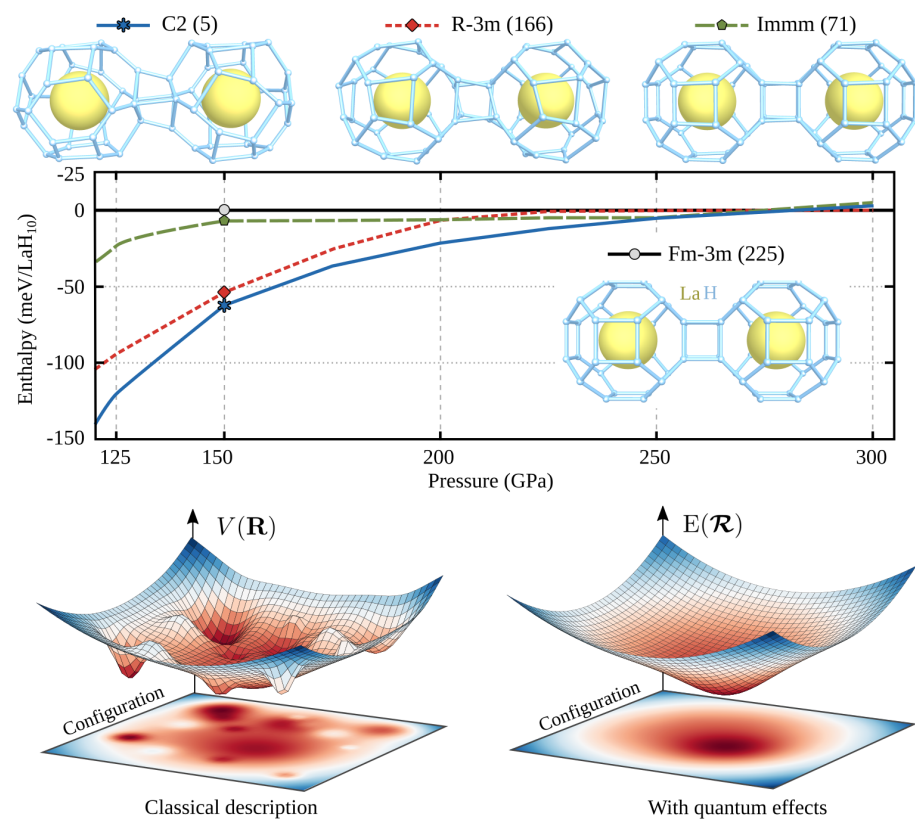
Received: 24 July 2019

Accepted: 14 November 2019

Published online: 5 February 2020

Ion Errea^{1,2,3}, Francesco Belli^{1,2}, Lorenzo Monacelli⁴, Antonio Sanna⁵, Takashi Koretsune⁶, Terumasa Tadano⁷, Raffaello Bianco², Matteo Calandra⁸, Ryotaro Arita^{9,10}, Francesco Mauri^{4,11} & José A. Flores-Livas^{4*}

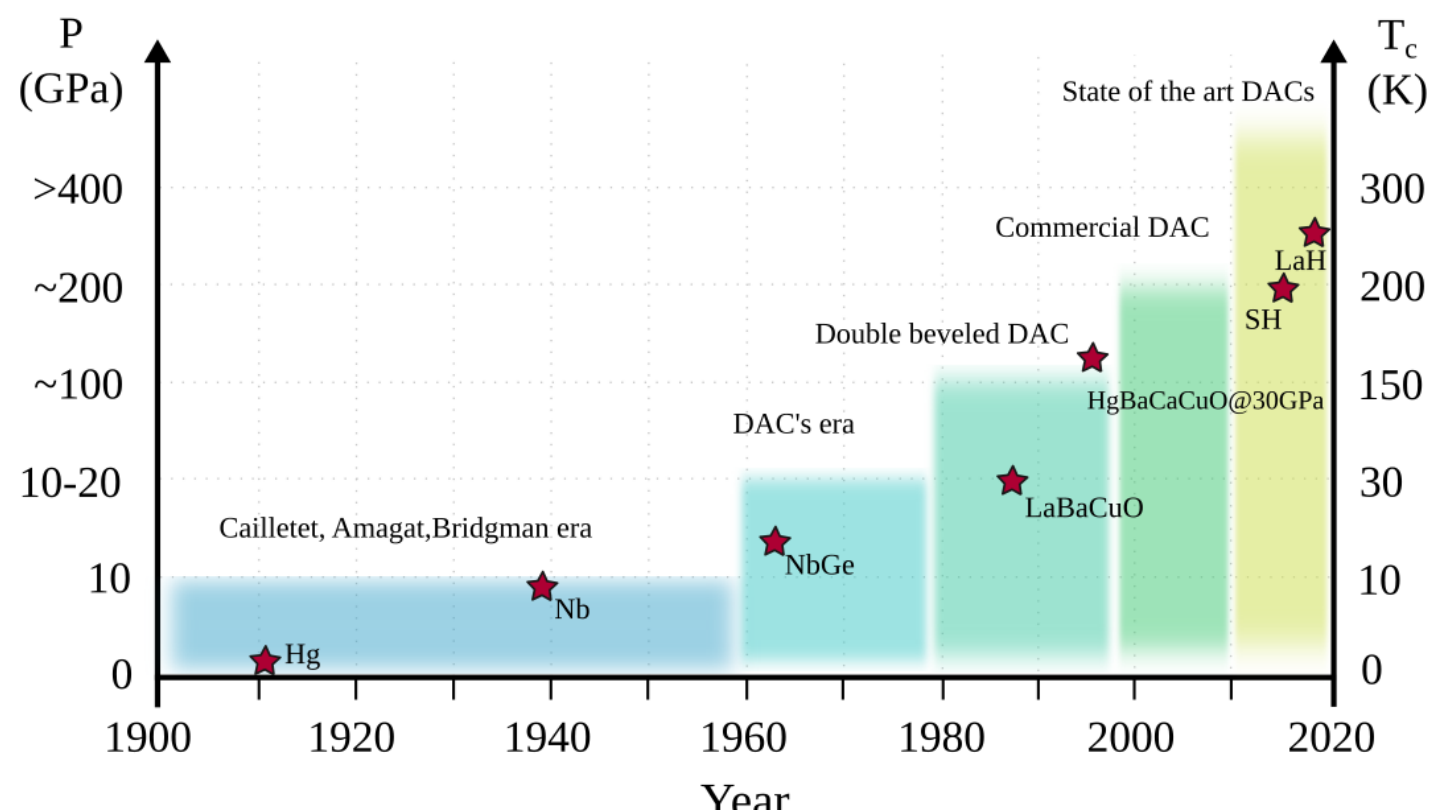
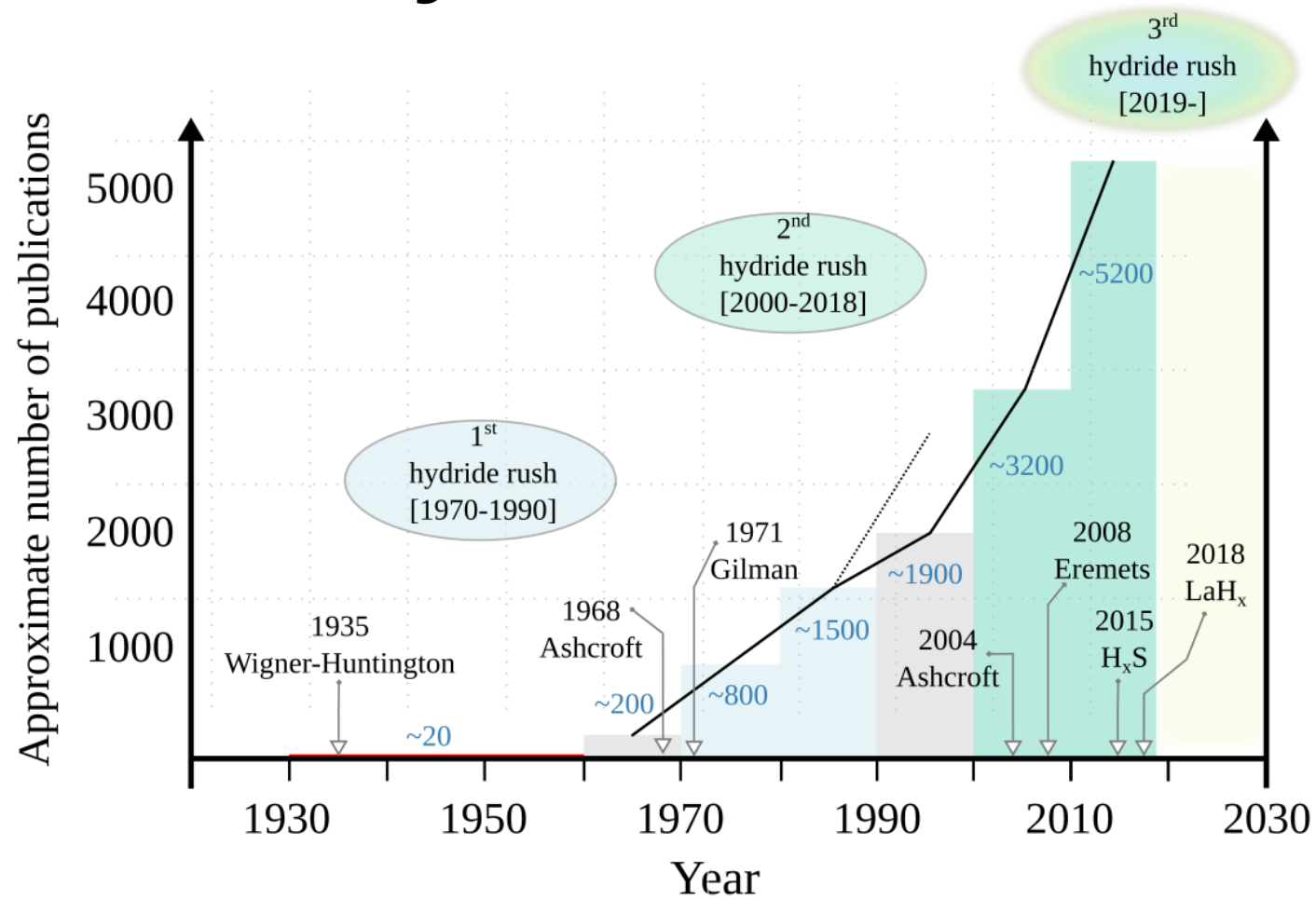
The discovery of superconductivity at 200 kelvin in the hydrogen sulfide system at high pressures¹ demonstrated the potential of hydrogen-rich materials as high-temperature superconductors. Recent theoretical predictions of rare-earth hydrides with hydrogen cages^{2,3} and the subsequent synthesis of LaH₁₀ with a superconducting critical temperature (T_c) of 250 kelvin^{4,5} have placed these materials on the verge of achieving the long-standing goal of room-temperature superconductivity. Electrical and X-ray diffraction measurements have revealed a weakly pressure-dependent T_c for LaH₁₀ between 137 and 218 gigapascals in a structure that has a face-centred cubic arrangement of lanthanum atoms⁵. Here we show that quantum atomic fluctuations stabilize a highly symmetrical $Fm\bar{3}m$ crystal structure over this pressure range. The



Room temperature superconductivity

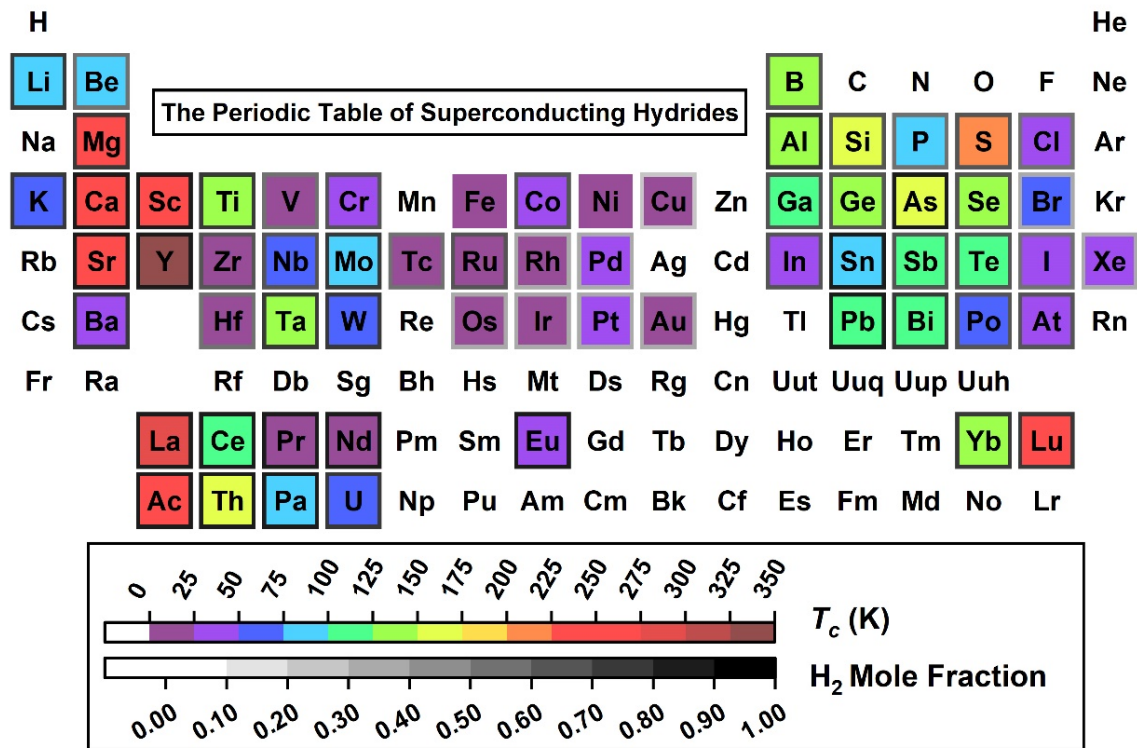


Hydride revolution



Better call....

Better call....



Better call....

Periodic table of binary hydride superconductors

H																	He
LiH ₆ 82	BeH ₂ 44											BH 21	C	N	O	F	Ne
Na	MgH ₄ 30											AlH ₅ 140	SiH _x ~20	PH ₂ 90	SH ₃ 200	Cl	Ar
KH ₁₀ 140	CaH ₆ 235	ScH ₉ 233	TiH ₁₄ 54	VH ₈ 72	CrH ₃ 81	Mn	Fe	Co	Ni	Cu	Zn	GaH ₃ 123	GeH ₄ 220	AsH ₄ 90	SeH ₃ 120	BrH ₂ 12	Kr
Rb	SrH ₁₀ 259	YH ₁₀ 240	ZrH ₁₄ 88	NbH ₄ 47	Mo	TcH ₂ 11	RuH ₃ 1.3	RhH 2.5	PdH 5	Ag	Cd	InH ₃ 41	SnH ₁₄ 90	SbH ₄ 95	TeH ₄ 100	IH ₂ 30	XeH 29
Cs	BaH ₆ 38		HfH ₂ 76	TaH ₆ 136	WH ₅ 60	Re	OsH 2	IrH 7	PtH 25	AuH 21	Hg	Tl	PbH ₈ 107	BiH ₅ 110	PoH ₄ 50	At	Rn
FrH ₇ 63	RaH ₁₂ 116		Rf	Db	Sg	Bh	Hs	Mt	Ds	Rg	Cn	Nh	Fl	Mc	Lv	Ts	Og
Lanthanides	LaH ₁₀ 250	CeH ₈ 117	PrH ₈ 31	NdH ₈ 6	Pm	Sm	Eu	Gd	Tb	Dy	HoH ₄ 37	ErH ₁₅ 30	TmH ₈ 21	Yb	LuH ₁₂ 7		
Actinides	AcH ₁₀ 250	ThH ₁₀ 170	PaH ₉ 62	UH ₈ 35	NpH ₇ 10	Pu	AmH ₈ 0.3	CmH ₈ 0.9	Bk	Cf	Es	Fm	Md	No	Lr		

T_c (K) Experimentally confirmed

T_c (K) Theoretically predicted

Better call....

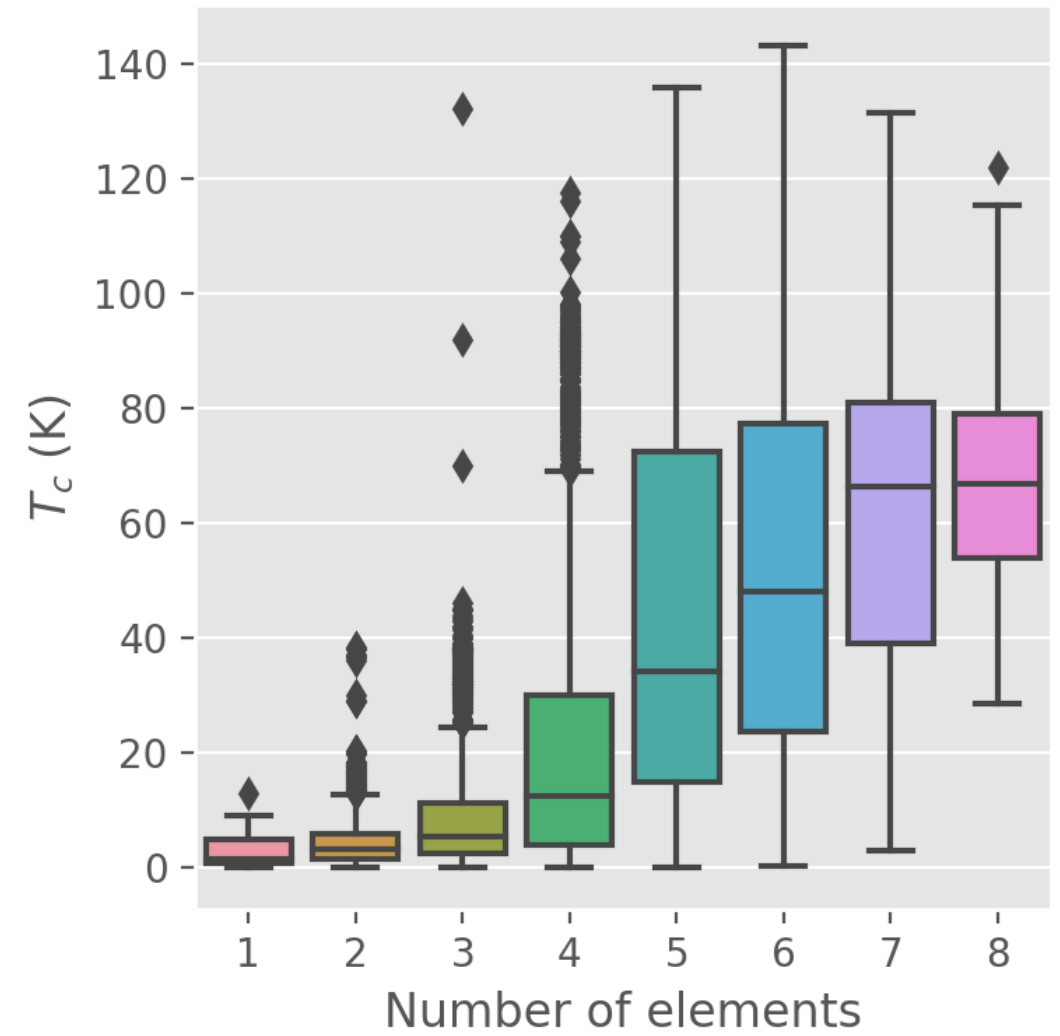
Periodic table of binary hydride superconductors

H																	He
LiH ₆ 82	BeH ₂ 44											BH 21	C	N	O	F	Ne
Na	MgH ₄ 30											AlH ₅ 140	SiH _x ~20	PH ₂ 90	SH ₃ 200	Cl	Ar
KH ₁₀ 140	CaH ₆ 235	ScH ₉ 233	TiH ₁₄ 54	VH ₈ 72	CrH ₃ 81	Mn	Fe	Co	Ni	Cu	Zn	GaH ₃ 123	GeH ₄ 220	AsH ₄ 90	SeH ₃ 120	BrH ₂ 12	Kr
Rb	SrH ₁₀ 259	YH ₁₀ 240	ZrH ₁₄ 88	NbH ₄ 47	Mo	TcH ₂ 11	RuH ₃ 1.3	RhH 2.5	PdH 5	Ag	Cd	InH ₃ 41	SnH ₁₄ 90	SbH ₄ 95	TeH ₄ 100	IH ₂ 30	XeH 29
Cs	BaH ₆ 38		HfH ₂ 76	TaH ₆ 136	WH ₅ 60	Re	OsH 2	IrH 7	PtH 25	AuH 21	Hg	Tl	PbH ₈ 107	BiH ₅ 110	PoH ₄ 50	At	Rn
FrH ₇ 63	RaH ₁₂ 116		Rf	Db	Sg	Bh	Hs	Mt	Ds	Rg	Cn	Nh	Fl	Mc	Lv	Ts	Og
Lanthanides	LaH ₁₀ 250	CeH ₈ 117	PrH ₈ 31	NdH ₈ 6	Pm	Sm	Eu	Gd	Tb	Dy	HoH ₄ 37	ErH ₁₅ 30	TmH ₈ 21	Yb	LuH ₁₂ 7		
Actinides	AcH ₁₀ 250	ThH ₁₀ 170	PaH ₉ 62	UH ₈ 35	NpH ₇ 10	Pu	AmH ₈ 0.3	CmH ₈ 0.9	Bk	Cf	Es	Fm	Md	No	Lr		

T_c (K) Experimentally confirmed

T_c (K) Theoretically predicted

Another actor: Al

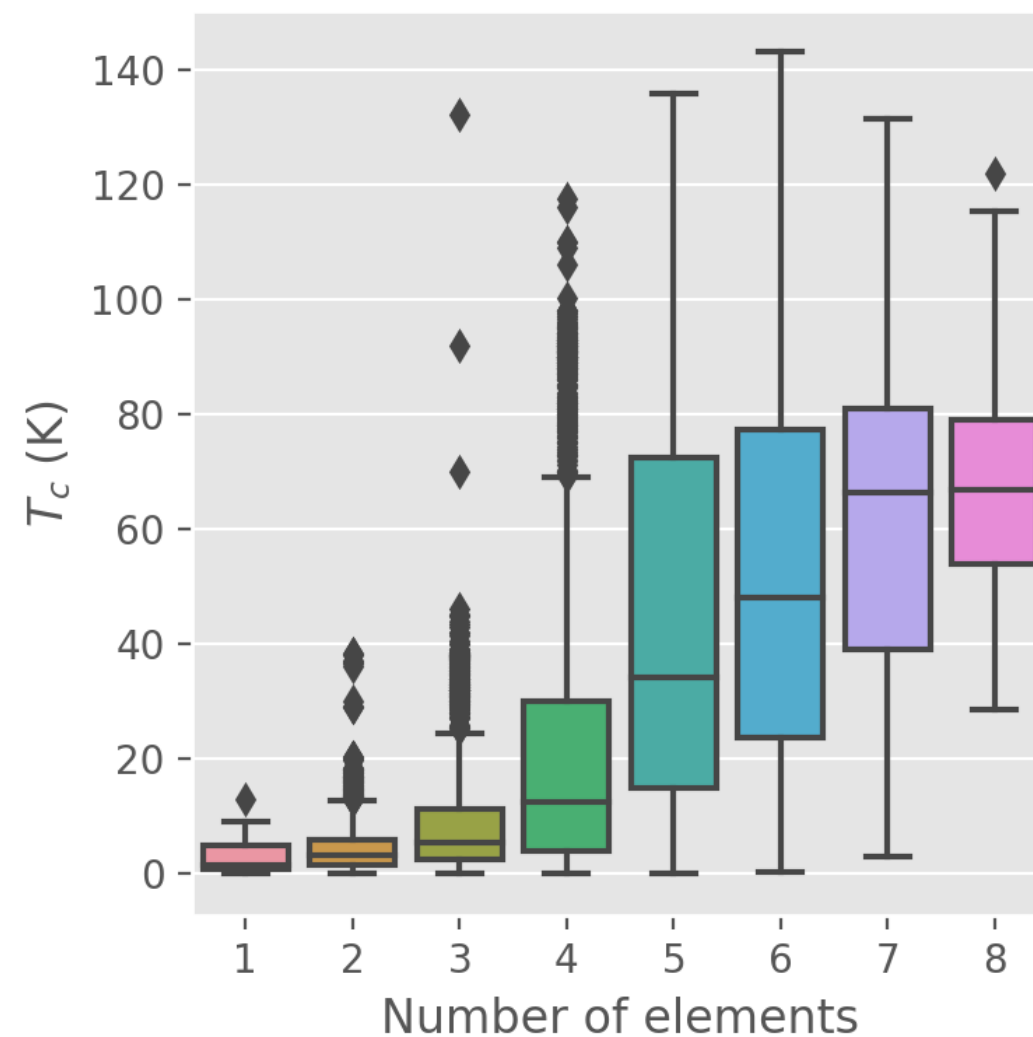
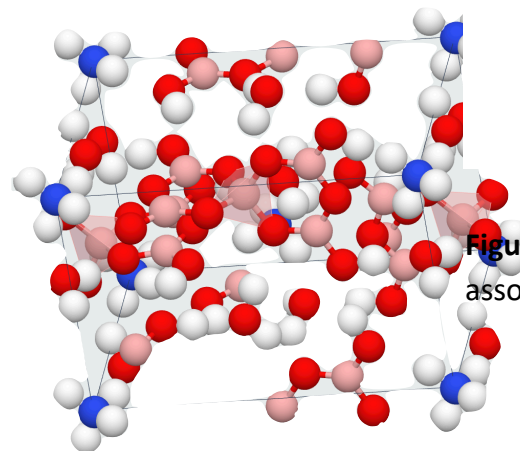
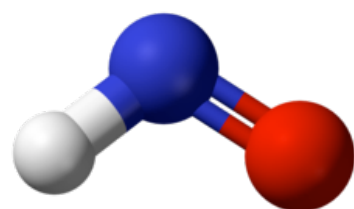
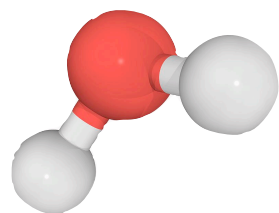
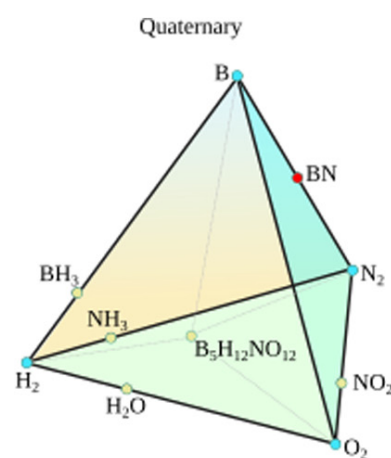
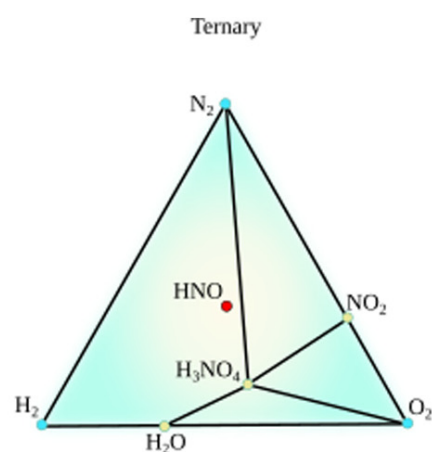
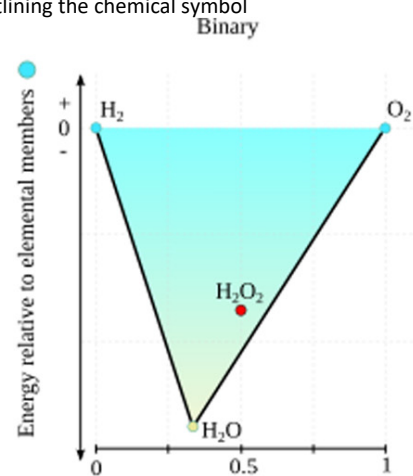


Better call....

Periodic table of binary hydride superconductors

H																	He				
LiH ₆ 82	BeH ₂ 44															BH 21	C	N	O	F	Ne
Na	MgH ₄ 30															AlH ₅ 140	SiH _x ~20	PH ₂ 90	SH ₃ 200	Cl	Ar
KH ₁₀ 140	CaH ₆ 235	ScH ₉ 233	TiH ₁₄ 54	VH ₈ 72	CrH ₃ 81	Mn	Fe	Co	Ni	Cu	Zn	GaH ₃ 123	GeH ₄ 220	AsH ₄ 90	SeH ₃ 120	BrH ₂ 12	Kr				
Rb	SrH ₁₀ 259	YH ₁₀ 240	ZrH ₁₄ 88	NbH ₄ 47	Mo	TcH ₂ 11	RuH ₃ 1.3	RhH 2.5	PdH 5	Ag	Cd	InH ₃ 41	SnH ₁₄ 90	SbH ₄ 95	TeH ₄ 100	IH ₂ 30	XeH 29				
Cs	BaH ₆ 38		HfH ₂ 76	TaH ₆ 136	WH ₅ 60	Re	OsH 2	IrH 7	PtH 25	AuH 21	Hg	Tl	PbH ₈ 107	BiH ₅ 110	PoH ₄ 50	At	Rn				
FrH ₇ 63	RaH ₁₂ 116		Rf	Db	Sg	Bh	Hs	Mt	Ds	Rg	Cn	Nh	Fl	Mc	Lv	Ts	Og				
Lanthanides		LaH ₁₀ 250	CeH ₈ 117	PrH ₈ 31	NdH ₈ 6	Pm	Sm	Eu	Gd	Tb	Dy	HoH ₄ 37	ErH ₁₅ 30	TmH ₈ 21	Yb	LuH ₁₂ 7					
Actinides		AcH ₁₀ 250	ThH ₁₀ 170	PaH ₉ 62	UH ₈ 35	NpH ₇ 10	Pu	AmH ₈ 0.3	CmH ₈ 0.9	Bk	Cf	Es	Fm	Md	No	Lr					

Another actor: Al



Room-temperature superconductivity in a carbonaceous sulfur hydride

<https://doi.org/10.1038/s41586-020-2801-z>

Received: 21 July 2020

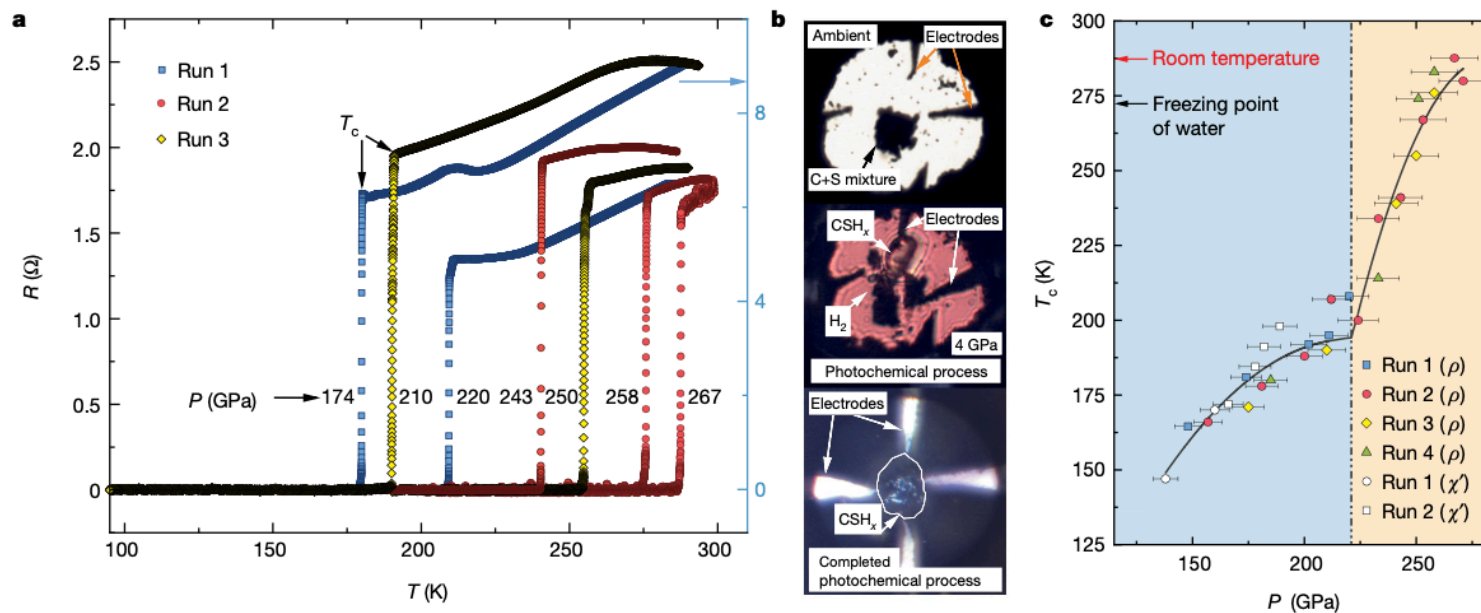
Accepted: 8 September 2020

Published online: 14 October 2020

 Check for updates

Elliot Snider^{1,6}, Nathan Dasenbrock-Gammon^{2,6}, Raymond McBride^{1,6}, Mathew Debessai³, Hiranya Vindana², Kevin Vencatasamy², Keith V. Lawler⁴, Ashkan Salamat⁵ & Ranga P. Dias^{1,2,6}

One of the long-standing challenges in experimental physics is the observation of room-temperature superconductivity^{1,2}. Recently, high-temperature conventional superconductivity in hydrogen-rich materials has been reported in several systems under high pressure^{3–5}. An important discovery leading to room-temperature superconductivity is the pressure-driven disproportionation of hydrogen sulfide (H₂S) to H₃S, with a confirmed transition temperature of 203 kelvin at 155 gigapascals^{3,6}. Both H₂S and CH₄ readily mix with hydrogen to form guest–host structures at lower pressures⁷, and are of comparable size at 4 gigapascals. By introducing methane at low pressures into the H₂S + H₂ precursor mixture for H₃S, molecular exchange is allowed within a large assemblage of van der Waals solids that are hydrogen-rich with H₂ inclusions; these guest–host structures become the building blocks of superconducting compounds at extreme conditions. Here we report superconductivity in a photochemically transformed carbonaceous sulfur hydride system, starting from elemental precursors, with a maximum superconducting transition temperature of 287.7 ± 1.2 kelvin (about 15 degrees Celsius) achieved at 267 ± 10 gigapascals. The superconducting state is observed over a broad pressure range in the diamond anvil cell, from 140 to 275 gigapascals, with a sharp upturn in transition temperature above 220 gigapascals. Superconductivity is established by the observation of zero resistance, a magnetic susceptibility of up to 190 gigapascals, and reduction of the transition temperature under an external magnetic field of up to 9 tesla, with an upper critical magnetic field of about 62 tesla according to the Ginzburg–Landau model at zero temperature. The light, quantum nature of hydrogen limits the structural and stoichiometric determination of the system by X-ray scattering techniques, but Raman spectroscopy is used to probe the chemical and structural transformations before metallization. The introduction of chemical tuning within our ternary system could enable the preservation of the properties of room-temperature superconductivity at lower pressures.



Room-temperature superconductivity in a carbonaceous sulfur hydride

<https://doi.org/10.1038/s41586-020-2801-z>

Received: 21 July 2020

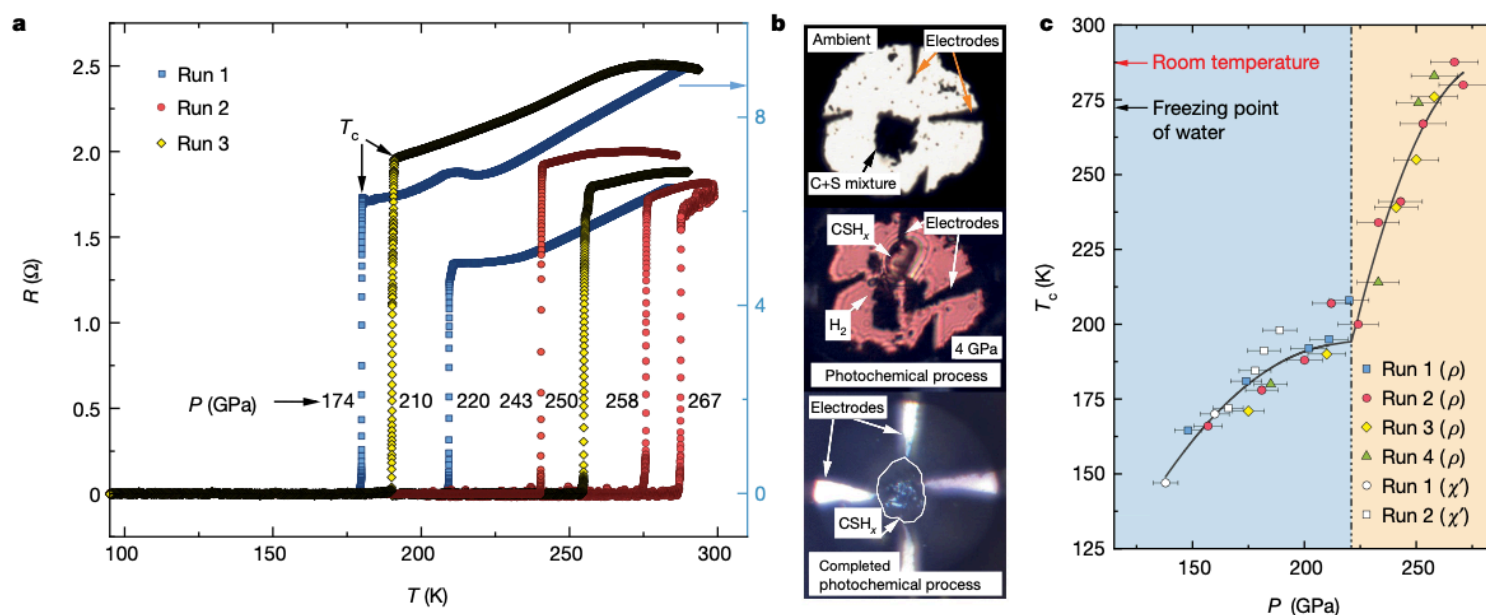
Accepted: 8 September 2020

Published online: 14 October 2020

 Check for updates

Elliot Snider^{1,6}, Nathan Dasenbrock-Gammon^{2,6}, Raymond McBride^{1,6}, Mathew Debessai³, Hiranya Vindana², Kevin Vencatasamy², Keith V. Lawler⁴, Ashkan Salamat⁵ & Ranga P. Dias^{1,2,6}

One of the long-standing challenges in experimental physics is the observation of room-temperature superconductivity^{1,2}. Recently, high-temperature conventional superconductivity in hydrogen-rich materials has been reported in several systems under high pressure^{3–5}. An important discovery leading to room-temperature superconductivity is the pressure-driven disproportionation of hydrogen sulfide (H₂S) to H₃S, with a confirmed transition temperature of 203 kelvin at 155 gigapascals^{3,6}. Both H₂S and CH₄ readily mix with hydrogen to form guest–host structures at lower pressures⁷, and are of comparable size at 4 gigapascals. By introducing methane at low pressures into the H₂S + H₂ precursor mixture for H₃S, molecular exchange is allowed within a large assemblage of van der Waals solids that are hydrogen-rich with H₂ inclusions; these guest–host structures become the building blocks of superconducting compounds at extreme conditions. Here we report superconductivity in a photochemically transformed carbonaceous sulfur hydride system, starting from elemental precursors, with a maximum superconducting transition temperature of 287.7 ± 1.2 kelvin (about 15 degrees Celsius) achieved at 267 ± 10 gigapascals. The superconducting state is observed over a broad pressure range in the diamond anvil cell, from 140 to 275 gigapascals, with a sharp upturn in transition temperature above 220 gigapascals. Superconductivity is established by the observation of zero resistance, a magnetic susceptibility of up to 190 gigapascals, and reduction of the transition temperature under an external magnetic field of up to 9 tesla, with an upper critical magnetic field of about 62 tesla according to the Ginzburg–Landau model at zero temperature. The light, quantum nature of hydrogen limits the structural and stoichiometric determination of the system by X-ray scattering techniques, but Raman spectroscopy is used to probe the chemical and structural transformations before metallization. The introduction of chemical tuning within our ternary system could enable the preservation of the properties of room-temperature superconductivity at lower pressures.



Room-temperature superconductivity in a carbonaceous sulfur hydride

<https://doi.org/10.1038/s41586-020-2801-z>

Received: 21 July 2020

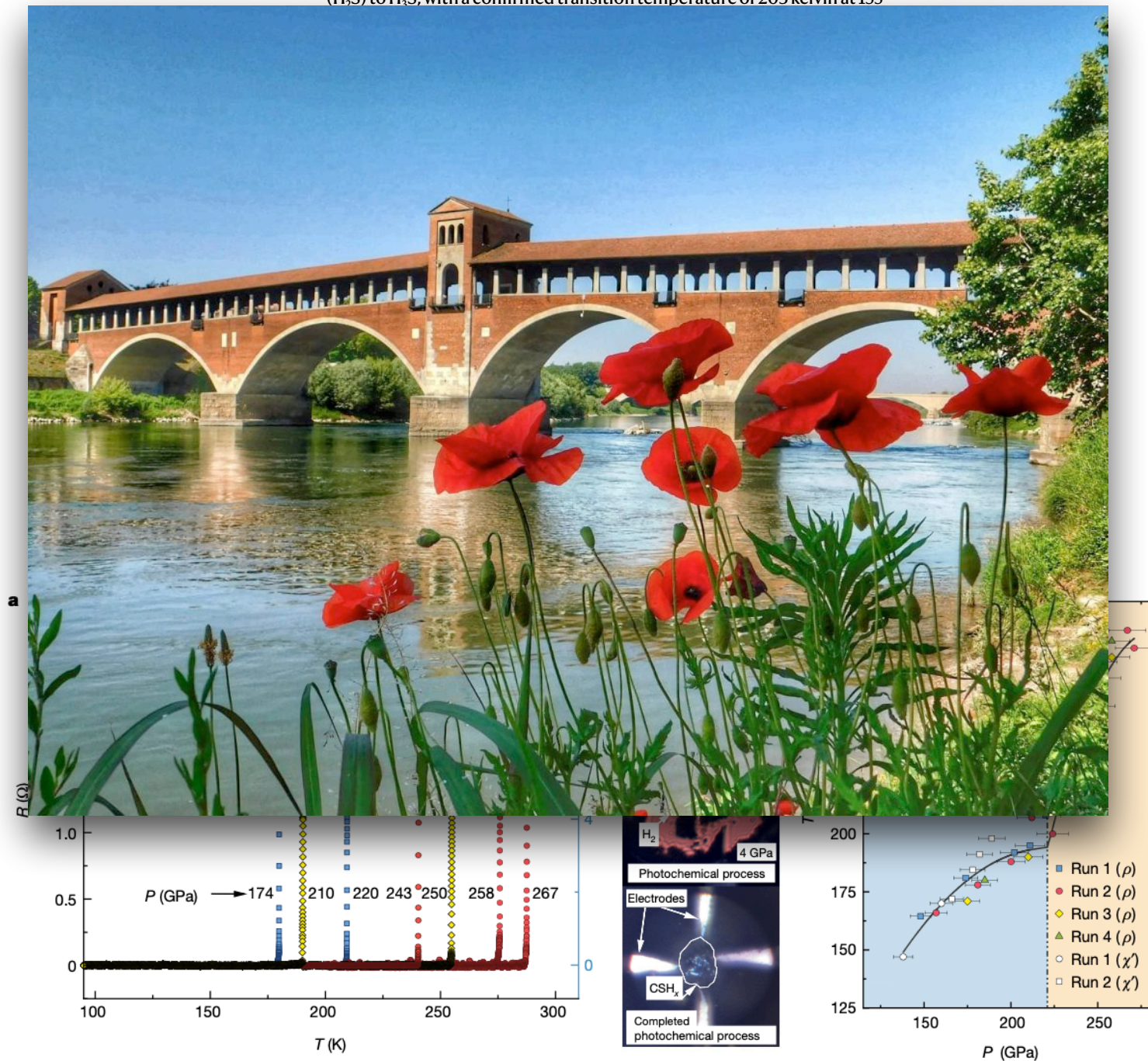
Accepted: 8 September 2020

Published online: 14 October 2020

 Check for updates

Elliot Snider^{1,6}, Nathan Dasenbrock-Gammon^{2,6}, Raymond McBride^{1,6}, Mathew Debessai³, Hiranya Vindana², Kevin Vencatasamy², Keith V. Lawler⁴, Ashkan Salamat⁵ & Ranga P. Dias^{1,2,6}✉

One of the long-standing challenges in experimental physics is the observation of room-temperature superconductivity^{1,2}. Recently, high-temperature conventional superconductivity in hydrogen-rich materials has been reported in several systems under high pressure^{3–5}. An important discovery leading to room-temperature superconductivity is the pressure-driven disproportionation of hydrogen sulfide (H₂S) to H₃S, with a confirmed transition temperature of 203 kelvin at 155



Room-temperature superconductivity in a carbonaceous sulfur hydride

https://doi.org/10.1038/s41586-020-2801-z

Received: 21 July 2020

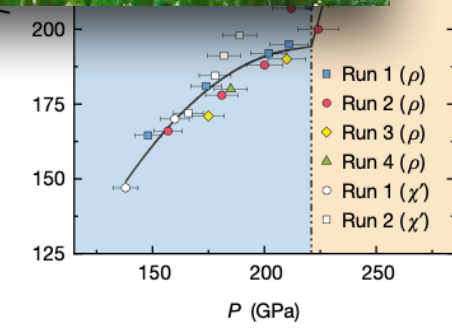
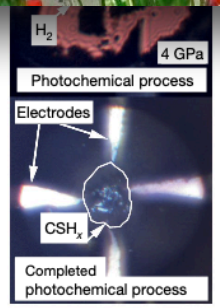
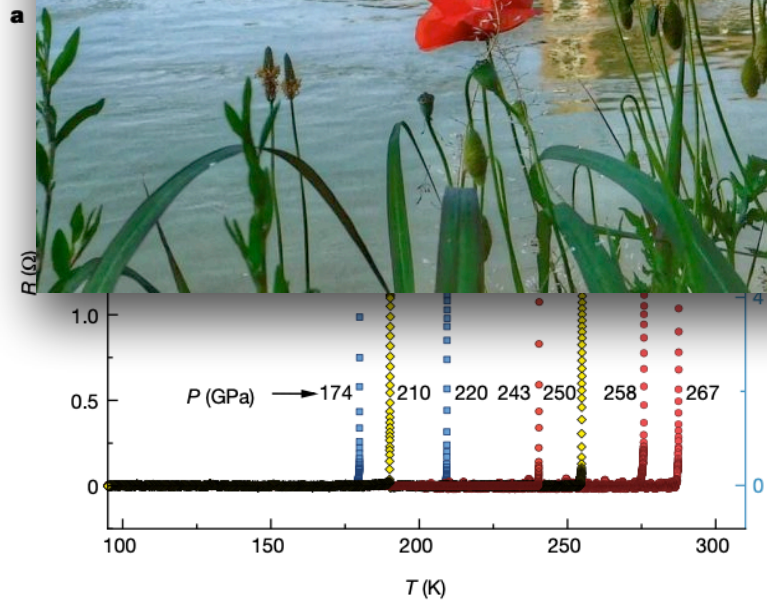
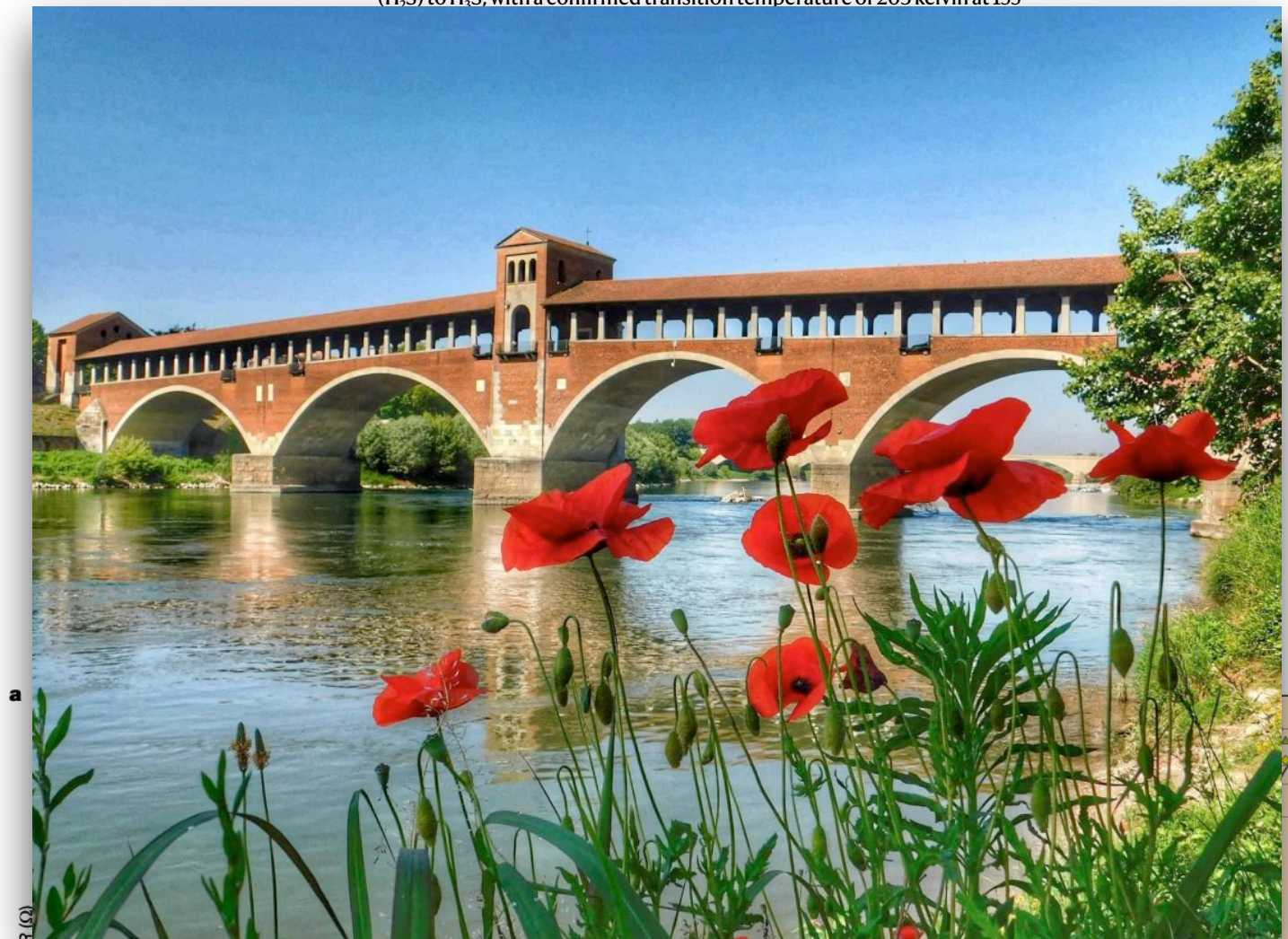
Accepted: 8 September 2020

Published online: 14 October 2020

Check for updates

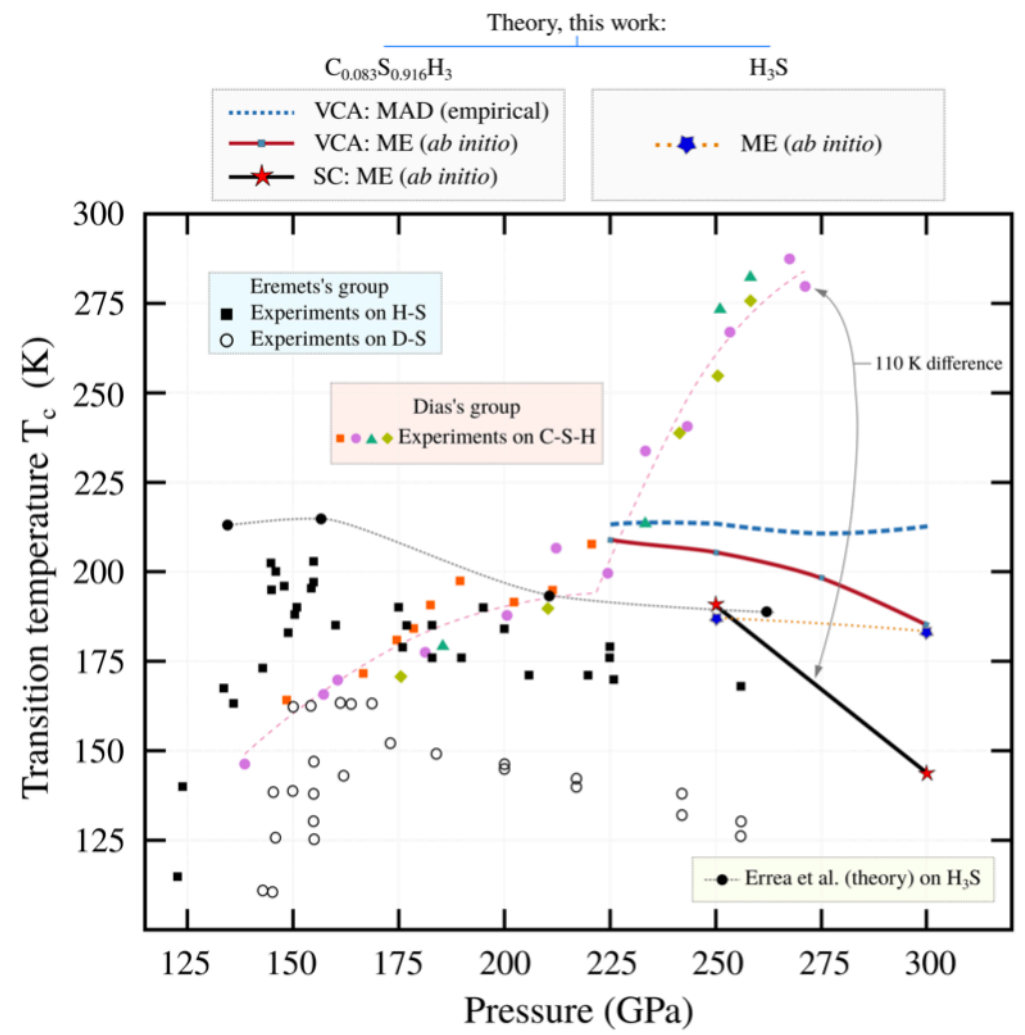
Elliot Snider^{1,6}, Nathan Dasenbrock-Gammon^{2,6}, Raymond McBride^{1,6}, Mathew Debessai³, Hiranya Vindana², Kevin Vencatasamy², Keith V. Lawler⁴, Ashkan Salamat⁵ & Ranga P. Dias^{1,2,6}

One of the long-standing challenges in experimental physics is the observation of room-temperature superconductivity^{1,2}. Recently, high-temperature conventional superconductivity in hydrogen-rich materials has been reported in several systems under high pressure³⁻⁵. An important discovery leading to room-temperature superconductivity is the pressure-driven disproportionation of hydrogen sulfide (H₂S) to H₃S, with a confirmed transition temperature of 203 kelvin at 155

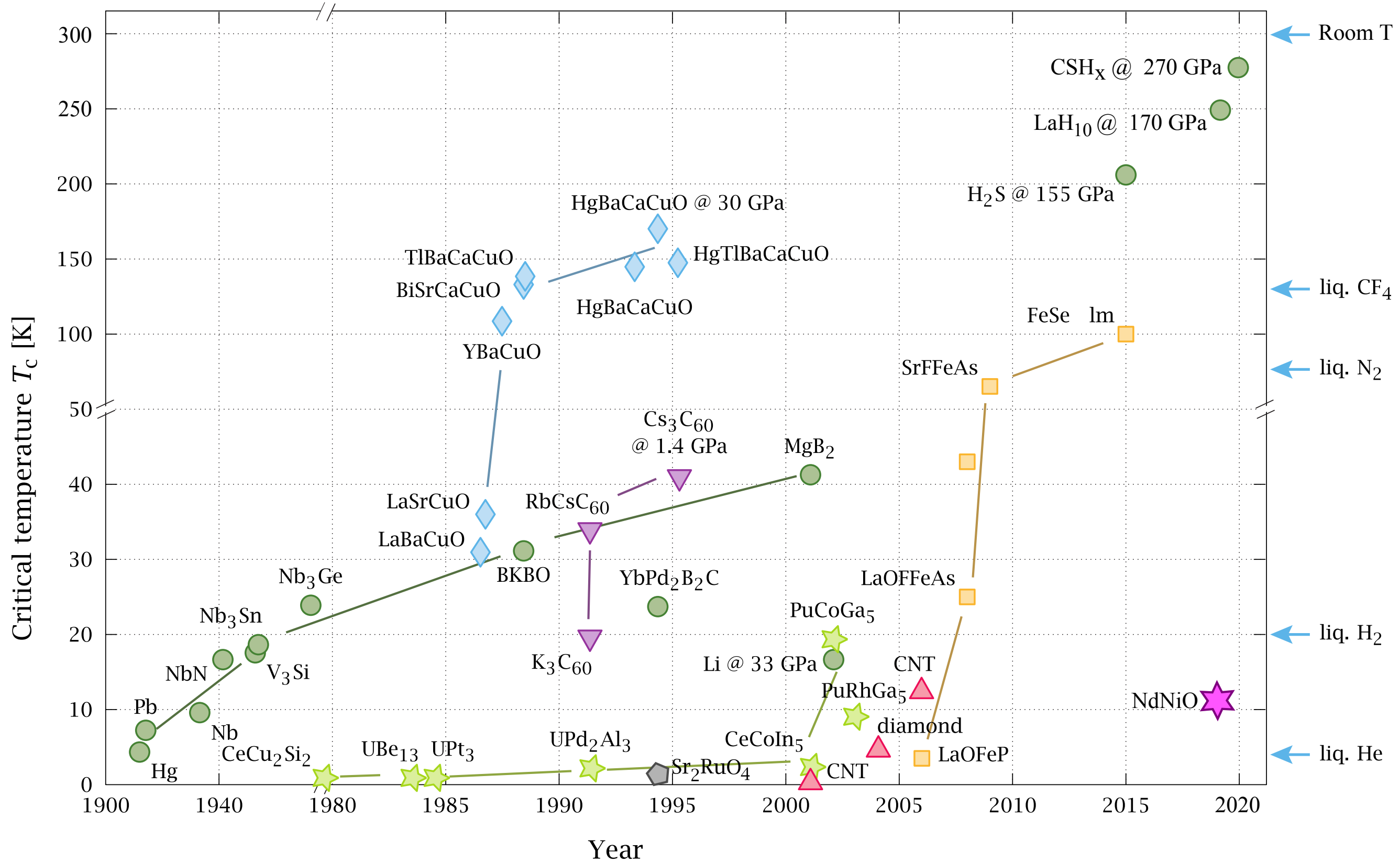


Absence of conventional room-temperature superconductivity at high pressure in carbon-doped H₃S

Tianchun Wang, Motoaki Hirayama, Takuya Nomoto, Takashi Koretsune, Ryotaro Arita, and José A. Flores-Livas
Phys. Rev. B **104**, 064510 – Published 25 August 2021



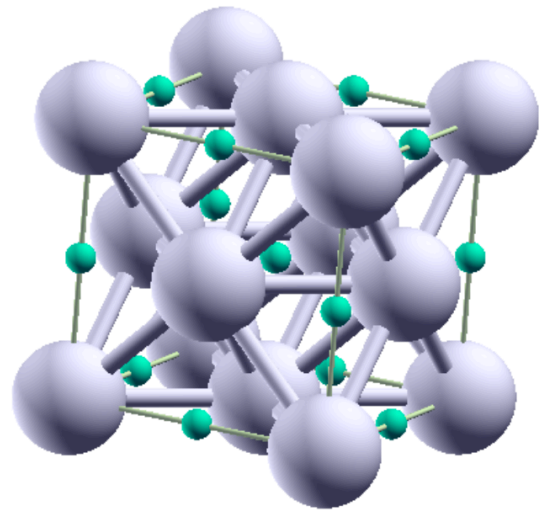
But theory fails (?)



From room temperature to ambient pressure: follow the hydrogen route

From room temperature to ambient pressure: follow the hydrogen route

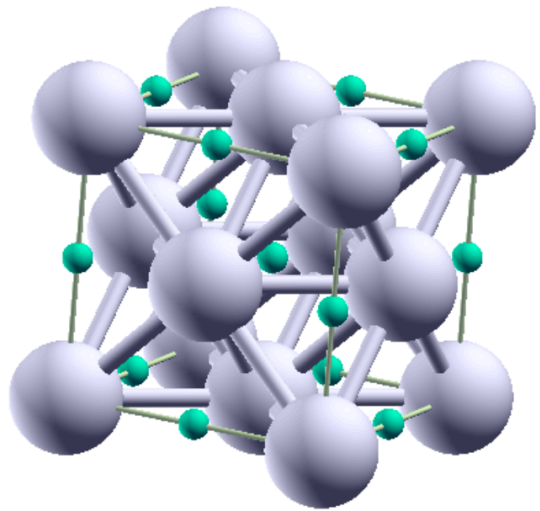
Palladium hydride



T_c=9 K

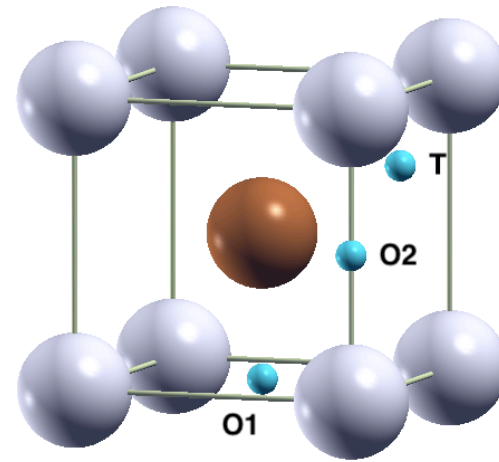
From room temperature to ambient pressure: follow the hydrogen route

Palladium hydride

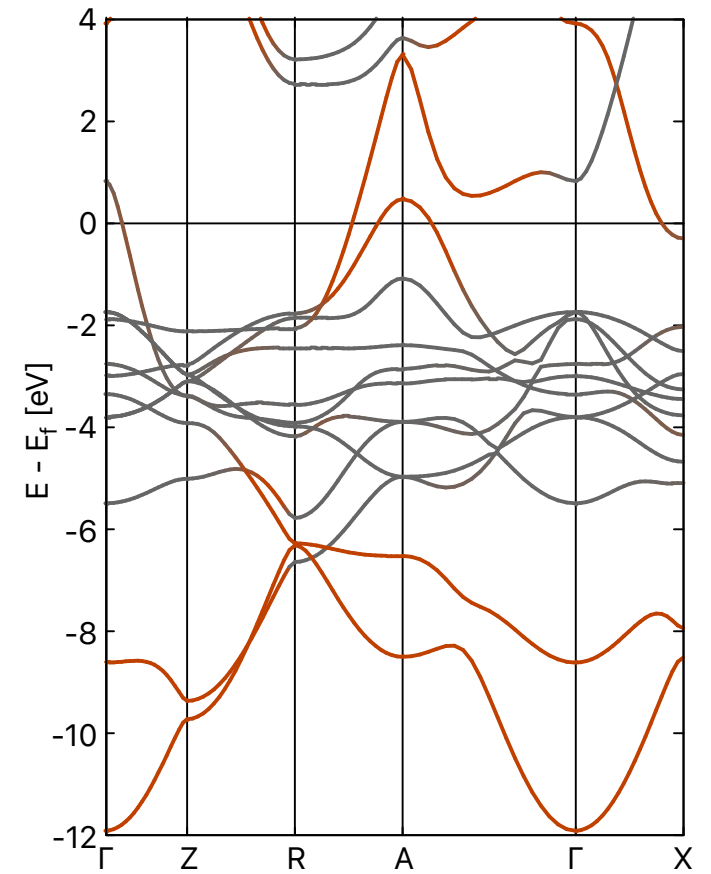


T_c=9 K

Palladium - Copper hydride

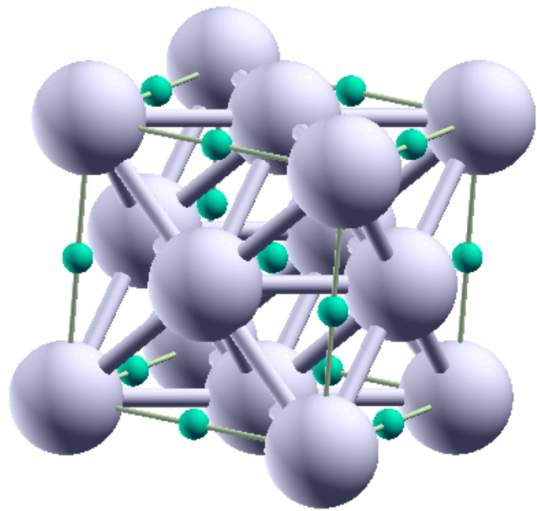


T_c=20 K



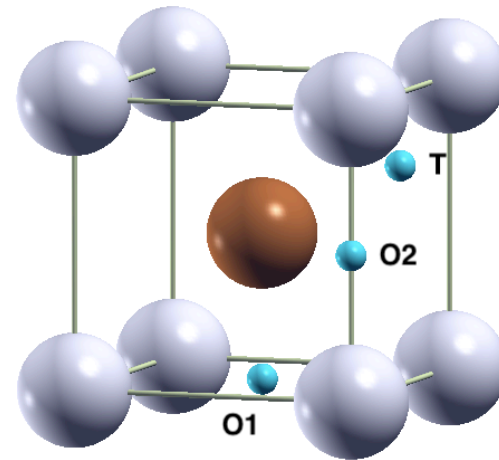
From room temperature to ambient pressure: follow the hydrogen route

Palladium hydride

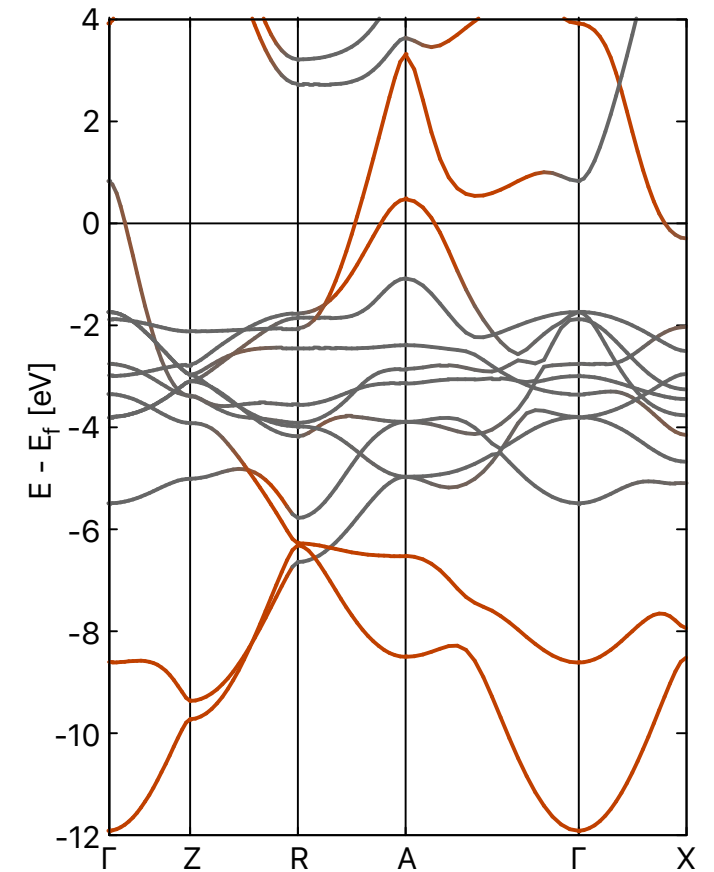


$T_c = 9 \text{ K}$

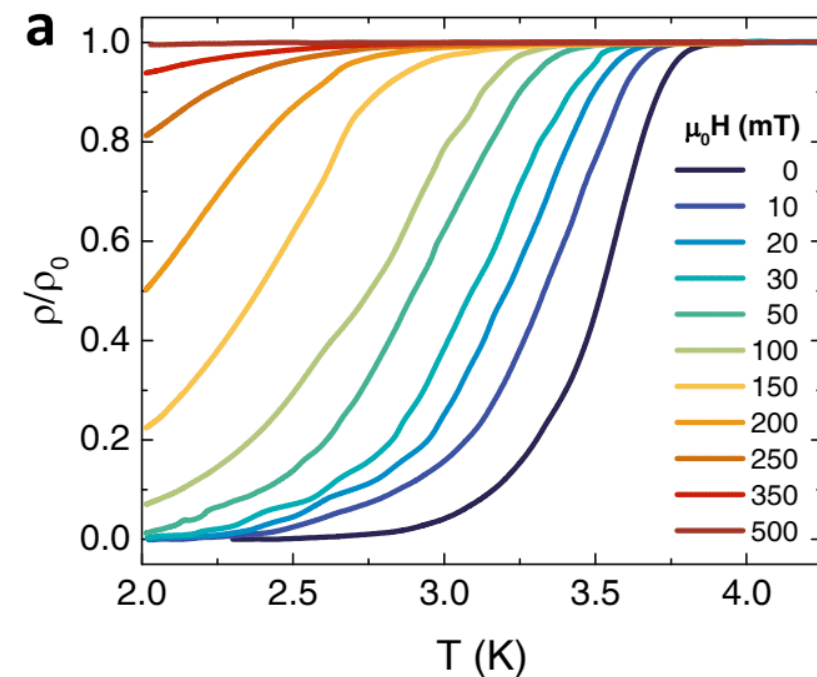
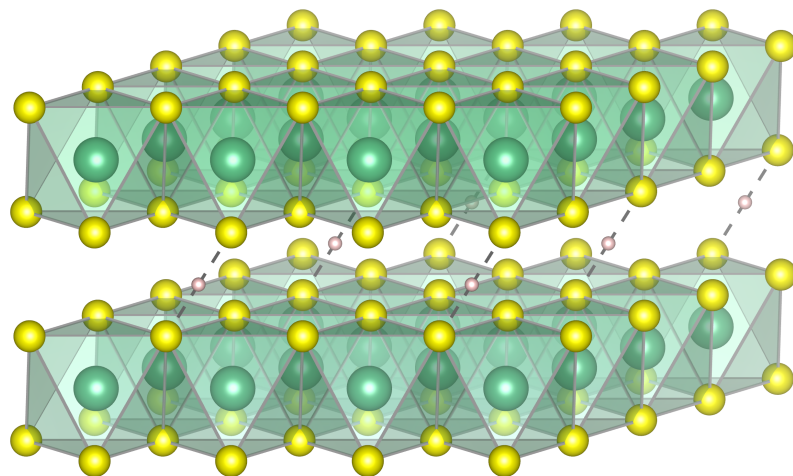
Palladium - Copper hydride



$T_c = 20 \text{ K}$



Hydrogenated TMD Titanium diselenide, TiSe_2



Any suggestions?

$$\frac{2}{\xi_k} \tanh\left(\frac{\xi_k}{2}\right) \sum_{\lambda q} |g_{kk'}^{\lambda q}|^2 [I(\xi_k, \xi_{k'}, \Omega_{\lambda q}) - I(\xi_k, -\xi_{k'}, \Omega_{\lambda q})] \quad (25)$$

does not depend on the nuclear masses (the sum is over the atoms of the crystal at cell position \mathbf{R}_l , with respect the reference cell \mathbf{R}_0).

From equation (30), and using, again, the (mass-independent) normalization of the eigenvectors we obtain (see appendix B for the details of the calculations):

$$\mathcal{K}_{kk'}^{\text{el}} = v_{kk'}. \quad (26)$$

$$\frac{\partial V_{\lambda q}}{\partial M_\alpha} = - \sum_{\mu} \frac{\zeta_{\alpha\mu}^{\lambda q} \zeta_{\alpha\mu}^{\lambda q}}{2M_\alpha} \Omega_{\lambda q}. \quad (32)$$

of the coupling constants $\zeta_{\alpha\mu}^{\lambda q}$ and $\chi_0(\mathbf{r}', \mathbf{r}'')$ are constants are given by the matrix elements of the self-consistent potential $(V_{\lambda q}(\mathbf{r}))$ with respect to the phonon mode λ at wave-vector \mathbf{q} between electrons at wavevectors \mathbf{k} and $\mathbf{k}' = \mathbf{k} + \mathbf{q}$.

$$V_{\lambda q}(\mathbf{r}) = \int d^3 r' \varphi_k^*(\mathbf{r}) V_{\lambda q}(\mathbf{r}')$$

The self-consistent potential can be written as [45]:

$$V_{\lambda q}(\mathbf{r}) = V_{\lambda q}^0(\mathbf{r}) + \int d^3 r' \int d^3 r'' \left(\frac{1}{|\mathbf{r} - \mathbf{r}'|} + f_{\text{ex}}(\mathbf{r}, \mathbf{r}') \right) \chi_0(\mathbf{r}', \mathbf{r}'') V_{\lambda q}^0(\mathbf{r}'') \quad (33)$$

where $\chi_0(\mathbf{r}, \mathbf{r}'')$ is the full response function and

$$V_{\lambda q}^0(\mathbf{r}) = \sum_{\alpha, \mu} \frac{Z_\alpha}{\sqrt{2M_\alpha \Omega_{\lambda q}}} e^{i\mathbf{q}\mathbf{R}_\alpha} \zeta_{\alpha\mu}^{\lambda q} \left(\frac{\partial}{\partial R_{\alpha i}^{\mu}} \frac{1}{|\mathbf{r} - \mathbf{R}_{\alpha i}|} \right) \quad (35)$$

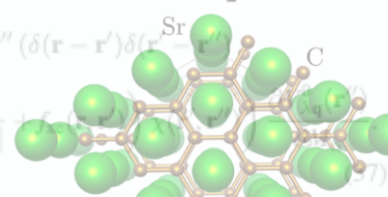
the derivative of the bare potential. Since the full response function is not explicitly known, the response equation (34) is normally rewritten as

$$V_{\lambda q}(\mathbf{r}) = V_{\lambda q}^0(\mathbf{r}) + \int d^3 r' \int d^3 r'' \left(\frac{1}{|\mathbf{r} - \mathbf{r}'|} + f_{\text{ex}}(\mathbf{r}, \mathbf{r}') \right) \chi_0(\mathbf{r}', \mathbf{r}'') V_{\lambda q}(\mathbf{r}'') \quad (36)$$

which involves only the Kohn-Sham response function ($\chi_0(\mathbf{r}', \mathbf{r}'')$), which is explicitly known, but it has to be solved self-consistently with respect to $V_{\lambda q}(\mathbf{r})$.

In order to calculate the partial derivative of the coupling constant with respect to the atomic masses, we write $V_{\lambda q}^0(\mathbf{r})$ as the partial derivative of the potential, $\frac{\partial V_{\lambda q}^0(\mathbf{r})}{\partial M_\alpha}$

$$\frac{\partial V_{\lambda q}(\mathbf{r})}{\partial M_\alpha} = \int d^3 r' \int d^3 r'' (\delta(\mathbf{r} - \mathbf{r}') \delta(\mathbf{r}' - \mathbf{r}'') + \left(\frac{1}{|\mathbf{r} - \mathbf{r}'|} + f_{\text{ex}}(\mathbf{r}, \mathbf{r}') \right) \chi_0(\mathbf{r}', \mathbf{r}'')) \frac{\partial V_{\lambda q}^0(\mathbf{r}'')}{\partial M_\alpha} \quad (37)$$



$$\frac{2}{\xi_k} \tanh\left(\frac{\xi_k}{2}\right) \sum_{\lambda q} |g_{kk'}^{\lambda q}|^2 [I(\xi_k, \xi_{k'}, \Omega_{\lambda q}) - I(\xi_k, -\xi_{k'}, \Omega_{\lambda q})] \quad (25)$$

does not depend on the nuclear masses (the sum is over the atoms of the crystal at cell position \mathbf{R}_l , with respect the reference cell \mathbf{R}_0).

From equation (30), and using, again, the (mass-independent) normalization of the eigenvectors we obtain (see appendix B for the details of the calculations):

$$K_{kk'}^{cl} = v_{kk'}. \quad (26)$$

$$V_{\lambda q} = -\sum_{\mu} \frac{\zeta_{\alpha\mu}^{\lambda q} \zeta_{\alpha\mu}^{\lambda q}}{2M_{\alpha}} \Omega_{\lambda q}. \quad (32)$$

of the coupling constants $\zeta_{\alpha\mu}^{\lambda q}$ and $\chi_0(\mathbf{r}', \mathbf{r}'')$ are constants are given by the matrix elements of the self-consistent potential $(V_{\lambda q}(\mathbf{r}))$ with respect to the phonon mode λ at wave-vector \mathbf{q} between electrons at wavevectors \mathbf{k} and $\mathbf{k}' = \mathbf{k} + \mathbf{q}$.

$$V_{\lambda q}(\mathbf{r}) = \int d^3 r' \varphi_{\mathbf{k}}^*(\mathbf{r}) V_{\lambda q}(\mathbf{r}').$$

The self-consistent potential can be written as [45]:

$$V_{\lambda q}(\mathbf{r}) = V_{\lambda q}^0(\mathbf{r}) + \int d^3 r' \int d^3 r'' \left(\frac{1}{|\mathbf{r} - \mathbf{r}'|} + f_{\alpha}(\mathbf{r}, \mathbf{r}') \right) \chi_0(\mathbf{r}', \mathbf{r}'') V_{\lambda q}^0(\mathbf{r}'') \quad (33)$$

where $\chi_0(\mathbf{r}, \mathbf{r}')$ is the full response function and

$$V_{\lambda q}^0(\mathbf{r}) = \sum_{\alpha, l, \mu} \frac{Z_{\alpha}}{\sqrt{2M_{\alpha} \Omega_{\lambda q}}} e^{i\mathbf{q}\mathbf{R}_l} \zeta_{\alpha\mu}^{\lambda q} \left(\frac{\partial}{\partial R_{\alpha l}^{\mu}} \frac{1}{|\mathbf{r} - \mathbf{R}_{\alpha l}|} \right) \quad (35)$$

the derivative of the bare potential. Since the full response function is not explicitly known, the response equation (34) is normally rewritten as

$$V_{\lambda q}(\mathbf{r}) = V_{\lambda q}^0(\mathbf{r}) + \int d^3 r' \int d^3 r'' \left(\frac{1}{|\mathbf{r} - \mathbf{r}'|} + f_{\alpha}(\mathbf{r}, \mathbf{r}') \right) \chi_0(\mathbf{r}', \mathbf{r}'') V_{\lambda q}(\mathbf{r}'') \quad (36)$$

which involves only the Kohn-Sham response function ($\chi_0(\mathbf{r}', \mathbf{r}'')$), which is explicitly known, but it has to be solved self-consistently with respect to $V_{\lambda q}(\mathbf{r})$.

In order to calculate the partial derivative of the coupling constant with respect to the atomic masses, we write $V_{\lambda q}^0(\mathbf{r})$ as the partial derivative of the potential, $\frac{\partial V_{\lambda q}^0(\mathbf{r})}{\partial M_{\alpha}}$

$$\frac{\partial V_{\lambda q}^0(\mathbf{r})}{\partial M_{\alpha}} = \int d^3 r' \int d^3 r'' (\delta(\mathbf{r} - \mathbf{r}') \delta(\mathbf{r} - \mathbf{r}'') + \left(\frac{1}{|\mathbf{r} - \mathbf{r}'|} + f_{\alpha}(\mathbf{r}, \mathbf{r}') \right) \chi_0(\mathbf{r}', \mathbf{r}'')) \frac{\partial V_{\lambda q}^0(\mathbf{r}')}{\partial M_{\alpha}} \quad (37)$$

$$Z_{\alpha} \zeta_{\alpha\mu}^{\lambda q} \frac{\partial V_{\alpha\mu}^{\lambda q}(\mathbf{r})}{\partial M_{\alpha} \Omega_{\lambda q}} \quad (38)$$

$$\left(\frac{\partial}{\partial R_{\alpha l}^{\mu}} \frac{1}{|\mathbf{r} - \mathbf{R}_{\alpha l}|} \right) \quad (39)$$

$$\frac{\partial V_{\lambda q}^0(\mathbf{r})}{\partial M_{\alpha} \Omega_{\lambda q}} \quad (40)$$

THANK YOU FOR YOUR ATTENTION

see more @ <http://www.aquila.infn.it/profeta/>

(BSE) [45]:

$$T(1,2,3,4) = w(1,3) \delta_{13} \delta_{24} + w(1,2) G(1,5) G(2,6) T(5,6,3,4). \quad (8)$$

The coordinate l is a compact notation: $l = \{\mathbf{r}_l, \tau_l, \sigma_l\}$, where \mathbf{r}_l is the real space vector, τ_l the Matsubara time, and σ_l the spin index. The diagrammatic form of this BSE and the self-energy contribution $\tilde{\Sigma}^T = \tilde{G}T$ corresponding to the T matrix are shown in Eq. (9).

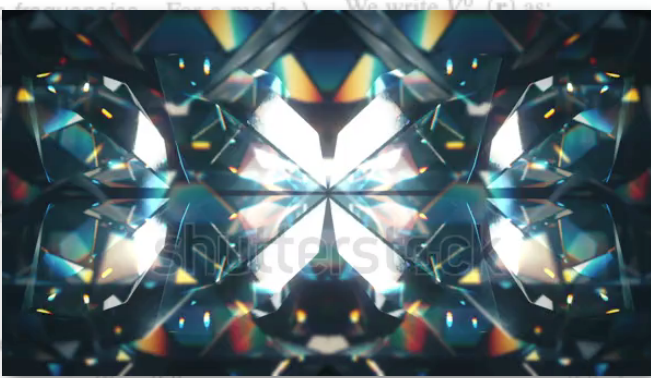
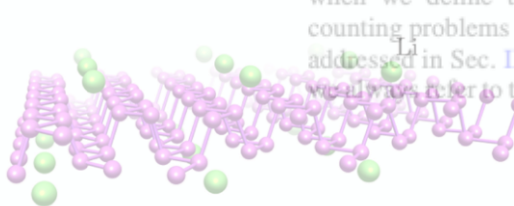
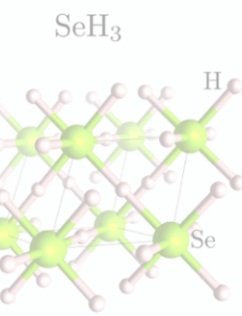
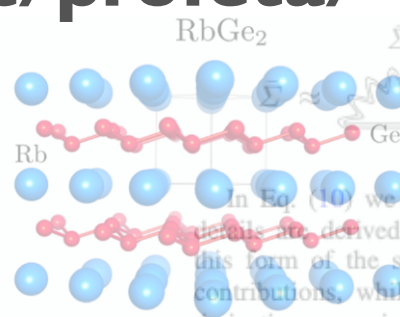
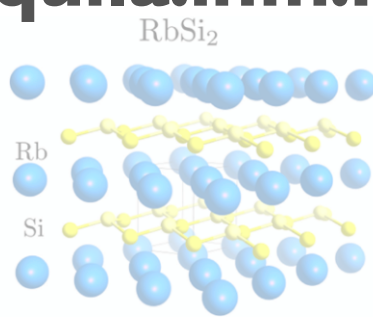
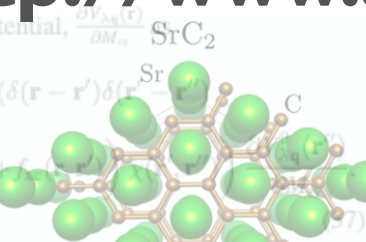


mathematically, it is well known that the matrix approximation of the magnetic response function is not sufficient for various studies to account for systems [46–49].

However, for reasons of simplicity, we do not make direct use of the T matrix and the corresponding self-energy for constructing the effective interaction. Instead we consider a larger set of diagrams, by starting from the particle-hole propagator Λ^P [50–52]. This object contains all proper particle-hole contributions. These are all diagrams which are irreducible with respect to a bare Coulomb interaction and have two incoming and two outgoing open coordinates. The T matrix is fully contained in Λ^P . We use the analogy with $\tilde{\Sigma}^T$ [see Eq. (9)], to formulate the self-energy containing magnetic contributions as

$$\Sigma^{GW} = \Sigma^{SF} + \Lambda^P + \Sigma^{Ph} \quad (10)$$

In Eq. (10) we only consider the diagrams that are derived from the self-energy contributions, while the derivative appearing in the self-energy contribution when we define the self-energy containing magnetic contributions is addressed in Sec. III C. We also refer to the



simplicity we restrict our calculation to the spin index σ , i.e., we assume a spin-independent interaction $\delta_{\sigma_1 \sigma_2} G(1,2)$. One of the diagrams contributing to the vertex $\Gamma(1,2,3,4)$ is shown in Fig. 1.



where the kernel of the irreducible vertex is

$$\Lambda_0^c(1,2,3,4)$$

and is called an irreducible vertex. The kernel Λ_0^c contains all connected diagrams which are irreducible with respect to a bare Coulomb interaction. The coordinates of the kernel are the coordinates of the external lines of the vertex. The kernel Λ_0^c is the sum of all diagrams which are irreducible with respect to a bare Coulomb interaction and have two incoming and two outgoing open coordinates. The kernel Λ_0^c is the sum of all diagrams which are irreducible with respect to a bare Coulomb interaction and have two incoming and two outgoing open coordinates. The kernel Λ_0^c is the sum of all diagrams which are irreducible with respect to a bare Coulomb interaction and have two incoming and two outgoing open coordinates.

After this definition, the contribution present in the self-energy is (1) The crossed contribution Σ^{Ph} containing the coordinates 1 and 2 in this set are

$$\Lambda_0^c(1,2,3,4)$$

Note that the contribution Σ^{Ph} is the sum of all diagrams which are irreducible with respect to a bare Coulomb interaction and have two incoming and two outgoing open coordinates.

Why and how does it happen?

Frohlich (1952)

$$H_F = H_e + H_p + H_{ep}$$

$$H_e = \sum_{k,\sigma} \epsilon_k c_{k,\sigma}^\dagger c_{k,\sigma}$$

$$H_p = \sum_{q,\lambda} \hbar\omega_{q,\lambda} [b_{q\lambda}^\dagger b_{q\lambda} + \frac{1}{2}]$$

$$H_{ep} = \sum_{k\sigma} \sum_{q,G\lambda} g_{k,\lambda}^{q+G} c_{k+q+G,\sigma}^\dagger c_{k\sigma} [b_{q\lambda} + b_{-q\lambda}^\dagger]$$

Why and how does it happen?

Frohlich (1952)

$$H_F = H_e + H_p + H_{ep}$$

$$H_e = \sum_{k,\sigma} \epsilon_k c_{k,\sigma}^\dagger c_{k,\sigma}$$

$$H_p = \sum_{q,\lambda} \hbar\omega_{q,\lambda} [b_{q\lambda}^\dagger b_{q\lambda} + \frac{1}{2}]$$

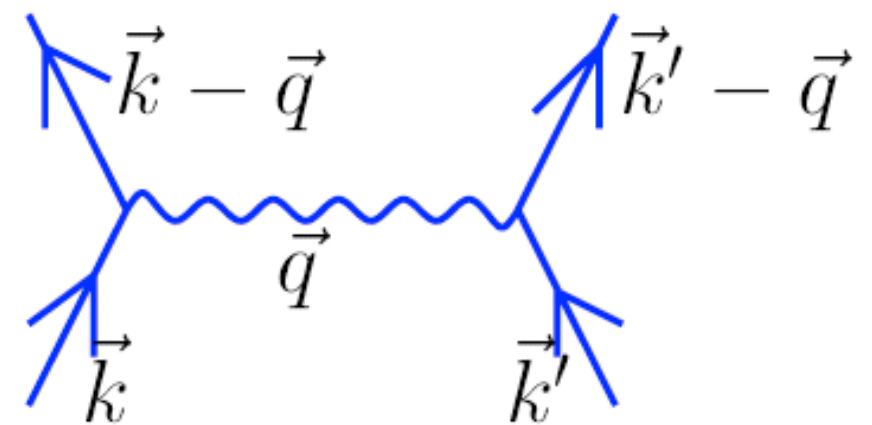
$$H_{ep} = \sum_{k\sigma} \sum_{q,G\lambda} g_{k,\lambda}^{q+G} c_{k+q+G,\sigma}^\dagger c_{k\sigma} [b_{q\lambda} + b_{-q\lambda}^\dagger]$$

Define an effective hamiltonian (not terms which couple e and ph)

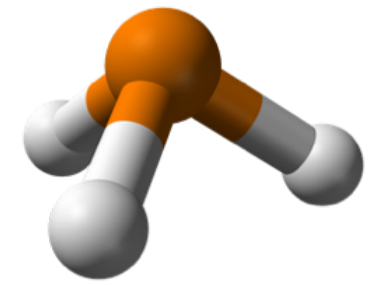
$$\tilde{H}_F = \sum_{k\sigma} \epsilon_k c_{k\sigma}^\dagger c_{k\sigma} + \frac{1}{2} \sum_{\substack{kk'qG \\ \sigma\sigma'}} V_{ph} c_{k+q+G\sigma}^\dagger c_{k'-q-G\sigma'}^\dagger c_{k'\sigma'} c_{k\sigma}$$

$$V_{ph} = \sum_{\lambda} \frac{\hbar\omega_{q\lambda} |g(q+G;\lambda)|^2}{[\epsilon_k - \epsilon_{k+q+G}]^2 - [\hbar\omega_{q\lambda}]^2}$$

if < 0 attraction !!



Isolated example? Superconducting phosphines (PH_3)



RAPID COMMUNICATIONS

PHYSICAL REVIEW B **93**, 020508(R) (2016)



Superconductivity in metastable phases of phosphorus-hydride compounds under high pressure

José A. Flores-Livas,¹ Maximilian Amsler,² Christoph Heil,³ Antonio Sanna,⁴ Lilia Boeri,³ Gianni Profeta,⁵ Chris Wolverton,² Stefan Goedecker,¹ and E. K. U. Gross⁴

¹Department of Physics, Universität Basel, Klingelbergstr. 82, 4056 Basel, Switzerland

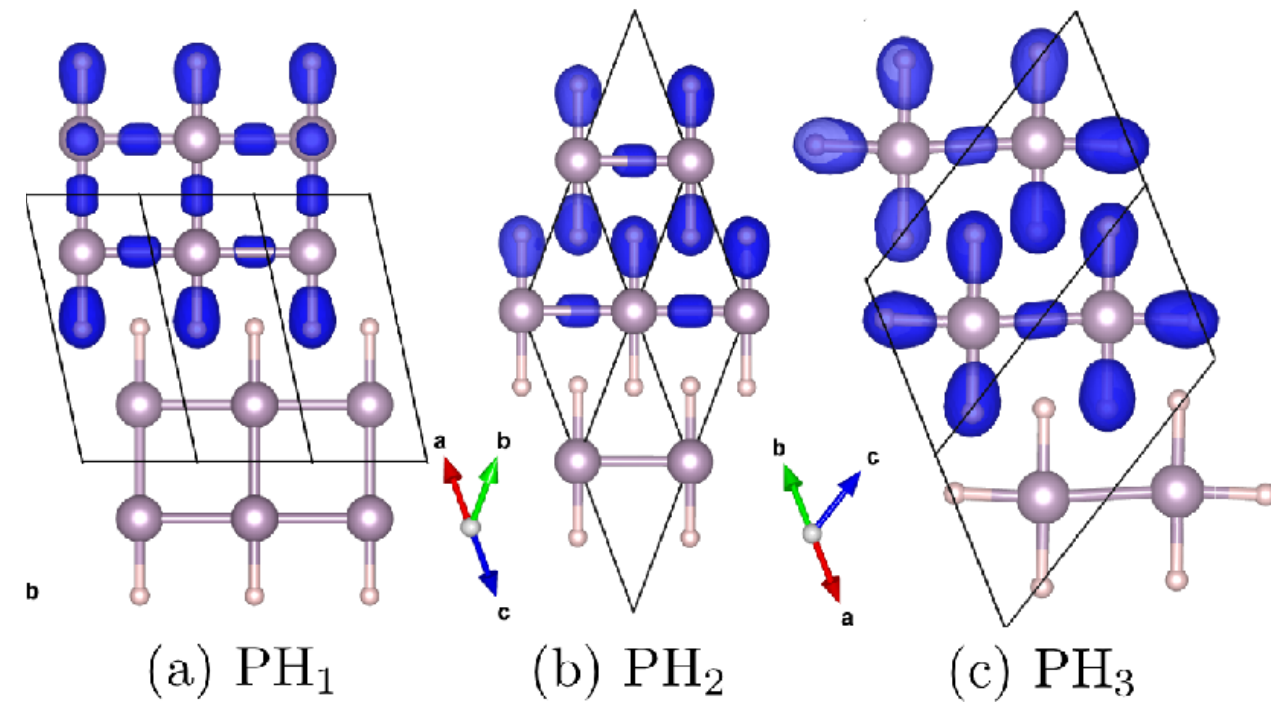
²Department of Materials Science and Engineering, Northwestern University, Evanston, Illinois 60208, United States

³Institute of Theoretical and Computational Physics, Graz University of Technology, NAWI Graz, 8010 Graz, Austria

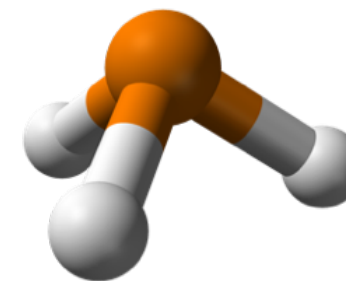
⁴Max-Planck Institut für Mikrostruktur Physik, Weinberg 2, 06120 Halle, Germany

⁵Dipartimento di Fisica Università degli Studi di L'Aquila and SPIN-CNR, I-67100 L'Aquila, Italy

(Received 7 December 2015; published 26 January 2016)



Isolated example? Superconducting phosphines (PH₃)



RAPID COMMUNICATIONS

PHYSICAL REVIEW B **93**, 020508(R) (2016)



Superconductivity in metastable phases of phosphorus-hydride compounds under high pressure

José A. Flores-Livas,¹ Maximilian Amsler,² Christoph Heil,³ Antonio Sanna,⁴ Lilia Boeri,³ Gianni Profeta,⁵ Chris Wolverton,² Stefan Goedecker,¹ and E. K. U. Gross⁴

¹Department of Physics, Universität Basel, Klingelbergstr. 82, 4056 Basel, Switzerland

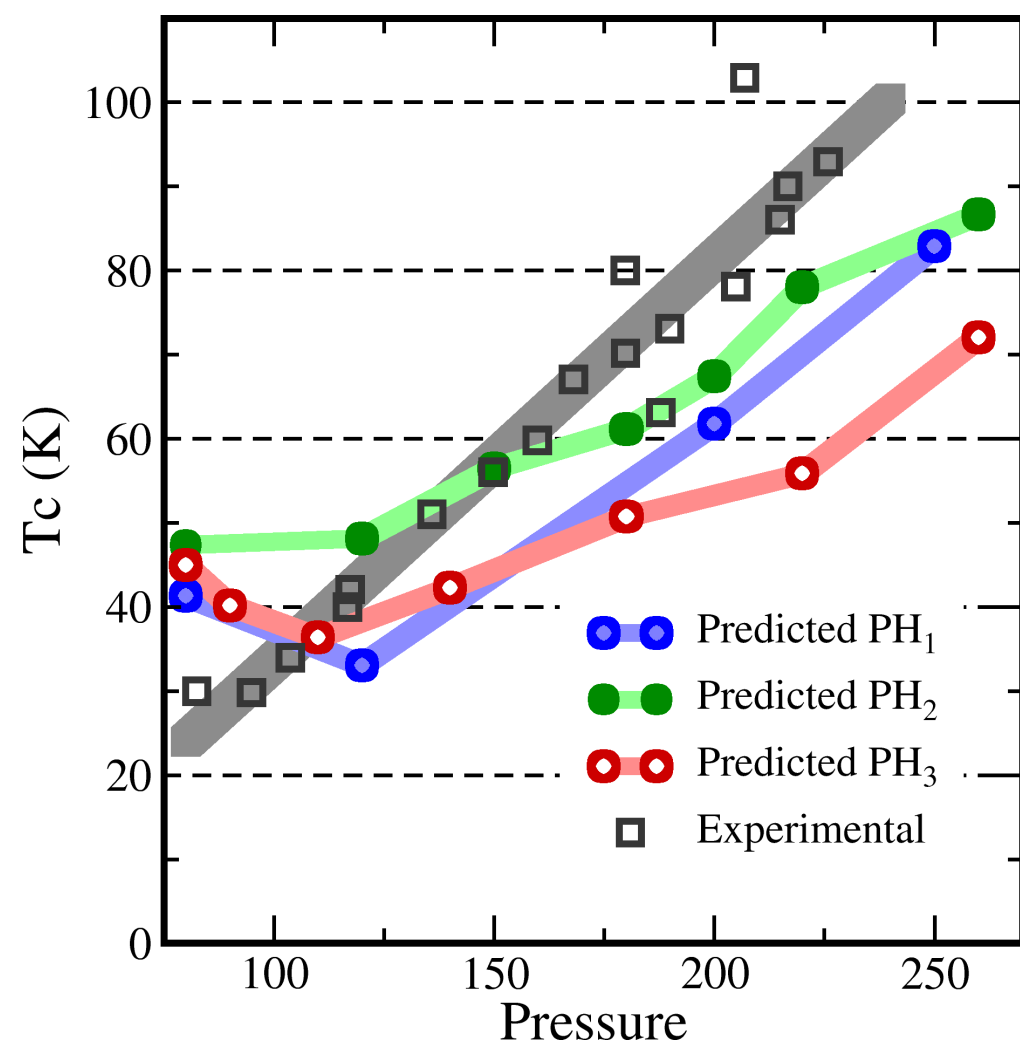
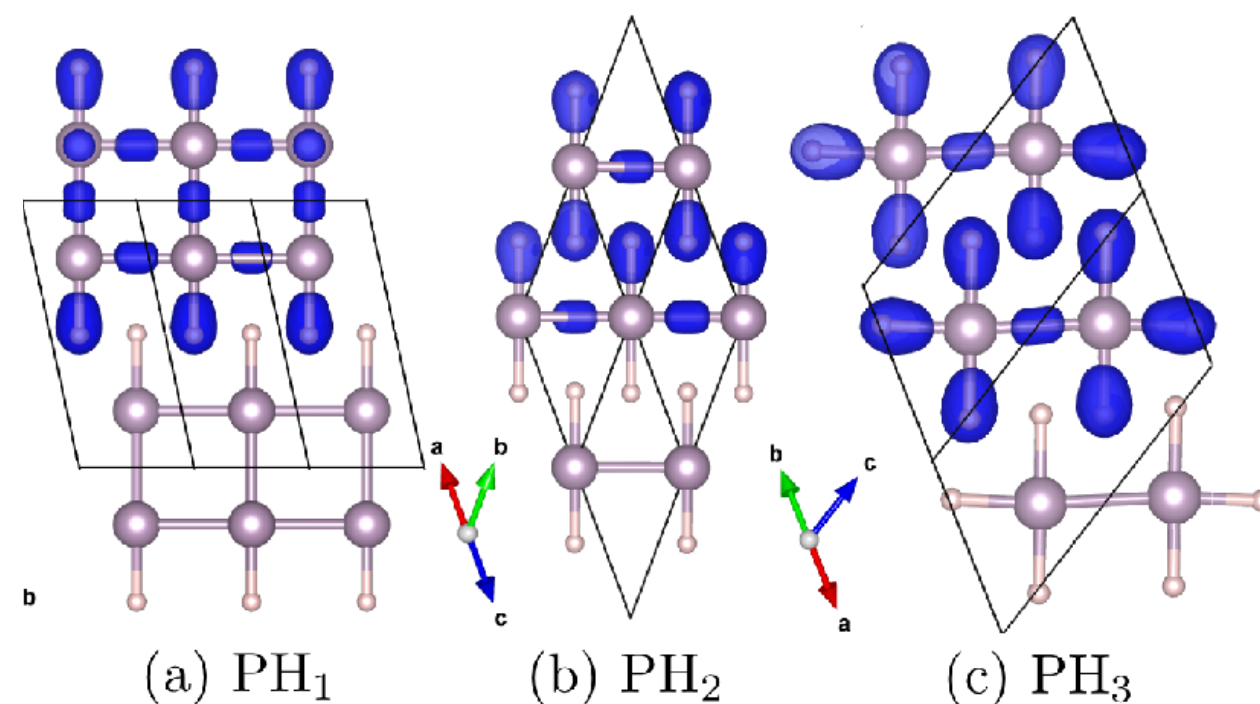
²Department of Materials Science and Engineering, Northwestern University, Evanston, Illinois 60208, United States

³Institute of Theoretical and Computational Physics, Graz University of Technology, NAWI Graz, 8010 Graz, Austria

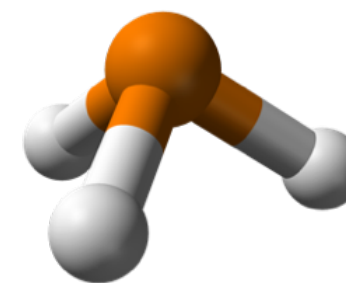
⁴Max-Planck Institut für Mikrostruktur Physik, Weinberg 2, 06120 Halle, Germany

⁵Dipartimento di Fisica Università degli Studi di L'Aquila and SPIN-CNR, I-67100 L'Aquila, Italy

(Received 7 December 2015; published 26 January 2016)



Isolated example? Superconducting phosphines (PH₃)



RAPID COMMUNICATIONS

PHYSICAL REVIEW B **93**, 020508(R) (2016)



Superconductivity in metastable phases of phosphorus-hydride compounds under high pressure

José A. Flores-Livas,¹ Maximilian Amsler,² Christoph Heil,³ Antonio Sanna,⁴ Lilia Boeri,³ Gianni Profeta,⁵ Chris Wolverton,² Stefan Goedecker,¹ and E. K. U. Gross⁴

¹Department of Physics, Universität Basel, Klingelbergstr. 82, 4056 Basel, Switzerland

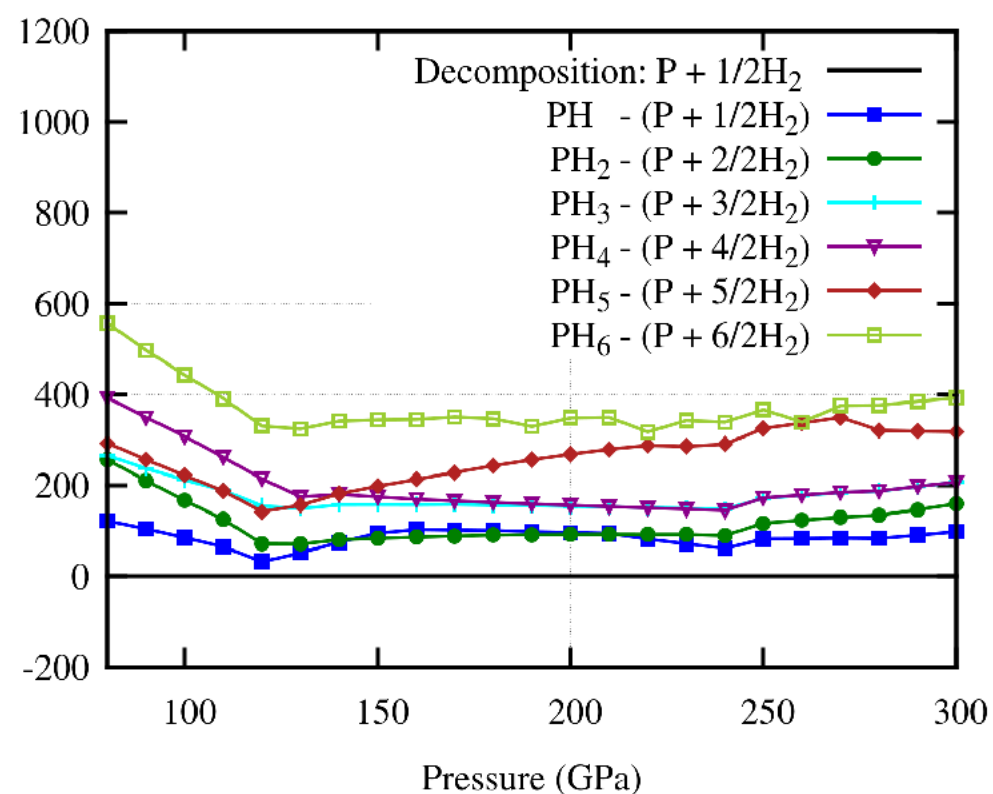
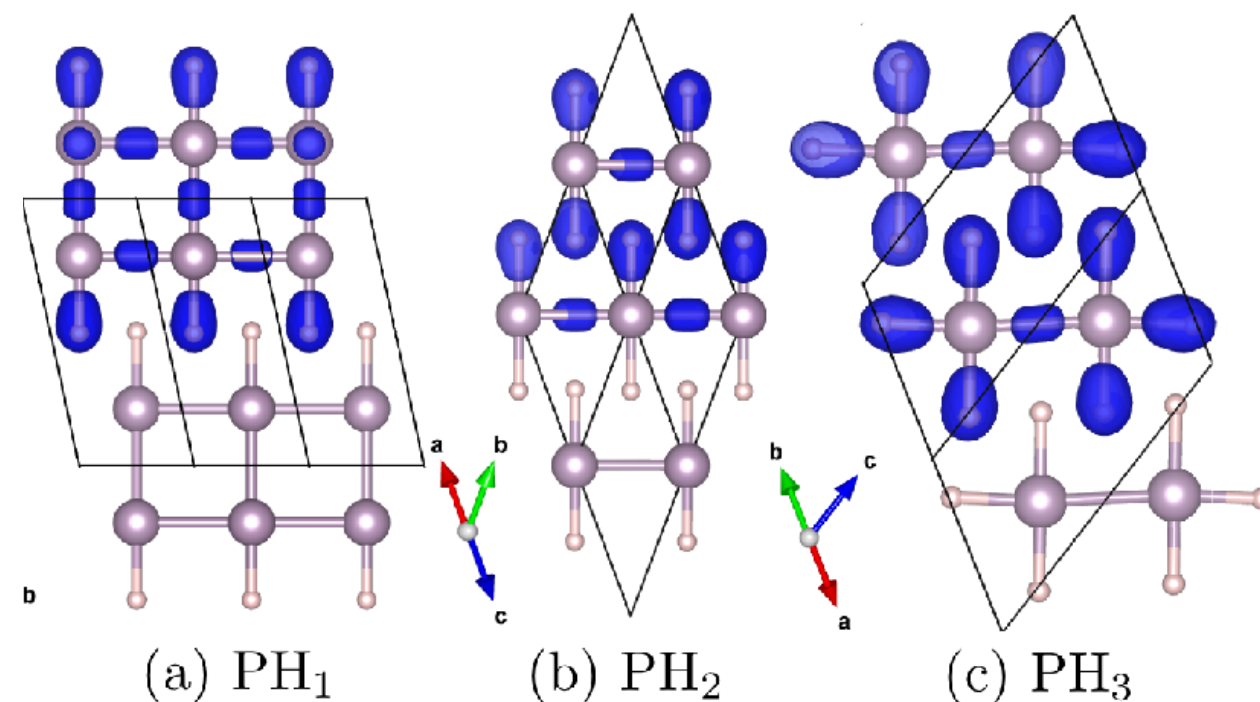
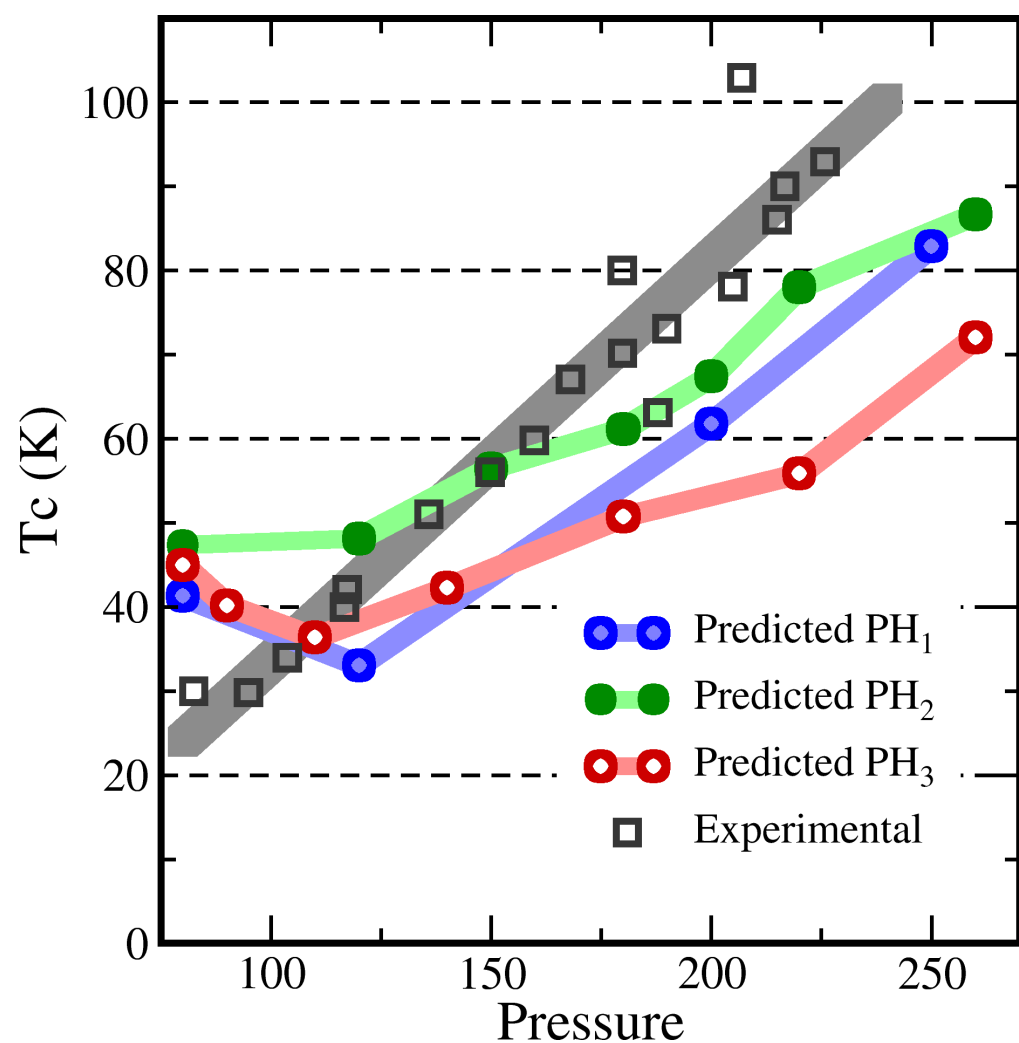
²Department of Materials Science and Engineering, Northwestern University, Evanston, Illinois 60208, United States

³Institute of Theoretical and Computational Physics, Graz University of Technology, NAWI Graz, 8010 Graz, Austria

⁴Max-Planck Institut für Mikrostrukturphysik, Weinberg 2, 06120 Halle, Germany

⁵Dipartimento di Fisica Università degli Studi di L'Aquila and SPIN-CNR, I-67100 L'Aquila, Italy

(Received 7 December 2015; published 26 January 2016)



Superconductivity up to 243 K in the yttrium-hydrogen system under high pressure

Panpan Kong^{1,7}, Vasily S. Minkov^{1,7}, Mikhail A. Kuzovnikov^{2,7}, Alexander P. Drozdov¹, Stanislav P. Besedin¹, Shirin Mozaffari³, Luis Balicas³, Fedor Fedorovich Balakirev⁴, Vitali B. Prakapenka⁵, Stella Chariton⁵, Dmitry A. Knyazev⁶, Eran Greenberg⁵ & Mikhail I. Erements¹✉

